UNIVERSITÉ DE STRASBOURG

EDSC
École Doctorale des Sciences Chimiques

UNIVERSITE DE STRASBOURG

ÉCOLE DOCTORALE des Sciences Chimiques

Laboratoire de Conception et Application de Molécules Bioactives UMR 7199

THÈSE

présentée par :

[SALMAN AKRAM]

soutenue le : **17 Octobre 2019**

pour obtenir le grade de : **Docteur de l'université de Strasbourg**

Discipline/ Spécialité : Sciences Pharmaceutiques

Synthèse, optimisation, caractérisation physico-chimique, fonctionnalisation et Application biomédicale de nanoparticules colloïdales

THÈSE dirigée par :

M ANTON Nicolas Professeur, Université de Strasbourg

RAPPORTEURS :

M BUKHARI Nadeem Irfan Professeur, Université de Punjab

M BEDUNEAU Arnaud Professeur, Université de Franche Comte

AUTRES MEMBRES DU JURY :

M VANDAMME Thierry Professeur, Université de Strasbourg

UNIVERSITY OF STRASBOURG

Logo
Ecole doctorale

ÉCOLE DOCTORALE des Sciences Chimiques

Laboratoire de Conception et Application de Molécules Bioactives UMR 7199

THESIS

PRESENTED BY:

SALMAN AKRAM

Defense on **October 2019**

For obtaining the degree of: **Doctorate of University of Strasbourg**

Discipline/ Specialisation: Pharmaceutical Sciences

Synthesis, Optimisation, Physico-chemical characterisation, Functionalisation and Applications of Colloidal Nano Particles

Thesis Supervised by:

M ANTON Nicolas	Professor, University of Strasbourg

Reporters :

M BUKHARI Nadeem Irfan	Professor, University of Punjab
M BEDUNEAU Arnaud	Professor, University of Franche Comte

Other Membres of Jury :

M VANDAMME Thierry	Professor, University of Strasbourg

Acknowledgment

Dawn is one of the most powerful experience observed by all those who share planet earth. Everyone loves it because it vanishes darkness & helps to observe this vast universe with a fresh look. Completing a PhD journey is similar experience as it vanishes darkness that reside in mind & helps to understand the nature around us in more detail. On this amazing but challenging voyage I have been supported by number of people without whom it would be impossible for me to finish this journey.

Firstly, I am thankful to my PhD supervisor **Dr Nicolas Anton** who was a source of continuous support through this whole journey. His vision, scientific advice & support helped me to achieve many milestones in this scientific journey. He not only provided his support during the PhD thesis but also invoked curiosity in my mind to try totally out of box ideas.

Secondly, I am thankful to my lab director **Professor Thierry Vandamme** for accepting me to this lab and providing me all the resources to complete this journey. He not only accepted and supported me but also gave his valuable scientific inputs throughout this journey.

Next, no one can achieve anything in this life without the support of **FAMILY**. I am thankful to my **Mother** for raising me after the death of my father. Being a single parent, she put all her energies to provide me all the financial resources and emotional support to carry out this study. She is the biggest reason today, that I am able achieve such a big milestone in my life. Then I am thankful to my **Brothers** and **Sisters** who provided me every resource, opportunities and motivation to continue my academic journey.

Moreover, I am thankful to my all lab mates who was always there to support me during the toughest times. Specially, **Asad Ur Rehman, Bilal Mustafa, Xinyue WANG, Justyn Wallyn, Mohammed Attia, Aidar Seralin, Sidy M. Dieng** & others. Their valuable inputs & friendly supported me made it easy for me to cross this difficult path with much ease. I had a wonderful time at lab memories of which will be with me for my lifetime.

Lastly, My PhD journey in Strasbourg journey would be incomplete without mentioning my **Pakistani Friends** here. They were here all the time here for me providing me a feeling of family & supported me in toughest times. They provided me with all the kind of emotional support to pass through difficult phases. I cannot thank them much for everything they have done for me.

RESUME DE LA THESE DE DOCTORAT

RESUME

Projet 1 : Formulation de doubles émulsions en deux étapes

Les émulsions doubles peuvent être réalisées soit par un processus en une seule étape ou en deux étapes (Figure 1 et la Figure 2). L'émulsion primaire E_1/H (eau-dans-huile) doit être de très petite taille, de préférence une nano-émulsion stabilisée par un tensioactif à HLB (Balance Lipophile Hydrophile) bas. L'émulsion inverse est généralement obtenue par une méthode à haute énergie, à l'aide d'un homogénéisateur à haute pression ou à ultrasons. Pour la deuxième émulsification, plusieurs approches peuvent être utilisées, mais une méthode à faible énergie peut être privilégiée afin d'éviter la libération prématurée du matériau hydrophile solubilisé dans les gouttelettes d'eau interne. En effet, les méthodes à haute énergie peuvent détruire l'émulsion primaire, produisant au final des émulsions H/E (huile-dans-eau) simples [1-3].

Depuis de nombreuses années, les émulsions doubles sont considérées comme une technologie émergente avec un intérêt potentiel élevé. Par conséquent, un énorme effort de recherche a été entrepris pour optimiser les formulations d'émulsions doubles pour les applications industrielles. Cependant, à ce jour, seuls quelques produits basés sur ce type d'émulsions sont sur le marché. La principale question est leur stabilité limitée, c'est-à-dire la formulation d'une émulsion double robuste capable de conserver ses spécifications sur le temps de stockage, comme l'apparence, la texture et le goût, ce qui implique une stabilité physique et chimique à long terme. Cette stabilité est très difficile à contrôler en raison de la différence de pression osmotique entre les phases interne et externe de l'eau qui doit être égalisée, et de la différence dans la pression hydrodynamique de Laplace qui tend à disparaître avec le temps et à modifier la morphologie globale du globule. Ces phénomènes d'équilibration sont également très dépendants des propriétés des tensioactifs utilisés pour la première émulsification, ce qui contribuent à stabiliser les minces films liquides entre les gouttelettes d'eau internes. En conséquence, l'équation de stabilité est complexe et très difficile. À ce stade, l'utilisation d'une nano-émulsion comme une émulsion primaire E_1/H peut être une option intéressante, en raison d'une plus grande stabilité de ce type d'émulsions, en comparaison avec les émulsions de tailles conventionnelles, *i.e.* micrométriques [4-6].

Ensuite, dans la partie suivante, nous avons optimisé la formulation des globules doubles à différentes échelles, de la taille micrométrique jusqu'à l'échelle nanométrique, en travaillant sur la seconde émulsification. Les nano-émulsions doubles ont été caractérisées par la diffusion dynamique de la lumière (DLS), la spectroscopie UV-visible, la spectroscopie de fluorescence, la

transmission et la microscopie électronique à transmission Cryo (TEM), ainsi que par la mesure de l'efficacité d'encapsulation (EE) et le profil de relargage des espèces modèles hydrophiles encapsulées dans les gouttelettes aqueuses internes, ce qui a donné lieu à la publication de deux articles : Akram S. *et al.* Langmuir 2019, et Ding, S. *et al.* Soft Matter 2017.

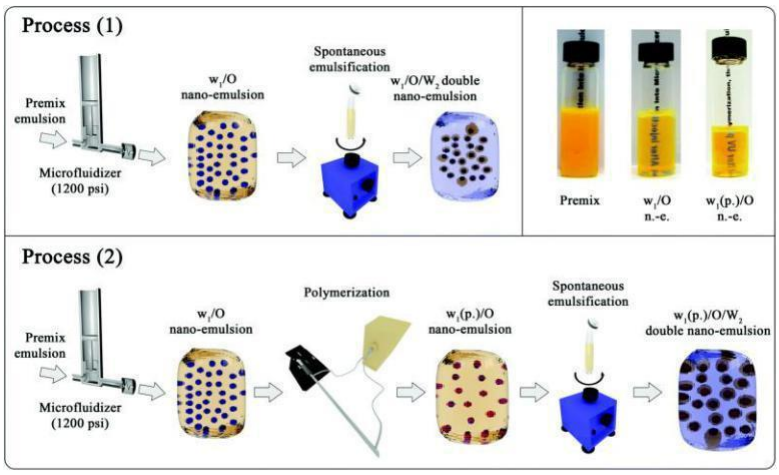

Figure 1 : partie A représentation schématique

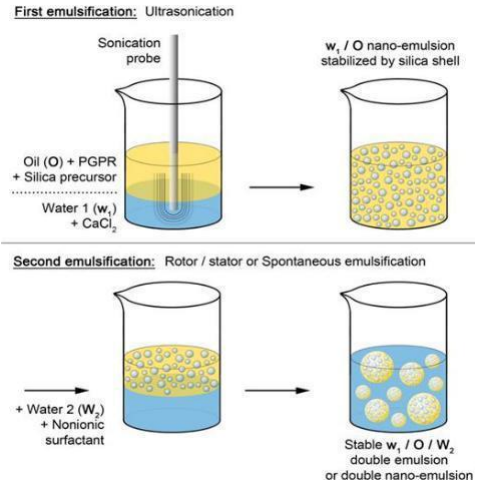

Figure 2 : partie B représentation schématique

Les résultats montrent que nous avons pu formuler les émulsions primaires et doubles à l'échelle nanométrique. Les résultats montrent dans le projet 1 partie A que l'efficacité d'encapsulation a été optimisée lorsque la phase aqueuse interne a été transformée en hydrogel (polymérisation UV). Dans la seconde partie (B), l'efficacité d'encapsulation a été augmentée en créant la coquille de silice à l'interface de l'émulsion primaire d'E/H.

Projet 2 : Etude de la nano-émulsification spontanée pour formuler des émulsions H/E

Dans le deuxième projet, nous nous sommes intéressés à des nano-émulsions inverses E/H par deux méthodes différentes d'émulsification spontanée. Les nano-émulsions E/H sont un outil

intéressant pour encapsuler les molécules hydrophiles, ce qui revêt un intérêt particulier pour des applications biomédicales après re-dispersion dans une phase aqueuse [7-9].

Dans la première méthode (méthode A), le surfactant lipophile est initialement mélangé avec de l'huile et homogénéise pendant cinq minutes. Ensuite, la phase aqueuse est ajoutée à débit constant (pompe péristaltique) permettant de fabriquer les nano-émulsions E/H. Premièrement, nous avons étudié l'effet des différents paramètres du procédé, comme le taux d'addition de la phase aqueuse, la vitesse d'homogénéisation à différents aux rapports de phase et différents rapports tensioactis/huile, sur la taille des particules et la dispersité des suspensions. Les différents tensioactifs lipophiles tels que le Span 80, le Span 85 et le PGPR (polyricinoléate de polyglycérol) ont été étudiés ainsi que leur impact sur le procédé d'émulsification. Ensuite, différents mélanges de ces tensioactifs et leur effet sur les propriétés des nano-émulsions ont été étudiés. Dans la dernière étape, différentes huiles telles que l'huile d'olive et d'autres ont été explorées.

Dans la deuxième méthode (méthode B), l'agent tensioactif lipophile a été mélangé avec la phase aqueuse à un taux d'homogénéisation prédéterminé pendant cinq minutes. Puis, l'huile a été ajoutée instantanément pour former les nano-émulsions E/H. Les différents aspects de la composition des formulations ont été étudiés comme précédemment et comparés.

Les résultats de ce projet indiquent que nous avons pu formuler les émulsions E/H nanométriques par les deux méthodes de formulations avec des propriétés comparables. Toutefois, la méthode A été préférée par rapport à la méthode B parce que les résultats présentés étaient meilleurs en termes de taille et d'indice de polydispersité. Les résultats ont également montré que plusieurs huiles et tensioactifs peuvent être utilisés pour faire ces émulsions E/H nanométriques par les deux méthodes.
Lors de dans cette partie, nous avons développé une nouvelle méthodologie pour fabriquer des émulsions inverses, ce qui est très novateur et qui servira de marchepied à de nombreuses recherche dans le domaine.

Conclusion

Les nanoparticules colloïdales sont un outil intéressant pour transporter les entités hydrohiles et lipophiles. Elles peuvent être efficacement produites par des méthodes de microfluidisation, d'ultrasonication et d'émulsification spontanée. Dans nos études, nous avons produit et caractérisé ces microparticules et nanoparticules sous forme d'émulsions simples, inverses et doubles, à la fois à l'échelle micrometrique et nanométrique montrant qu'elles peuvent être utilisées comme vecteurs de médicaments.

Références

(1) Lamba, H.; Sathish, K.; Sabikhi, L. Double Emulsions: Emerging Delivery System for Plant Bioactives. Food Bioprocess Technol. 2015, 8 (4), 709–728.

(2) Hearn, T. L.; Olsen, M.; Hunter, R. L. Multiple Emulsions Oral Vaccine Vehicles for Inducing Immunity or Tolerance. Ann. N. Y. Acad. Sci. 1996, 778 (1), 388–389.

(3) Okochi, H.; Nakano, M. Preparation and Evaluation of W/O/W Type Emulsions Containing Vancomycin. Adv. Drug Deliv. Rev. 2000, 45 (1), 5–26.

(4) Muschiolik, G.; Dickinson, E. Double Emulsions Relevant to Food Systems: Preparation, Stability, and Applications. Compr. Rev. Food Sci. Food Saf. 2017, 16 (3), 532–555.

(5) Assadpour, E.; Maghsoudlou, Y.; Jafari, S.-M.; Ghorbani, M.; Aalami, M. Evaluation of Folic Acid Nano-Encapsulation by Double Emulsions. Food Bioprocess Technol. 2016, 9 (12), 2024–2032.

(6) Esfanjani, A. F.; Jafari, S. M.; Assadpoor, E.; Mohammadi, A. Nano-Encapsulation of Saffron Extract through Double-Layered Multiple Emulsions of Pectin and Whey Protein Concentrate. J. Food Eng. 2015, 165, 149–155.

(7) Esfanjani, A. F.; Jafari, S. M.; Assadpour, E. Preparation of a Multiple Emulsion Based on PectinWhey Protein Complex for Encapsulation of Saffron Extract Nanodroplets. Food Chem. 2017, 221, 1962–1969

(8)Mohammadi, A.; Jafari, S. M.; Assadpour, E.; Esfanjani, A. F. Nano-Encapsulation of Olive Leaf Phenolic Compounds through WPC–Pectin Complexes and Evaluating Their Release Rate. Int. J. Biol. Macromol. 2016, 82, 816–822.

(9) Matsumoto, S. Development of W/O/W-Type Dispersion during Phase Inversion of Concentrated W/O Emulsions. J. Colloid Interface Sci. 1983, 94 (2), 362–368.

LISTE DES PRESENTATIONS

1. Enhancing Encapsulation Efficiency of Double Emulsion by Silica Stabilization

Poster Presentation at EMRS (European Material Research Society) Spring Meeting 18-22 June, 2018, Strasbourg, France

Akram S, Wang X, Vandamme TF, Collot M, Rehman AU, Messaddeq N, Mély Y, Anton N

LISTE DES PUBLICATIONS

1. Toward the Formulation of Stable Micro and Nano Double Emulsions through a Silica Coating on Internal Water Droplets. Akram S, Wang X, Vandamme TF, Collot M, Rehman AU, Messaddeq N, Mély Y, Anton N. ***Langmuir. 2019*** *Feb 12;35(6):2313-2325.*

2. Development of doxorubicin hydrochloride loaded pH-sensitive liposomes: Investigation on the impact of chemical nature of lipids and liposome composition on pH-sensitivity. Rehman AU, Omran Z, Anton H, Mély Y, Akram S, Vandamme TF, Anton N. ***European Journal of Pharmaceutics and Biopharmaceutics, 2018*** *Dec;133:331-338.*

3. A new method for the formulation of double nanoemulsions. Ding S, Anton N2, Akram S, Er-Rak M, Anton H, Klymchenko A, Yu W, Vandamme TF, Serra CA ***Soft Matter. 2017*** *Feb 22;13(8):1660-1669*

4. Biomedical Imaging: Principles, Technologies, Clinical Aspects, Contrast Agents, Limitations and Future Trends in Nanomedicines Justine Wallyn, Nicolas Anton, Salman Akram, Thierry F. Vandamme ***Pharmaceutical Research 2019****, 36:78*

5. Book title: Nano-emulsions, Elsevier, 2017. Editors: Seid Mahdi Jafari and David Julian McClements Chapiter title: Transitional nanoemulsification methods Anton, N.; Salman Akram, Thierry F. Vandamme. 77-100*

6. Book title: Smart Nanocontainers, Elsevier, 2019. Editors: Tuan Anh Nguyen Chapiter title: Lipid nanocarriers: Formulation, properties, and applications Rehman, A.; Akram, S.; Seralin, A.; Vandamme, T.; Anton, N. (Just Accepted)*

Contents

General Overview

The thesis manuscript is divided into three sections & is written in monogram form. Each section is complete in sense of its theoretical representation of topic & independent from each other. Thus, the manuscript does not have general list of abbreviations or list of figures.

The first section consists of three chapters. The first chapter is about general introduction on double emulsions & is part of book chapter written by me in partnership with fellow colleagues. The second & third chapters contain research articles published in peer review journals “Soft Matter” & “Langmuir” respectively.

The second section consists of two chapters. The fourth chapter consists of general overview of transitional nano-emulsification methods & is taken from book chapter written by my supervisor & me & published in book on nano-emulsions. The fifth chapter consists of research findings on formation of inverse nano-emulsions by spontaneous emulsification. This research article is in process of submission & review currently.

The third section consists of one chapter & appendices. The chapter 7 contains general conclusion of the thesis & perspectives of our different research projects. In the last appendixes contain additional research work carried out in collaboration.

Further detail about these different sections is given in the start of each section.

SECTION 1

Synthesis & Characterization of Double Emulsions

Executive Summary

This section contains 3 chapters all related to different concepts about double emulsions. Double emulsions are systems in which water in oil or oil in water emulsion is further emulsified into an out most continuous phase. The double emulsions are an interesting system because of the possibility they provide of carrying the both hydrophilic & lipophilic contents in the same system.

Chapter 1 contains introduction about the basic ideas of double emulsions. It provides a historical perspective about their development as drug delivery system, some of most important factors that impact their stability, their potential applications & at the end a very short review of their formation at nano scale. This part is taken from my academic writing work accepted by academic press to be published in a book.

Chapter 2 contains my research article published on the topic of double emulsions at nano scale in soft matter. This research article provides a ground-breaking research in the field of nano double emulsions by transposing conventional methods of formation of double emulsions at micro scale to form double emulsions at nano scale. The main highlight from study is first time use of combination of high & low energy methods for production of double emulsions at nano scale. The other main highlight is improvement of low encapsulation efficiency of double emulsions at nano scale by formation of hydrogel through UV-Polymerization.

Chapter 3 contains my research article published on the topic of double emulsions in Langmuir. This study provides another alternative for encapsulating hydrophilic drug at both micro & nano scale. The study mentions formation of double emulsions by combination of ultrasonication & spontaneous emulsification methods. The main highlight from study is that it addresses the low encapsulation efficiency problem of double emulsions by formation of silica shell at the interface of primary water in oil nano emulsion phase.

CHAPTER 1

General Introduction of Double Emulsions

1. Background, History & Introduction

Innovation is a tool that scientists use around the globe in many ways. The innovation allows scientists to improve the already developed systems as well as address the new problems and propose sustainable pragmatic solutions for these emerging problems. One of the major problem in the field of pharmaceuticals is to create smart drug delivery systems. The drug delivery systems which have high encapsulation efficiency, properties of targeted drug delivery, biocompatibility, high stability as well as safety are still challenge to many. Scientists have responded to these challenges in many ways which resulted in number of new dosage forms in the field of pharmaceuticals. Double emulsions is also one of these answers to challenge of developing optimum drug delivery system.

William Seifriz was the first person to observe the phenomenon of double emulsions in 1925[1]. The double emulsions reported by him had a very short life and were considered as transient systems between O/W and W/O emulsion system. After the first observation by Seifriz, double emulsions did not attracted attention of scientists for three decades. But in 1968, first application of this system as drug delivery carrier was reported in literature [2]. As these structures are inherently instable, historically their stability study was an important area of interest for researchers working in the field of double emulsions and there are number of studies available that give us some of the most important factors affecting their stability [3-11]. Besides exploring their stability, formulation and progress in the field of pharmaceuticals was also another important area of research [5, 6, 8]. Over the years, scientists also focused their potential as drug delivery system and their manufacturing on nano scale [2, 12-16].

Double emulsions are complex colloidal dispersions in which the two different emulsions coexist in the same system. The multilayer structure is composed in such a manner that the inner most globules are dispersed in a continuous phase, which is subsequently dispersed as globules in another outermost continuous phase [1, 8]. As this multilayered colloidal system can encapsulate both hydrophilic and lipophilic entities at the same time, this system can be exploited to number of applications in the pharmaceutical field [15, 17].

Depending on the continuous and dispersed phases double emulsions can be divided in two different following types

I. W/OW

II. O/W/O

The first type is mainly used in pharmaceutical field so we will mainly focus on the first type of double emulsions in this chapter.

Double emulsions are composed of three main components: oil Phase, surfactant and aqueous phase. The type of oil can have practical effect on double emulsion properties as one of the most important component of double emulsion system. Sometimes a mixtures of oil is also used to have some specific properties of double emulsion system. The most important factor by which oil can effect on the double emulsion system is the viscosity of oil. The highly viscous liquids can alter the rate of solutes transport from inner phase to out phase [5].

In most cases, the double emulsions have at least two surfactants which are opposite in nature and have different HLB values. For the creation of primary W1/O emulsion, a surfactant with relatively low HLB value is used, this surfactant is lipophilic in nature. HLB range 2-7 is generally suitable for primary emulsion while HLB range 6-16 is generally suitable for creating secondary emulsion. The secondary surfactant is mainly hydrophilic in nature and used to stabilize the secondary O/W2 emulsion. The higher amount of surfactants are not appreciated from safety point of view. The secondary surfactant concentration is also important from stability point of view as higher secondary surfactant concentration can lead to instability of the double emulsion system [4, 5, 7]. (More details in 4.2.3. stability of double emulsions)

2. Strategies to form double nano emulsions

The double emulsions can be made in single-step [6, 18] or by a two-step approach [19, 20]. In one step method the two different aqueous phases have same composition. Moreover, double emulsions prepared by one step method have relatively low encapsulation efficiency as well as they need an additional step of purification of bulk formulation and are not suitable for high added value active compounds. On the other hand, double emulsions prepared by two step method have different aqueous phases and potentially higher encapsulation efficiencies [3, 21-23].

The primary emulsion is mainly prepared by high energy method which break down the particles from micro to nano range depending upon the type of instrument used and energy applied. High

speed homogenizer with low energy range usually produce primary W1/O emulsion in micro range. While the high speed homogenizer with high energy input or shear such as micro fluidizer is mainly used to prepare emulsions in the nano range [20]. Ultrasonicator is another such instrument which create high energy waves and used to create primary emulsions in nano range [11]. (We have discussed these methods in start of chapter). The secondary emulsion is usually prepared by low energy method such as spontaneous emulsification [11, 20]. The low energy method is used because the high energy method can destroy the primary emulsion and can result in simple O/W emulsion [5].

Since their inception in 1925[1], a number of different techniques has been used to formulate the double emulsions. In a very recent review by Ding et al [24], they have summarized the different formulation strategies for double emulsion manufacturing. Different strategies used over the years for formulation of double emulsions are one step emulsification by hand shake [1], two step emulsification by mechanical stirring [25], two-step emulsifications with small vibrating mixer [4], double emulsions by UltraTurrax [11, 26], double emulsions prepared by a fractionated crystallization technique [27], double emulsion prepared with pin-mixer and UltraTurrax for W/O and W/O/W emulsions, respectively [3], double emulsion prepared with Micro fluidizer and Spontaneous emulsification for W/O and W/O/W emulsions, respectively [20], double emulsion prepared with Ultrasonicator and Spontaneous emulsification for W/O and W/O/W emulsions, respectively [11] and preparation of double emulsions by membrane emulsification [28].

A schematic diagram of formation of double emulsions is given in Figure 1 to understand the formation of double emulsions by two-step emulsification.

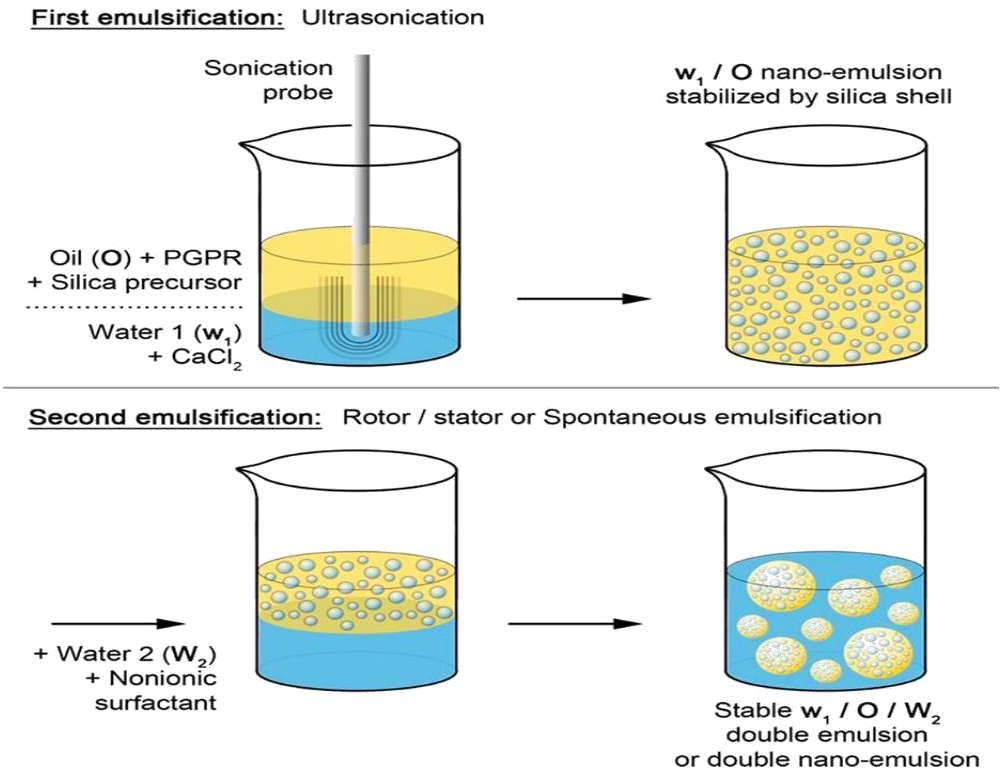

Figure 1: General process of the formulation of the double droplets and double nano-droplets stabilized by silica shell. First emulsification is the formulation of the primary reverse nano-emulsion for which water / oil interface is stabilized by both PGPR and silica shell. Second emulsification is done either by a rotor / stator apparatus (Ultraturrax®) for micro-double emulsions, or by spontaneous emulsification for double nano-emulsion.

The figure is retrieved from the work of Akram et al and shows the formation of double emulsion at both micro and nano scale formation by two step method.

3. Stability of double emulsions

Despite having many advantages, the double emulsions use is mainly limited because of their instability. The stability of double emulsions has been studied over many years and there is a lot of literature on stability of double emulsions. Below, there are some of the most recent and important representative studies. These studies give a comprehensive view of some important stability criteria of double emulsions.

In 1998, Ficheux et al [7] studied some of the important features of the stability criteria of double emulsions. They identified two different type of instabilities

a. Coalescence of the small inner water droplets with the globules surface
b. Coalescence between the small inner droplets inside the globules

They proposed that conversion from double to simple emulsion is exclusively due to coalescence of internal droplets with the large globule interface. Indeed, there is no detectable solubility of the oil soluble surfactant into water within exploration range of the water soluble surfactant concentration. Coalescence requires the formation of hole, which is associated with the activation energy E_a.

They showed that hydrophilic surfactant concentration in external phase and internal droplets as well as increasing the droplet diameter and temperature significantly increase the coalescence rate and conversion from double to simple inverse emulsion can be done from several months to few hours.

In 2001, K. Pays et al [9] investigated stability of double emulsions and proposed two methods that leads to release of chemical substances in surfactant stabilized double emulsions

a. Coalescence of thin film separating internal droplets from globules
b. Compositional ripening which occurs due to diffusion or permeation of the chemical substances across the oil phase

Firstly, the concentration of hydrophilic surfactant (C_h) in double emulsions can have an impact on the stability of the double emulsions. When the hydrophilic surfactant concentration (C_h), is less than critical micellar concentration (CMC) double emulsions are stable and there is no structural evolution even after few days of storage. While when the concentration of hydrophilic surfactant C_h=10CMC, the double emulsions takes almost five hours to be converted to simple inverted W/O emulsion. Coalescence of internal aqueous droplets on globule surface leads to this conversion.

Later on in 2003, Héctor González-Ochoa et al [10] also studied the coalescence phenomenon in double emulsions and they proposed that coalescence takes place in two different stages. In this study, hydrophilic surfactant concentration was increased up to 30 CMC and evolution of globules with respect to time was noted. Inner droplets escape due to coalescence and globule is shrunk in size and some of the inner droplets merge to form large droplet and eventually that too escape from the globule. By varying the concentration of surfactant the time for this destruction can be varied.

The coalescence happens very similarly for globules of different size being faster for the smaller ones.

The two stages of coalescence were identified although coalescence is thought to be instantaneous. In the first stage of the coalescence the external oil-water interface breakage takes place the oil enveloping the water peels off and transient water in water emulsion is formed. This leaves the water droplet immersed in continuous water phase supported by the film of oil and surfactants. In the second stage the film made of oil and surfactants thins continuously and breaks eventually to release inner water droplet content into the external water. The droplets close to the globule surface can exit early as compared to those that are in center of the oil globule. The time span for the first stage is determined by the properties of the oil phase such as viscosity, surface tensions, initial and final curvature and so on. The time span for the second stage depends on formulation of a film of oil and surfactants around the water and its properties such as thickness, structure and molar composition.

Carlos H. Villa et al [29] studied the instability due to internal coalescence in details. They showed that hydrophobic emulsifier promotes the stability of the double emulsion by creating a thickened adsorbed layer. This layer creates repulsive forces between the inner water W1 droplets or a droplet and the O/W2 interface. While the ionic and nonionic hydrophilic emulsifier have a destabilizing effect. Internal coalescence to occur before external coalescence, the hydrophilic surfactant must be more concentrated at the inner W_1/O as compared to W_2/O. Moreover, the internal coalescence will happen only when the overall hydrophilic surfactant is more in W1 as compared to W2. This higher surfactant in the oil layer can be present because of higher interfacial area to volume ratio of water W1 as compared to W2.

Martín Chávez-Páez et al recently studied the time evolution of double emulsions as interplay of two coalescence processes namely internal and external coalescence. They were able to identify four different regimens of this time evolution. In the first regimen, external coalescence was high due to presence of large internal droplets and their collision with the globule surface. At this stage the globule volume decrease significantly. During this inner water droplets also start to merge to form bigger nuclei. Later on, in second regimen as all the water droplets close to the surface of the globules are released so external coalescence rate becomes lower. In this case, the most of the inner droplets united together and form bigger droplets. There was no difference in the globule

diameter and only evolution is in texture of globule due to inner coalescence of droplets. In the third regimen, these bigger droplets of many micrometer settle down at the bottom of the globule and eventually leave the globule and we observe again a decrease in the diameter of globule. In the fourth regimen, as most of the droplets have left already the globule so we do not observe any significant internal coalescence.

These four stages can be better differentiated in case of smaller globules as in case of larger globules there are lot of inner droplets and the change in size is smooth. Moreover, the predominance of these two coalescence procedures over one another leads to different evolutions and this predominance depends on the surfactant compositions of both the interfaces. Such compositions are difficult to assess experimentally [30].

In another set of studies, Schuch et al [31-33] and her team tried to understand the coalescence in double emulsions by various other aspects. It was shown that coalescence of inner droplets could only be observed when there is second surfactant in the continuous phase. Choice of surfactants also impact on the stability of double emulsions. Moreover, coalescence is independent of double emulsion droplet deformation and break up. Coalescence does not take place within seconds but can be observed over several minutes. This implies that instabilities in double emulsion does not governed by process conditions but rather are an intrinsic consequence of formulation. Moreover, the coalescence of the droplets is only indirectly influenced by process parameters and emulsification devices as these different processes can produce droplets with different geometrical parameters. These geometrical parameters such as inner and outer droplets size strongly effect the coalescence. Lastly, they showed that usage of biopolymer does not necessarily guarantee on stabilizing the double emulsion by impacting on coalescence of the droplets produced and it varies from one to another biopolymer.

4. Stability of double emulsions at nano scale

The stability of double emulsions can be assessed in number of ways. For instance, increase in the size of internal droplets or external globules on storage for longer duration. In determining the stability, encapsulation efficiency is one of the major criteria when it comes to double emulsions at nano scale. The stability constraints has limited the formulation of double emulsions at micro scale[20]. In literature, Double emulsion formulations at the nanoscale are widely reported [21-23,

34, 35].However, these efforts did not gave deep insights into the improved encapsulation efficiency at nano scale or co-encapsulation of hydrophilic and lipophilic entities.

During my PhD, I have performed two studies related to double emulsions [11, 20]. These studies used a two-step method approach for creation of double emulsions at nano scale. The first step is creation of W1/O emulsion by high energy method followed by second step in which W1/O/W2 emulsion at nano scale is created by low energy method. So, we did transposition of classical method of generating double emulsions at micro scale by two step method approach to create double emulsion at nano scale. The first method involves the increase in stability by polymerization of inner aqueous phase while the second study reported the improvement in stability of double emulsions by reinforcement of inner aqueous with silica shell.

In first study, primary Nano-emulsions [20], W1/O was made by high pressure homogenizer (Microfluidizer®). The formulations of primary emulsion were mainly dependent on the formulation composition. The surfactant concentrations of more than 7%, and higher viscosity of the dispersed phase leads to reduction in size and hence increase in stability of primary emulsion droplets. The second step of the process was the low-energy emulsification of this primary nano emulsion, giving rise of double Nano-emulsion W1/O/W2, and the characterization of the leakage of an encapsulated small hydrophilic molecule (CF). We showed that the encapsulation efficiency
(EE) can strongly differ in function of the formulation parameters like the polymerization of the inner aqueous phase leads to higher encapsulation efficiency and hence higher stability. We took very interesting images by confocal and cryoTEM Figure 2.

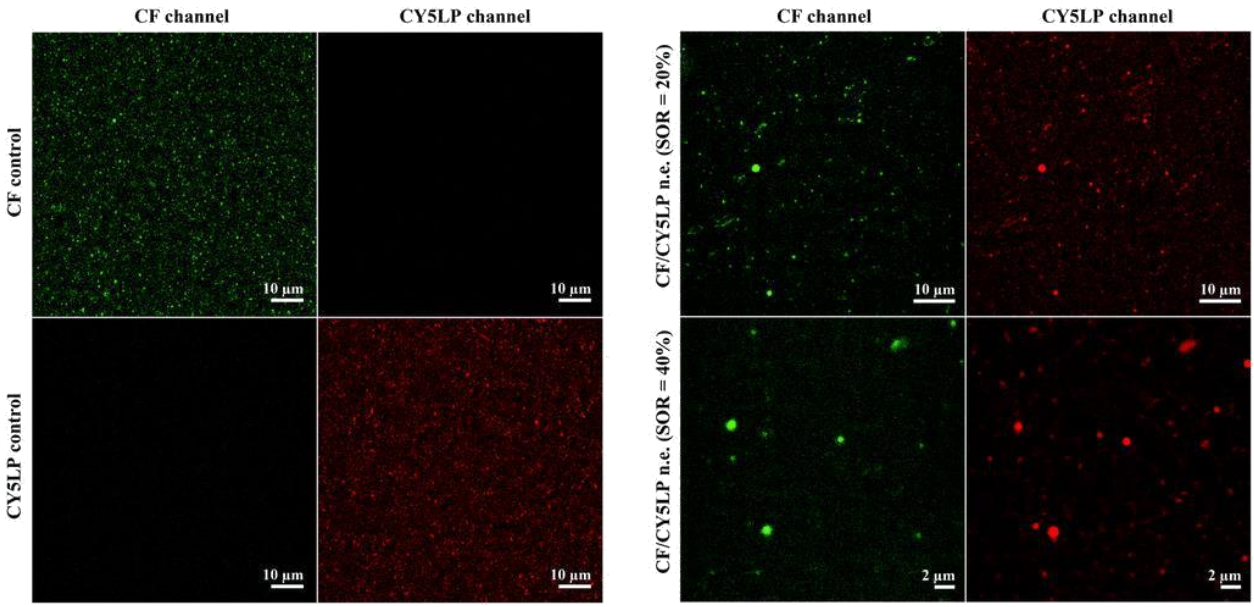

(Figure 2: Fluorescence confocal microscopy of w1 (p.)/O/W2 double nano-emulsions. Carboxyfluorescein (CF) and lipophilic cyanine 5 (CY5LP) are used as hydrophilic and lipophilic model dyes, respectively. CF control is double nano-emulsions containing only CF in aqueous core, and CY5LP is a nano-emulsion only containing CY5LP in oil phase.)

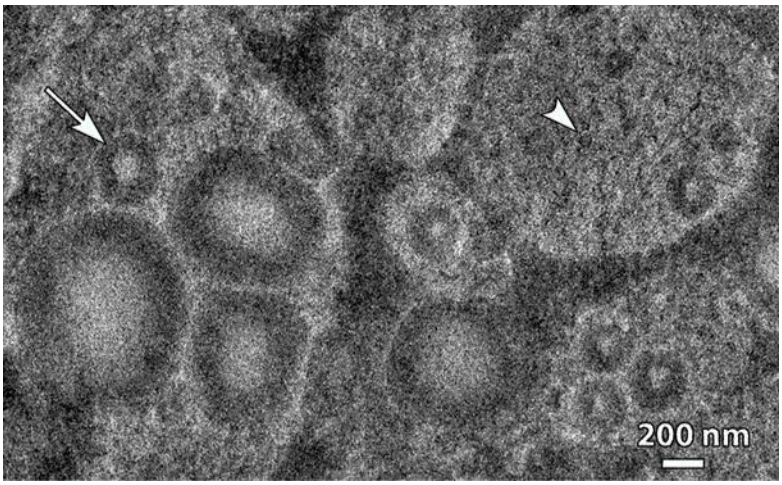

Figure 3: Cryo TEM micrographs of w1 (p.)/O/W2 double nano-emulsions. The darkest areas are the supporting lacey film.

The second study by us involves another novel technique for enhancing encapsulation efficiency. The double emulsion at nano scale was formed by two step method combining ultrasonication and spontaneous emulsification for primary and double emulsion respectively.

The system showed higher encapsulation efficiency and higher stability at both micro and nano scale when the primary emulsion droplets were reinforced by silica coating. Silica precursors were added to primary emulsion oil phase which created strong shell and protected the leakage of inner droplets on secondary emulsification to form double emulsions at nano scale. The study showed that modulating the silica membrane thickness (by playing on the formulation parameters) can result in modulating the encapsulation efficiency (up to hundred percent encapsulation), size and release kinetics. The following micrographic images show the double emulsions produced at micro and nano scale respectively.

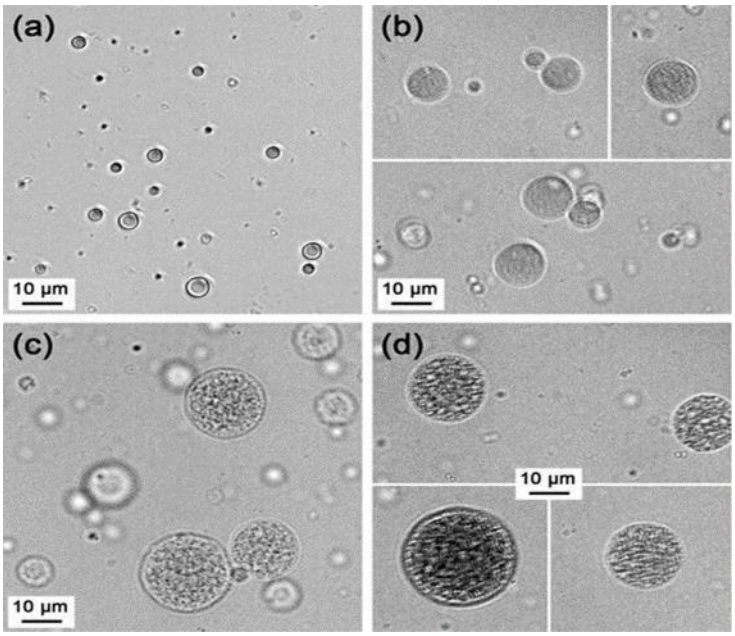

Figure 5: Optical observation of control emulsification without primary emulsions O/W2 (a), of the double emulsion w1/O/W2 without silica precursor (b), of the double emulsion w1/O/W2 with 2.5 wt.% APTES (c) and with 10 wt.% APTES (d) (ϕ_V^(Oil phase)=20 % and [Kolliphor ELP®] = 25 %).

The above figure shows the double emulsions at micro scale, without and with different amount of silica precursors. This multiple structure is reserved at nano scale too which is shown in following TEM images.

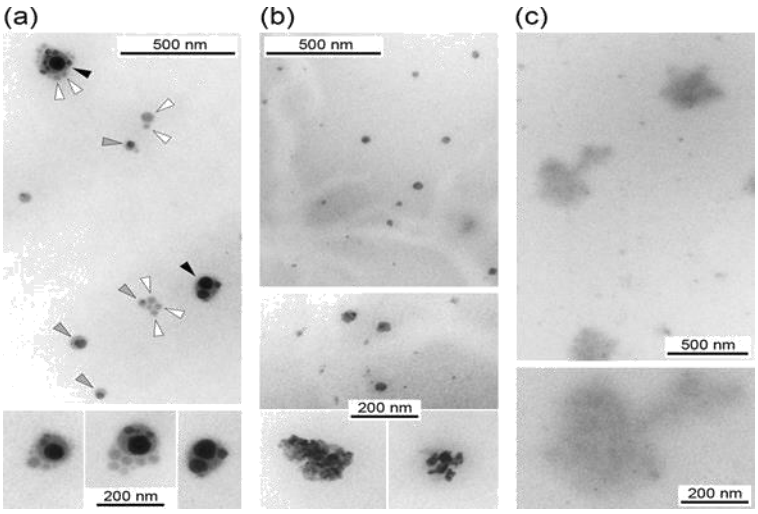

Figure 6: Transmission electron microscopy of double nano-emulsions for different concentrations of APTES, (a) 10 wt. %, (b) 2.5 wt. %, and (c) control without APTES.

The TEM images showing preservation of double emulsion structure even at nano scale when using silica precursor. In part (a) we can see multiple inner droplets inside the oil phase.

5. Applications of double emulsions

Adjuvant drug carriers which can carry both hydrophilic and lipophilic components in the same system are very interesting from drug delivery point of view. Components of different nature if combined in a single system can be advantageous as they can enhance the efficacy of the drug as well they can give synergistic effect. Core shell polymers, conjugate polymeric nano particles as well as liposomes are all efforts to take additional benefit from such adjuvant drug carrier system. The major drawback of all these systems is however their low encapsulation efficiency [14, 17, 36-40].

To meet the need of adjuvant therapy double emulsions appear as practical alternate solution. The double emulsion system ensures higher encapsulation efficiency of both hydrophilic and lipophilic entities as the system is itself constructed by these two type of phases. That is why, double emulsions have attracted attention of scientists around the globe over the past thirty years and their potential in drug delivery, cancer therapy and vaccine development has been explored.

Double emulsions have a wide use in field of pharmaceuticals. They are normally exploited to encapsulate the anticancer drugs [12, 17, 41-43]. In addition to their use as anticancer agents they

are used for loading of active compounds [44], to encapsulate the water soluble dyes [45], antifungal drugs [46], to antidiabetic actives [15], plant bioactive [16], food ingredients [19], vaccines [13].In addition to their applications in pharmaceutical field as drug carriers they are also used for purification of hydrocarbons [47], for enzyme immobilization [48] and for treatment of drug overdose [49].

6. Research Projects

The next chapters contains published version of two research projects (discussed briefly above) completed during my PhD that are described in summary above.

References

1. Seifriz, W., *Studies in Emulsions. III-V.* The Journal of Physical Chemistry, 1924. **29**(6): p. 738-749.
2. Engel, R.H., S.J. Riggi, and M.J. Fahrenbach, *Insulin: Intestinal Absorption as Water-in-Oil-in-Water Emulsions.* Nature, 1968. **219**(5156): p. 856-857.
3. Matsumoto, S., Y. Kita, and D. Yonezawa, *An attempt at preparing water-in-oil-in-water multiple-phase emulsions.* Journal of Colloid and Interface Science, 1976. **57**(2): p. 353-361.
4. Florence, A.T. and D. Whitehill, *Some Features of Breakdown in Water-in-Oil-in-Water Multiple Emulsions.* Journal of Colloid and Interface Science, 1981. **79**(1): p. 243-256.
5. Florence, A.T. and D. Whitehill, *The formulation and stability of multiple emulsions.* International Journal of Pharmaceutics, 1982. **11**(4): p. 277-308.
6. Matsumoto, S., *Development of W/O/W-type dispersion during phase inversion of concentrated W/O emulsions.* Journal of Colloid and Interface Science, 1983. **94**(2): p. 362-368.
7. Ficheux, M.F., et al., *Some stability criteria for double emulsions.* Langmuir, 1998. **14**(10): p. 2702-2706.
8. Garti, N. and C. Bisperink, *Double emulsions: Progress and applications.* Current Opinion in Colloid & Interface Science, 1998. **3**(6): p. 657-667.
9. Pays, K., et al., *Coalescence in surfactant-stabilized double emulsions.* Langmuir, 2001. **17**(25): p. 7758-7769.
10. Gonzalez-Ochoa, H., L. Ibarra-Bracamontes, and J.L. Arauz-Lara, *Two-stage coalescence in double emulsions.* Langmuir, 2003. **19**(19): p. 7837-7840.
11. Akram, S., et al., *Toward the Formulation of Stable Micro and Nano Double Emulsions through a Silica Coating on Internal Water Droplets.* Langmuir, 2019. **35**(6): p. 2313-2325.
12. Khopade, A.J., K.S. Nandakumar, and N.K. Jainb, *Lectin-Functionalized Multiple Emulsions for Improved Cancer Therapy.* Journal of Drug Targeting, 1998. **6**(4): p. 285-292.
13. Verma, R. and T.N. Jaiswal, *Haemorrhagic septicaemia vaccines.* Vaccine, 1998. **16**(11): p. 1184-1192.
14. Allen, C., D. Maysinger, and A. Eisenberg, *Nano-engineering block copolymer aggregates for drug delivery.* Colloids and Surfaces B: Biointerfaces, 1999. **16**(1): p. 3-27.
15. Garber, A.J., *Benefits of Combination Therapy of Insulin and Oral Hypoglycemic Agents.* Archives of Internal Medicine, 2003. **163**(15): p. 1781-1782.
16. Lamba, H., K. Sathish, and L. Sabikhi, *Double Emulsions: Emerging Delivery System for Plant Bioactives.* Food and Bioprocess Technology, 2015. **8**(4): p. 709-728.
17. Lane, D., *Designer combination therapy for cancer.* Nature Biotechnology, 2006. **24**: p. 163.
18. Pradhan, M. and D. Rousseau, *A one-step process for oil-in-water-in-oil double emulsion formation using a single surfactant.* Journal of Colloid and Interface Science, 2012. **386**(1): p. 398-404.
19. O' Dwyer, S.P., et al., *Formation, rheology and susceptibility to lipid oxidation of multiple emulsions (O/W/O) in table spreads containing omega-3 rich oils.* LWT - Food Science and Technology, 2013. **51**(2): p. 484-491.
20. Ding, S., et al., *A new method for the formulation of double nanoemulsions.* Soft Matter, 2017. **13**(8): p. 1660-1669.
21. Zhang, M., et al., *Controlling Complex Nanoemulsion Morphology Using Asymmetric Cosurfactants for the Preparation of Polymer Nanocapsules.* Langmuir, 2018. **34**(3): p. 978-990.
22. Malo de Molina, P., et al., *Oil-in-Water-in-Oil Multinanoemulsions for Templating Complex Nanoparticles.* Nano Letters, 2016. **16**(12): p. 7325-7332.

23. Zhang, M., et al., *Synthesis of Oil-Laden Poly(ethylene glycol) Diacrylate Hydrogel Nanocapsules from Double Nanoemulsions.* Langmuir, 2017. **33**(24): p. 6116-6126.
24. Ding, S., et al., *Double emulsions prepared by two–step emulsification: History, state-of-the-art and perspective.* Journal of Controlled Release, 2019. **295**: p. 31-49.
25. Kawashima, Y., et al., *Shear-induced phase inversion and size control of water/oil/water emulsion droplets with porous membrane.* Journal of Colloid and Interface Science, 1991. **145**(2): p. 512-523.
26. Ohwaki, T., et al., *Drug Release from the Water-in-Oil-in-Water Multiple Emulsion in Vitro. II. Effects of the Addition of Hydrophilic Surfactants to the Internal Aqueous Compartment on the Release Rate of Secretin.* CHEMICAL & PHARMACEUTICAL BULLETIN, 1993. **41**(4): p. 741-746.
27. Bibette, J., *Depletion interactions and fractionated crystallization for polydisperse emulsion purification.* Journal of Colloid and Interface Science, 1991. **147**(2): p. 474-478.
28. van der Graaf, S., C.G.P.H. Schroën, and R.M. Boom, *Preparation of double emulsions by membrane emulsification—a review.* Journal of Membrane Science, 2005. **251**(1): p. 7-15.
29. Villa, C.H., et al., *Internal coalescence as a mechanism of instability in water-in-oil-in-water double-emulsion globules.* Langmuir, 2003. **19**(2): p. 244-249.
30. Chavez-Paez, M., et al., *Coalescence in Double Emulsions.* Langmuir, 2012. **28**(14): p. 5934-5939.
31. Schuch, A., L.G. Leal, and H.P. Schuchmann, *Production of W/O/W double emulsions. Part I: Visual observation of deformation and breakup of double emulsion drops and coalescence of the inner droplets.* Colloids and Surfaces a-Physicochemical and Engineering Aspects, 2014. **461**: p. 336-343.
32. Schuch, A., J. Wrenger, and H.P. Schuchmann, *Production of W/O/W double emulsions. Part II: Influence of emulsification device on release of water by coalescence.* Colloids and Surfaces a-Physicochemical and Engineering Aspects, 2014. **461**: p. 344-351.
33. Schuch, A., et al., *Observations on the influence of different biopolymers on coalescence of inner water droplets in W/O/W (water-in-oil-in-water) double emulsions.* Colloids and Surfaces a-Physicochemical and Engineering Aspects, 2015. **475**: p. 2-8.
34. Hanson, J.A., et al., *Nanoscale double emulsions stabilized by single-component block copolypeptides.* Nature, 2008. **455**: p. 85.
35. Mehrnia, M.-A., et al., *Rheological and release properties of double nano-emulsions containing crocin prepared with Angum gum, Arabic gum and whey protein.* Food Hydrocolloids, 2017. **66**: p. 259-267.
36. Rubinfeld, B., et al., *Identification and immunotherapeutic targeting of antigens induced by chemotherapy.* Nature Biotechnology, 2006. **24**: p. 205.
37. Xu, C., et al., *Dopamine as A Robust Anchor to Immobilize Functional Molecules on the Iron Oxide Shell of Magnetic Nanoparticles.* Journal of the American Chemical Society, 2004. **126**(32): p. 9938-9939.
38. Santra, S., et al., *Conjugation of Biomolecules with Luminophore-Doped Silica Nanoparticles for Photostable Biomarkers.* Analytical Chemistry, 2001. **73**(20): p. 4988-4993.
39. Burns, A., H. Ow, and U. Wiesner, *Fluorescent core–shell silica nanoparticles: towards "Lab on a Particle" architectures for nanobiotechnology.* Chemical Society Reviews, 2006. **35**(11): p. 1028-1042.
40. Wu, S.-H., Y. Hung, and C.-Y. Mou, *Compartmentalized Hollow Silica Nanospheres Templated from Nanoemulsions.* Chemistry of Materials, 2013. **25**(3): p. 352-364.

CHAPTER 2

A new method for the formulation of double nanoemulsions

Published on 16 January 2017. Downloaded by Université de Strasbourg, Service Commun de la Documentation on 03/02/2017 03:53:38.

Soft Matter

PAPER

View Article Online
View Journal

Cite this: DOI: 10.1039/c6sm02603f

A new method for the formulation of double nanoemulsions

Shukai Ding,[a] Nicolas Anton,*[bc] Salman Akram,[bc] Meriem Er-Rafik,[a] Halina Anton,[d] Andrey Klymchenko,[d] Wei Yu,[a] Thierry F. Vandamme[bc] and Christophe A. Serra*[ae]

Double emulsions are very attractive systems for many reasons; the most important of these are their capacity to encapsulate hydrophilic and lipophilic molecules simultaneously in a single particle and their potentiality to protect fragile hydrophilic molecules from the continuous phase. Double emulsions represent a technology that is widely present down to the micrometer scale; however, double nano-emulsions, with their new potential applications as nanomedicines or diagnosis agents, currently present a significant challenge. In this study, we propose an original two-step approach for the fabrication of double nanoemulsions with a final size below 200 nm. The process consists of the formulation of a primary water-in-oil (w1/O) nanoemulsion by high-pressure homogenization, followed by the re-emulsification of this primary emulsion by a low-energy method to preserve the double nanostructure. Various charac-terization techniques were undertaken to confirm the double structure and to evaluate the encapsulation efficiency of a small hydrophilic probe in the inner aqueous droplets. Complementary fluorescence confocal and cryo-TEM microscopy experiments were conducted to characterize and confirm the double structure of the double nanoemulsion.

Received 18th November 2016,
Accepted 15th January 2017

DOI: 10.1039/c6sm02603f

rsc.li/soft-matter-journal

Introduction

Aqueous core nanovectors have attracted considerable research over the past quarter of a century due to their ability to form barrier globules suspended in an aqueous phase, which in turn contain smaller dispersed aqueous droplets.[1–3] Such a complex structure results in a multifunctional nanocarrier that is able to encapsulate hydrophilic molecules, hence this presents a huge potential for pharmaceutical application. Double emulsions, that is to say water-in-oil-in-water, present the great advantage of allowing co-encapsulation of hydrophilic (in the inner aqueous compartments) and lipophilic molecules (in the lipophilic envelope).[4,5] The combination of several components with different natures in one single carrier is a propitious solution with respect to improving the efficiency of treatment, produ-cing a synergistic effect in situ.[5,6] Thus, to satisfy this need, a variety of vehicles have been designed, such as conjugated polymer nanoparticles,[7–9] core–shell polymer nanoparticles,[10,11] and liposomes.[12] Even if, theoretically speaking, these solutions seem to fulfill the specifications of co-encapsulation, their main limitation remains their encapsulation efficiency. This point emphasizes the need to accelerate research efforts to create efficient multifunctional nanocarriers.

Double emulsions appear as a rational and pragmatic system in this scenario. This system not only meets the requirements for cocktail therapies but, directly using hydrophilic and lipophilic phases, guarantees the best possible encapsulation efficiency of both hydrophilic and lipophilic molecules. This is one of the main reasons why double emulsions triggered substantial inter-est with respect to pharmaceutical applications, such as drug delivery,[13] cancer therapy,[14] and vaccines.[15]

However, up to now, the formulation constraints only restricted the fabrication of double emulsions at the micro-scale. This is due to the instability of the double structure when the size reaches scales lower than 100 nm,[16,17] which is probably due to the great increase in the Laplace pressure in the inner aqueous droplets. Different strategies were used to reinforce the double structure and stabilize the particle, such as replacing the oil phase with a lipophilic polymer/solvent phase (using PLA, poly(lactic acid)), which gave rise to a water/poly-mer/water vehicle that encapsulated hydrophilic proteins (HSA, human serum albumin) at around 20–30% without co-encapsulation of the lipophilic component in the PLA phase.[18] Another example described the formulation of double

[a] Institut Charles Sadron (ICS) – UPR 22 CNRS, Strasbourg, France

[b] CNRS 7199, Laboratoire de Conception et Application de Mole´cules Bioactives (CAMB), Equipe de Pharmacie Biogale´nique, 74 route du Rhin, 67401 Illkirch Cedex, France

[c] Universite´ de Strasbourg, Faculte´ de Pharmacie, 74 route du Rhin, 67401 Illkirch Cedex, France. E-mail: nanton@unistra.fr

[d] CNRS 7213, Laboratoire de Biophotonique et Pharmacologie, 74 route du Rhin, 67401 Illkirch Cedex, France

[e] Universite de Strasbourg, Ecole Europeenne de Chimie, Polymeres et Materiaux (ECPM), Strasbourg, France. E-mail: ca.serra@unistra.fr

Published on 16 January 2017. Downloaded by Université de Strasbourg, Service Commun de la Documentation on 03/02/2017 03:53:38.

nanoemulsions stabilized with very specific block copoly-peptides; however, no further information was provided on encapsulation efficiency, yields, and the potential loading of the hydrophilic molecules[19] Another reported mechanism for obtaining a nano double emulsion is cavitation, which was applied for the nanoencapsulation of an anti-inflammatory.[20] In spite of some reported examples, the production and industrial scale-up of nano-sized double emulsions with very high encapsula-tion efficiency remains a challenge.

A microscopic water-in-oil-in-water double emulsion was first observed in 1925,[21] when W. Seifriz researched the effects of changing the specific gravity of the oil phase and the type of electrolyte on the type of emulsion. Since then, the synthesis and applications of double emulsions have been extensively investigated, and different methods of preparation have been developed. In general, double emulsions are prepared via two steps: the w1/O emulsion is first prepared as a primary emulsion, and then this primary emulsion is used as the oil phase with another aqueous phase in order to formulate a direct second emulsion, w1/O/W2.[22,23]

In the present paper, the formulation of double nano-emulsions is envisaged through transposing the classical method undertaken for the fabrication of double emulsions to processes normally followed to generate nanoemulsions. It follows that the two dispersed phases are generated separately; the first emulsification provides the reverse emulsion, w1/O, followed by a second emulsification giving w1/O/W2. Similarly, for micro-scale double emulsions, this methodology aims to ensure the best encapsulation efficiency; however, since the compositions of the two aqueous phases are different, special care needs to be devoted to the study of stability, drug leakage, and the equilibrium osmotic pressure.

This transposition requires that the process integrates several constraints; the primary emulsion should present a size typically below 50 nm, which is small enough to allow the second nanoencapsulation and stable enough to undergo a second emulsification process without breaking. The nano-emulsion formulations are divided into high energy and low-energy methods,[24] where high-energy methods involve the use of specific devices such as sonication or high-pressure appara-tus (e.g. high-pressure homogenizer or Microfluidizer^{S}) and low-energy ones use the physicochemical properties of the components to generate stable nanoemulsions.

Herein we focus on the development of a general emulsifica-tion method to obtain and understand the formulation of a double nanoemulsion through a two-step method. The primary w1/O nanoemulsion was stabilized by low-HLB surfactants and generated with a high-pressure Microfluidizer^{S}. Then, a double nanoemulsion was formulated by using a classical low-energy emulsification process and simply replacing the oil phase with the primary emulsion.[25] In order to improve the encapsulation efficiency, the inner aqueous nanodroplets were polymerized by acrylamide to form polyacrylamide hydrogel. Evaluation of the double structure was performed by cryo-transmission electron microscopy (cryo-TEM) and fluorescence microscopy, and the encapsulation efficiency within the aqueous inner compartment was characterized by using a hydrophilic fluorescent probe placed in the first water phase.

Methods and materials

Materials

The medium-chain triglyceride used in the preparation of nanoemulsions was exclusively Labrafac^{S} WL 1349 (Gattefosse´ S.A., Saint-Priest, France), a mixture of capric and caprylic acid triglycerides, as a model parenteral-grade oil. The use of such an oil helps to avoid Ostwald ripening of the droplets.[26] Non-ionic surfactant (polyglycerol polyricinoleate, PGPR, Pan Oil PGPR E476), which was used as a low-HLB surfactant (HLB = 1.5 0.5) for the preparation of the primary nanoemulsion, w1/O, was kindly gifted by Ste´arinerie Dubois (Boulogne-Billancourt, France). PGPR is a lipophilic stabilizer that is used in many formulations, and it is generally recognized as safe for human consumption by the FDA. Non-ionic surfactant, Kolliphor ELP^{S} (BASF, Ludwigshafen, Germany), is a polyoxyethylated-35 castor oil (HLB = 12–14), which was used as a hydrophilic surfactant in the secondary emulsifica-tion. Maltodextrin C* Dry 01915 (MD) was kindly provided by Cargill (Saint-Germain-en-Laye, France). MD is a polysaccharide that is generally used as a food additive. Genocure* DMHA was provided by RAHN (USA), and 5(6)-carboxyfluorescein (CF), N,N^{0}-methylene-bisacrylamide (MBA), acrylamide, potassium phos-phate monobasic, and sodium hydroxide were purchased from Sigma-Aldrich Chemical Company (Saint-Louis, USA).

Preparation of carboxyfluorescein solution

A given amount of CF was added to PBS (pH = 7.4 UPS), which resulted in a drastic decrease in pH. Sodium hydroxide solution (0.1 M) was used to increase the pH until a completely trans-parent brown CF solution was obtained. Then, sodium hydroxide solution was continually added until a pH of 7.4 was reached.

Preparation of primary emulsions w1/O by high-pressure microfluidizer

Let us focus on one of the most efficient high-pressure devices, which is the Microfluidizer^{S} (Microfluidics Corp., Westwood, MA, USA)[27] and precisely the lab-scale model, LV1. This works on the principle of injecting a coarse emulsion (premixed aqueous phase and oil phase) into an interaction chamber at a high pressure of up to 1200 psi. A decrease in the size of the emulsion droplets results from the great shear forces, which are supported by the special structure inside the interaction chamber. Microfluidizers have been used in the pharmaceutical industry.[28,29] The first step is the preparation of the inner aqueous w1 and oily phases. The aqueous w1 phase contains maltodextrin (C* Dry 01915), Milli-Q water or PBS, and a fluorescent probe (CF solution). Other additives, such as poly-merizing agents, crosslinkers, and initiators, can potentially be added. The oil phase was prepared by mixing the oil Labrafac WL^{S} and PGPR. The proportions of the different components as well as the volume fraction of the dispersed phase were the subjects of a part of the study. Both phases were roughly mixed

 This journal is © The Royal Society of Chemistry 2017

Published on 16 January 2017. Downloaded by Université de Strasbourg, Service Commun de la Documentation on 03/02/2017 03:53:38.

in a 50 mL Falcon-type flask with a volume around 10 mL. This coarse emulsion was mixed in a vortex for 1 min and then placed in a thermomixer (Eppendorf Thermomixer C, French) at 1000 rpm and 50 1C for 3 min. The premix was completed using an Ultra-Turrax® instrument (IKA T25M, Germany) operating at 24 000 rpm for 3 min. Next, the premix obtained was directly injected into the Microfluidizer®, operating at 1200 psi, to obtain the w1/O nanoemulsion after one passage. These stages aim to impact on the reproducibility of the experiments in order to ensure that all the premixes formulated and intro-duced to the high-pressure device were formulated under the same conditions.

On the other hand, complementary to this first formulation process, a second strategy was developed that involved poly-merizing the aqueous droplets to further reduce the risk of leakage. These agents were monomers (acrylamide) plus a crosslinker (N,N′-methylene-bisacrylamide) and a photoinitiator (Genocure* DMHA). The polymerization was performed by UV-irradiation (Hamamatsu Lightningcure LC8 operated at 365 nm) in a residence loop of 20 cm for typically 120 s, which was achieved by passing the primary emulsion through a PTFE tube. The light intensity was ca. 140 mW cm^{-2} for all formulations and this was measured with a light power meter (model C6080-13, Hamamatsu).

Nano double emulsions produced by low-energy nanoemulsification

Once the primary emulsion is generated, it is used as the oily phase for the low-energy emulsification process with or without reinforcement of its structure by polymerization. Low-energy emulsification takes advantage of the intrinsic physicochemical properties of the surfactants, co-surfactants, and excipients in the formulation in order to promote dispersion of the oil phase within the continuous aqueous phase at the nanometric scale. Several low-energy nanoemulsification methods have been described, such as spontaneous emulsification and phase-inversion temperature methods, but these were recently shown to be based on similar mechanisms.[30] In general, a nanoemul-sion is formed by mixing an aqueous phase (which can be pure water) with an oily phase containing a high-HLB non-ionic surfactant (which is fully miscible under certain temperature conditions). When these phases are mixed, the water-miscible surfactants diffuse into the water phase; this may occur so rapidly that turbulence is generated along with spinodal-like decomposition, which causes oil nanoscale droplets to form.[31]

It is noteworthy that the mechanism of double emulsifica-tion is not related to emulsion phase inversion; even though a literature report[32] proposes an accurate description of the relationship between emulsion inversion phenomena and the formation of double emulsions, this is not the case here. Emulsion phase inversion is generally used to produce O/W nanoemulsions; namely, the transitional phase inversion method utilizes the temperature (at constant composition) to create the best conditions for producing the nanoemulsifica-tion. On the other hand, the so-called catastrophic phase inversion method utilizes the composition (volume fraction of dispersed phase at constant temperature) to induce the emulsion phase inversion. Besides these two methods, it is important to mention that phase inversion can also occur because of hydrodynamic phenomena and notably as a result of stress induced by the flow.[32–35] Therefore, since multiple emulsions commonly form before the emulsion phase inver-sion due to interfacial instabilities causing changes in the surface concavity and giving rise to inclusion of the continuous phase within the droplets,[36] it is important to note that a hydrodynamic phenomenon can generate multiple emulsions without changes in temperature or composition.[32] However, it is likewise important to note that such multiple emulsions that are formed before emulsion phase inversion remain as inter-mediate states and rapidly destabilize, e.g. once emulsion inversion is complete. The process developed in the current study is different because it is based on a two-step procedure. This is designed for the formulation of stable double struc-tures, specifically encapsulating materials in the inner aqueous droplets that are not mixed with the continuous phase, and the inner droplets are not mixed with the continuous phase at any point in the process.

The aim here was to transpose the low-energy nanoemulsi-fication method to fabricate double emulsions using the primary emulsions as the oil phase; it was assumed that low-energy emulsification would be a smooth method that preserved the inner droplet structure. Thus, low-energy nano-emulsification was performed by mixing a primary emulsion with high-HLB non-ionic surfactant at room temperature and then rapidly pouring PBS into it. This system was then rapidly homogenized (vortex) to produce double nanoemulsions. We note that the vortex was used herein to optimize the homo-genization of the samples and not for nanoemulsification. Similar results were obtained using magnetic stirring instead of a vortex.[37,38] The dispersion properties, size, and polydisper-sity index (PDI) were closely linked to the relative proportions between the different components, which are defined as:

(i) high-HLB surfactant/primary emulsion weight ratio: SOR = 100 $w_{surfactant}/(w_{surfactant} + w_{oil})$, where w indicates the weight of the different compounds, and (ii) surfactant + oil/water weight ratio: $SOWR = 100 w_{surfactant+oil}/(w_{surfactant+oil} + w_{water})$.

The influence of the SOR was studied, whereas the SOWR was kept constant at 40% throughout this study; since its influence is negligible it only impacts on the droplet concentration to a reasonable extent (see ref. 25 for more details).

Characterization of primary nanoemulsion

Nanoemulsion-sized distributions were assessed by dynamic light scattering (DLS, Malvern ZS90). The primary emulsion was collected from the outlet of the microfluidizer and diluted with Labrafac WL®. The concentration of CF effectively present in the primary emulsion was determined by destroying a sample of the dispersion by heating it at 70 1C for 10 min along with the addition of hydrophilic non-ionic surfactant (Kolliphor ELP®) (at a ratio of 1 : 1). Centrifugation (14 000 rpm, 20 min, Eppendorf Minispin Centrifuge) was then performed to allow collection of the aqueous phase at the bottom of the flask. The supernatant

Published on 16 January 2017. Downloaded by Université de Strasbourg, Service Commun de la Documentation on 03/02/2017 03:53:38.

was removed and washed with dichloromethane three times. The dichloromethane was then completely evaporated, and the CF was dissolved in PBS and quantified with UV spectrometers. This quantification method was followed for every primary emul-sion formulated and was performed in triplicate.

Characterization of double nanoemulsion

Likewise, the size distribution of the double nanoemulsion was determined by DLS after dilution with PBS. Evaluation of the fraction of CF encapsulated in the inner aqueous w1 phase of the double nanoemulsion was performed by separation of the double nanodroplets from free dye that potentially escaped in the external water phase, W2. This separation is achieved by size exclusion chromatography using a desalting column (PD-10 Sephadex^{S} G-25 M, GE Healthcare). Before injection of the sample, columns were equilibrated with 25 mL of PBS (also used as an eluent), and 0.8 mL of the sample was deposited. We observed a clear boundary of pure PBS between the first passage of the double nanoemulsions (milky) and the free dyes (colored), which ensured the efficiency of the separation. The concentration of free CF was finally assessed by UV spectrometers (experiment done in triplicate), giving the encapsulation efficiency EE as follows:

$$EE = \frac{W_{tot.} - W_{free}}{W_{tot.}}$$

where $w_{tot.}$ and w_{free} are the weight of the total amount of CF in the primary emulsion and the weight of the unencapsulated CF, respectively. The EE values were quantified by UV spectrophotometry for the free fraction after separation with size exclusion chromatography. The double structure of the emulsion was imaged by cryogenic transmission electron microscopy (cryo-TEM) after performing sample dialysis to remove free surfactant in W2 (1 mL sample into the dialysis membrane, Spectra/Por^{S}, Spectrum Europe B.V., Breda, the Netherlands, cut-off 12 kDa, immersed 50 mL PBS for 12 h).

The double nanoemulsion structure was further character-ized by confocal microscopy. By adding a lipophilic fluorescent probe in the oil phase in addition to CF in the aqueous inner compartments, this characterization technique aims to show the co-localization of the two dyes. Double nanoemulsions were loaded with extremely hydrophobic cyanine dye, CY5LP. This dye was prepared as reported in previous studies.[34] Briefly, small hydrophilic counter ions (i.e. perchlorate) of a cationic cyanine dye, 1,1^{0}-dioctadecyl-3,3,3^{0},3^{0}-tetramethylindocarbocyanine (Dil), were replaced with a bulky hydrophobic tetraphenylborate (TPB) anion to form CY5LP. Double nanoemulsions were deposited in an 8 well imaging chamber (Ibidi, Biovalley) and imaged with a confocal microscope (Leica SP2) using a 20 dry objective (Leica). CF was excited with a 488 nm laser and the emitted fluorescence was detected in the spectral range 500–550 nm; on the other hand, CY5LP was excited with a 632 nm laser and the emitted fluorescence was detected in the spectral range 650–710 nm.

Cryo-TEM experiments were performed on double nanoemul-sions. The primary emulsions correspond to entry 2 of Table 2, and the double emulsion was formulated by adopting SOR = 30 wt%. Then, the sample was dialyzed for 24 h (Spectra/Por^{S}, Spectrum Europe B.V., Breda, the Netherlands, cut-off 12 kDa) to remove free surfactants. The vitrification of the samples was carried out with a homemade vitrification system. The chamber was held at 22 1C and the relative humidity at 80%. A 5 mL drop of the sample was deposited onto a lacey carbon film covered grid (Ted Pella), which was rendered hydrophilic using an ELMO glow discharge unit (Cordouan Technologies). The grid was automatically blotted to form a thin film that was plunged in liquid ethane held at 190 1C with liquid nitrogen. In this way, a vitrified film was obtained, in which the native structure of the objects was preserved. The grid was mounted onto a cryo holder (Gatan 626) and observed under low-dose conditions with a Tecnai G2 microscope (FEI) at 200 kV. Images were acquired using an Eagle slow scan CCD camera (FEI).

Results and discussion

As theoretically described above, the formulation of a double nanoemulsion is a multistep process, which is schematically illustrated in Fig. 1. Two formulation conditions were investi-gated: without (process (1)) and with (process (2)) polymeriza-tion of the aqueous inner w1 phase. In the first section below, we will focus on the influence of the composition and formula-tion parameters on the properties of the primary emulsion, w1/O. In process (2), acrylamide, MBA, and DMHA are added to the carboxyfluorescein solution to convert the aqueous nano-droplets of the w1/O nanoemulsion into hydrogel after UV polymerization. The inset of Fig. 1 shows photographs of the primary emulsions before and after their passage into the Microfluidizer^{S} and after polymerization. The premix appears completely turbid while the reverse nanoemulsion, w1/O, and the polymerized reverse nanoemulsion, w1(p.)/O, appear clear and translucent.

Impact of the composition on the properties of the primary nanoemulsion w1/O

To summarize, the aqueous phase is composed of Milli-Q water, maltodextrin (thickener), carboxyfluorescein (probe), and potentially acrylamide (monomer), crosslinker (MBA), and photoinitiator (DMHA). The oil phase is composed of Labrafac WL^{S} (medium-chain triglycerides) and PGPR (low-HBL stabilizer). We investigate the influence of the composition of these different components on the size and size distribution of the w1/O nanoemulsions; the results are shown in Table 1. The different entries are sorted by size to emphasize the potential impact of the formulation parameters on the nanoemulsion properties.

Overall, the nanoemulsification process appears to be efficient, resulting in hydrodynamic diameters between 200 nm and ca. 50 nm along with PDI values varying from 0.15 to 0.05; this confirms the good monodispersity of the suspension. The most important parameter affecting the size of the nanodroplets is the surfactant concentration. Increasing the weight content of PGPR induces a decrease in the size of the aqueous-phase nanodroplets

Published on 16 January 2017. Downloaded by Université de Strasbourg, Service Commun de la Documentation on 03/02/2017 03:53:38.

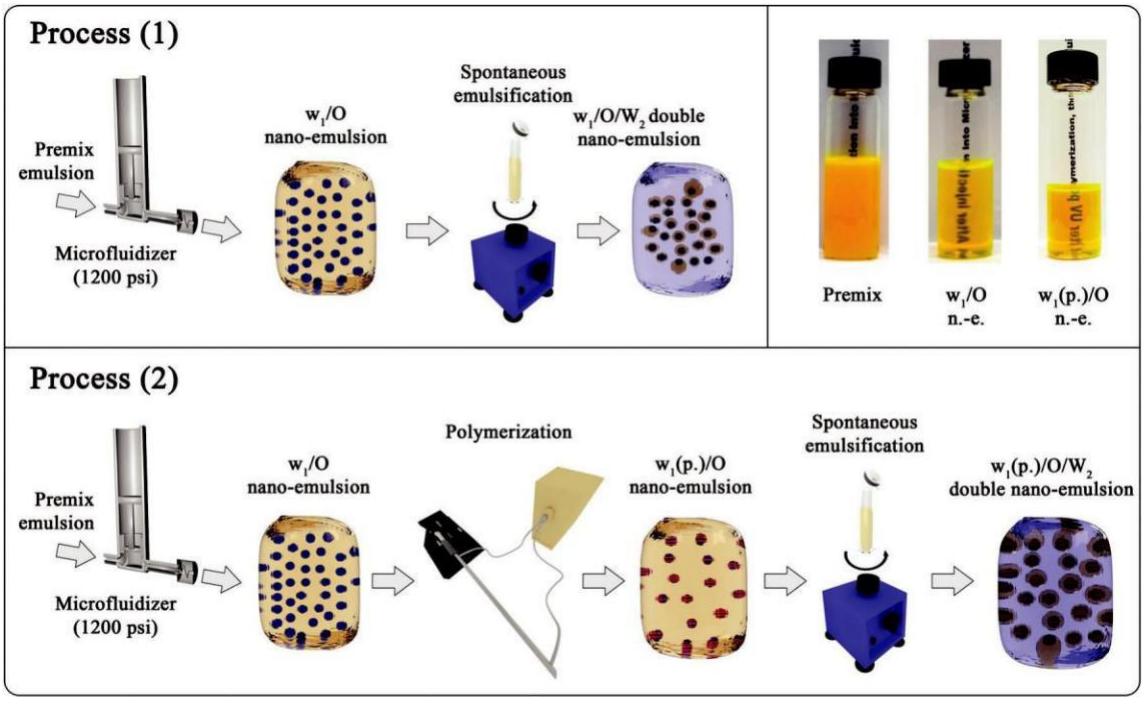

Fig. 1 Schematic drawings of the two-step processes to produce either fluorescent double nanoemulsions (process (1)) or fluorescent double nanohydrogels (process (2)). In the first process, the premix emulsion is injected into the high-pressure Microfluidizer^{S} to obtain a primary emulsion of water nanodroplets in the oil phase (w1/O), which is then used in the low-energy emulsification to obtain the double nanoemulsion (w1/O/W2). In process (2), the premix emulsion containing acrylamide, photoinitiator, and crosslinker is injected into the high-pressure Microfluidizer^{S} to obtain a polymerizable primary emulsion of water/acrylamide nanodroplets in the oil phase (w1/O). Then, the primary emulsion is polymerized by UV irradiation to obtain nanohydrogels in the oil phase (w1(p.)/O), which are then used in the low-energy emulsification to obtain double nanohydrogels (w1(p.)/O/W2). The inset shows photographs of the primary emulsions before and after their passage into the Microfluidizer^{S} and after polymerization.

Table 1 Compositions and sizes of the primary emulsions in process (1)

	Aqueous phase (AP)			Oil phase (OP)				
#Entry	f^{bulk} (%)	MD (wt% in AP)	PBS[a] (wt% in AP)	$f_{disp.}$ (%)	Oil (wt% in OP)	PGPR (wt% in OP)	Size (nm)	PDI
1	19	72	28	81	98.75	1.25	195	0.12
2	19	72	28	81	99.25	0.75	193	0.06
3	25	72	28	75	92.86	7.14	150	0.12
4	15	72	28	85	93.75	6.25	123	0.03
5	10	30	70	90	94.12	5.88	111	0.15
6	15	30	70	85	93.75	6.25	111	0.10
7	25	30	70	75	92.86	7.14	110	0.08
8	25	50	50	75	92.86	7.14	104	0.12
9	15	50	50	85	93.75	6.25	101	0.15
10	10	40	60	90	87.50	12.5	55	0.16
11	13	50	50	87	90.62	9.375	55	0.28
12	10	50	50	90	87.50	12.5	50	0.11
13	10	60	40	90	87.50	12.5	77	0.08

[a] No CF in PBS buffer solutions.

produced by the Microfluidizer^{S} regardless of the viscosity (i.e. regardless of the weight content of maltodextrin) and the weight content of the aqueous phase. On the other hand, the weight contents of maltodextrin in water $[MD]_{water}$ have a limited impact on the size as one can observe when $[PGPR]_{oil}$ is kept constant at 6.25 wt%. This result is probably correlated to the phenomenon by which the droplets are created and stabilized during processing. The reason for the increase in the viscosity of the aqueous phase was related to the impact of the viscosity ratio on the critical Weber number Wec, which shows a minimum for values between 10 [2] and 1.[40] Based on these observations, our methodology was empirical and we gradually increased the viscosity of the aqueous phase while measuring the resulting size distributions of the reverse nanoemulsion. With a minimum maltodextrin weight content of 30 wt% in the aqueous phase, this is precisely what we obtained. The other key parameters are the weight contents of the aqueous phase and PGPR in oil. These parameters will influence, respectively, the number of droplets

Documentation on 03/02/2017 03:53:38.

Published on 16 January 2017. Downloaded by Université de Strasbourg, Service Commun de la

Table 2 Compositions and sizes of the primary emulsions used in low-energy emulsifications in process (2)

	Aqueous phase (AP)							Oil phase (OP)				
#Entry	f_{bulk} (%)	MD (wt% in AP)	PBS (wt% in AP)	CF (mM in PBS)	AM (wt% in PBS)	MBA (wt% in AM)	DHMA (wt% in AM)	$f_{disp.}$ (%)	Labrafac (wt% in OP)	PGPR (wt% in OP)	Size (nm)	PDI
1	10	50	50	50	—	—	—	90	87.50	12.5	58	0.17
2	10	50	50	50	40	10	5	90	87.50	12.5	50	0.13
3	10	50	50	200	40	10	5	90	87.50	12.5	53	0.23
4	10	50	50	50	40	2	5	90	87.50	12.5	47	0.17

created and their potential stabilization before coalescence during emulsification. This clarifies the effect of the PGPR concentration on the resulting size of the droplets, which is due to better stabilization of the nanodroplets after generation.

For process (2) (Fig. 1), the resulting polymerizable primary emulsion was then pumped through PTFE tubing (1.6 mm ID), which was placed inside a 20 cm long stainless tube with both ends connected by means of two T-junctions (Swagelok, France) to the two light waveguides of a UV source (Lightningcure LC8, Hamamatsu, Japan) operating at a wavelength of 365 nm and a suitable intensity (ca. 140 mW cm^{-2}). At such settings, the residence time of the primary emulsion under the UV light was about 120 s, which was sufficient to polymerize acrylamide inside the nanodroplets, resulting in the formation of nano-hydrogels in oil due to the presence of the MBA crosslinker. The sizes and PDIs of the obtained polymerized primary nanoemulsions as determined by DLS measurements are reported in Table 2.

From this table, it can be seen that the presence of the fluorescent contrast agent (CF) and the polymeric compounds (AM, MBA, & DHMA) does not significantly affect the size of the aqueous phase nanodroplets (see entries 1 & 3 of Table 2 and entry 12 of Table 1 as well as entries 1–4 of Table 2).

Synthesis of double nanoemulsions

After obtaining the primary emulsion, the $w_1/O/W_2$ double emulsions are prepared by a low-energy emulsion method. Since the volume ratio of water compared to that of the primary emulsion (i.e. value of SOWR, see above) was recognized as not having a substantial influence on the nanoemulsion properties,[25] it was fixed at 40%. On the other hand, a key parameter influencing the droplet size is the surfactant-to-oil ratio (namely SOR, see above). The SOR was varied from 20 to 40%, and the sizes of the resulting double nanoemulsion are reported in Tables 3 and 4. As expected, increasing the value of the SOR induces a reduction in the double droplet size to below 100 nm for SOR = 40%.[30,41] In addition, to confirm the limited impact of the viscosity of the aqueous phase on the process, we have investigated its effect on the size of the double droplets, selecting $[MD]_{water}$ = 40, 50, and 60 wt%. The resulting sizes and PDIs of the secondary double nanoemulsions for-mulated by processes (1) and (2) are reported in Tables 3 and 4, and these show that the suspensions are very similar regardless of the MD concentration. This indicates that the low-energy emulsification is not affected by the oil content but is affected by the surfactant-to-oil ratio. Once the high-HLB non-ionic

Table 3 Surfactant-to-oil weight ratios (SORs) used in low-energy emul-sion process (1) and the resulting double nanoparticle characteristics as a function of the weight content of MD in the aqueous phase of the primary emulsion (w_1) for process (1): 40, 50, and 60 wt%

40 wt%[a]			50 wt%[b]			60 wt%[c]		
SOR (%)	Size (nm)	PDI	SOR (%)	Size (nm)	PDI	SOR (%)	Size (nm)	PDI
20	178	0.51	20	161	0.31	20	168	0.37
25	156	0.34	25	137	0.13	25	153	0.29
30	127	0.17	30	113	0.15	30	119	0.13
35	103	0.12	35	113	0.22	35	98	0.11
40	83	0.14	40	81	0.12	40	87	0.15

[a] Based on aqueous formulation of entry 10 of Table 1 containing 50 mM of 5(6)-CF. [b] Based on aqueous formulation of entry 12 of Table 1 containing 50 mM of 5(6)-CF. [c] Based on aqueous formulation of entry 13 of Table 1 containing 50 mM of 5(6)-CF.

Table 4 Surfactant-to-oil ratio (SOR) used in low-energy emulsion process (2) and the resulting double nanoparticle characteristics for three different compositions of the primary aqueous phases (w_1)

Composition A (entry #2 of Table 2)			Composition B (entry #3 of Table 2)			Composition C (entry #4 of Table 2)		
SOR (%)	Size (nm)	PDI	SOR (%)	Size (nm)	PDI	SOR (%)	Size (nm)	PDI
30	130	0.21	30	145	0.37	30	162	0.39
35	120	0.21	35	133	0.23	35	128	0.20
40	106	0.22	40	116	0.22	40	111	0.25

surfactant (Kolliphor ELP^S) is mixed with the primary nano-emulsion, it appears to preserve the inner droplets. Then, mixing this oily phase with PBS induces the immediate solubi-lization of Kolliphor ELP^S by the buffer and results in low-energy emulsification. The size distribution obtained by dynamic light scattering of the primary and double emulsions of a representative sample is reported in Fig. 2 (entry 2 in Table 2 for the primary emulsion and composition A in Table 4, with SOR = 40 wt%, for the double emulsion). It is interesting to note that the primary emulsions w_1(p.)/O are centered at 50 nm and the double emulsions w_1(p.)/O/W_2 reached 122 nm; these both had a relatively good monodispersity. Even though the two distributions appear to overlap, they are still compatible with engulfment of the former in the latter. It is interesting to note that, like common nanoemulsions made with triglycerides that inhibit Ostwald ripening, the suspensions present excellent stability. After several weeks of storage, the values were checked again and remained unchanged (data not shown).

Published on 16 January 2017. Downloaded by Université de Strasbourg, Service Commun de la Documentation on 03/02/2017 03:53:38.

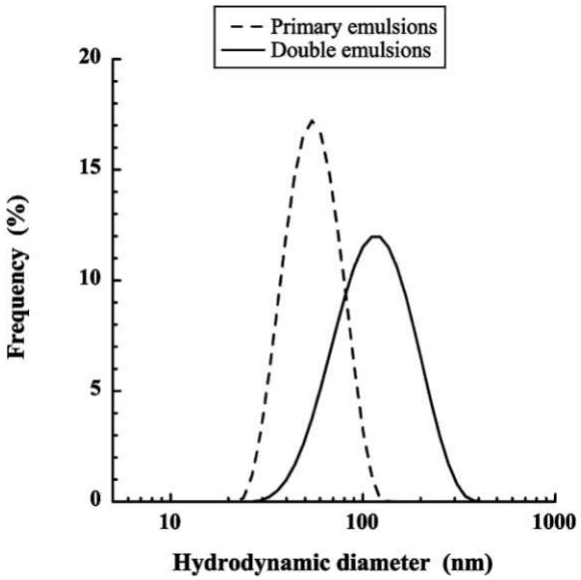

Fig. 2 Size distribution (obtained by dynamic light scattering) of primary emulsion (w_1(p.)/O) corresponding to entry 2 in Table 2, and double emulsion (w_1(p.)/O/W_2) corresponding to composition A in Table 4, with SOR = 40 wt%.

Considering the whole process of double nanoemulsion formulation, the critical question is whether the secondary nanoemulsification preserves the inner aqueous nanodroplets. Indeed, low-energy emulsification involves mixing oil with hydrophilic non-ionic surfactant, which can potentially solubilize and destabilize the hydrophilic materials, and the turbulence generated could also induce their leakage into the bulk W_2 phase. To this end, we developed a method based on the encapsulation of a fluorescent probe, which was easily quantified by absorption. We selected 5(6)-carboxyfluorescein for this purpose, and this was encapsulated in the inner aqueous w_1 phase at a concentration of 50 mM (200 mM was also tested for comparison, see below). Once the double nanoemulsion was formulated, free CF was physically separated from the double nanodroplets by phase exclusion chromatography (PD10 Sephadex G25), and the free portion was quantified.

The first system is the double nanoemulsion (process (1)) with SOR = 20% and [MD] = 50 wt%, which results in quite polydisperse droplets (PDI = 0.51) with sizes around 177 nm. The encapsulation efficiency obtained reached ca. 19% (Table 5).

When the droplet size was reduced and the monodispersity increased, along with increasing the SOR (concentration of high-HLB surfactant), the encapsulation dropped to zero. This is probably due to the polydispersity, which allowed the bigger droplets to be less affected by the emulsification process. A similar result was obtained from [MD] = 40 wt%, probably for the same reason. When [MD] was increased to 60 wt%, a very slight rise in the encapsulation value was obtained, between 7 and 12%. Owing to the fact that the MD mainly impacts on the viscosity of the w_1 phase, one can imagine that this increase in CF encapsulation may be related to the slightly higher retention of CF during emulsification.

On the other hand, when the inner w_1 phase is polymerized and turned into hydrogel (process (2)), the double nanoemulsi-fication allows much greater encapsulation of CF, up to about 50%. Compared to the double nanoemulsion prepared with process (1), here the droplets integrate monomer, crosslinker, and initiator, and we observed a limited impact on the size of both the primary and double nanoemulsions. The hydrogel formed probably creates a network to trap the hydrophilic species within the inner aqueous droplets.[42] According to the trend observed for process (1), increasing the value of the SOR results in a decrease in the double droplet size (see Table 4), e.g. from 130 nm to 120 nm to 106 nm for a decrease in the SOR from 30 wt% to 35 wt% to 40 wt%. Compared to the results for process (1), the size and PDI are slightly increased, which may be related to the fact that more water droplets are encapsulated inside the oil globules. However, in any event, converting internal aqueous droplets into hydrogels has a significant impact on the encapsulation of the small hydrophilic probe. This gives EE values as high as 50–60%, which are significantly higher and probably related to the fact that crosslinked polyacryl-amide creates a water cage that slows down the CF leakage during and after the low-energy emulsification. It is interesting to note that the presence of crosslinker (MBA, 2 wt%) has no influence on the results, indicating that the crosslinked polyacrylamide chains were sufficiently packed and tangled in the w_1 nanodroplets to retain CF. Another experiment was conducted by increasing the CF concentration to 200 mM. In this case, the encapsulation efficiency was decreased to approximately 20%. It follows from this that the maximum encapsulation capability was reached and the excess CF was largely expelled into the W_2 bulk phase.

To summarize, the efficient encapsulation of a small hydro-philic probe like CF is possible by reinforcement of the inner

Table 5 Encapsulation efficiency (EE) of 5(6)-CF for different surfactant-to-oil weight ratios (SOR), with different aqueous phase compositions and the same oil phase composition as in Table 2

	Aqueous phase composition/process (1)			Aqueous phase composition/process (2)		
SOR (%)	40 wt% MD in AP 60 mM 5(6)-CF in PBS	50 wt% MD in AP 50 mM 5(6)-CF in PBS	60 wt% MD in AP 40 mM 5(6)-CF in PBS	Comp. A (entry #2 of Table 2)	Comp. B (entry #3 of Table 2)	Comp. C (entry #4 of Table 2)
20	n/a	19.1	n/a	n/a	n/a	n/a
25	n/a	n/d	n/a	n/a	n/a	n/a
30	2.9	n/d	7.2	57.9	17.6	56.8
35	3.0	n/d	8.1	55.6	14.3	55.4
40	2	n/d	12.2	55.4	23.4	56.6

n/d: 5(6)-CF not detected.

Published on 16 January 2017. Downloaded by Université de Strasbourg, Service Commun de la Documentation on 03/02/2017 03:53:38.

droplet of the w1 aqueous phase by the creation of a hydrogel. The synthesized crosslinked polymer chains are sufficiently closely packed to prevent the leakage of at least half of the CF during the low-energy emulsification, but this reaches its limit when the probe concentration is increased. These results are relatively important since they provide evidence of the efficient encapsulation of hydrophilic molecules within nanoemulsion droplets. Moreover, these results prove that the nanodispersion we obtained is compatible with the structure of a double nano-emulsion with aqueous inner compartments, which is the first time that this has been achieved with a two-step formulation method.

Microscopic characterization

We have shown above that the supposed double nanoemulsions are able to encapsulate a small hydrophilic molecule (CF) with an efficiency that varies according to the formulation conditions. The objective of this section is to perform further characteriza-tion that will confirm the w1/O/W2 double structure of these nanoparticles through fluorescence microscopy. To this end, the aqueous phase contained CF, as in the above experiments, and the oil phase was formulated with a lipophilic dye, CY5LP, a lipophilic form of cyanine 5, which was stabilized by lipophilic counter ions.[39] The results are shown in Fig. 3.

On the one hand, control experiments were performed with formulations containing only one dye, either CF or CY5LP, in order to show that the two signals do not overlap (Fig. 3, left). On the other hand, the same acquisition was performed on double nanoemulsions containing both dyes with two different formulations having SOR values of 40% and 20%. The control experiments appeared very clear and the two emission spectra were sufficiently separated to allow differentiation between the two dyes. Regarding double nanoemulsions containing both drugs, the aim of this experiment was to show the co-localization of the green and red signals in order to corroborate the double structure. In Fig. 3, most of the visible nanodroplets appear to effectively nanoencapsulate both CF and CY5LP. However, to understand the picture, one has to remember that (i) acquisitions were performed in a liquid environment, which can potentially allow mobility of the droplets between the two acquisitions, and (ii) the droplet population presents a log-normal distribu-tion with both very large droplets (high brightness) and very small ones (cloudy, diffuse signal). Intermediate-sized droplets were still visible and were probably subject to move-ment in the liquid medium while larger droplets appeared to stick to the support. These results confirm that hydrophilic molecules encapsulated in the inner aqueous core of the nanoparticles are generally co-localized with lipophilic mole-cules, which is additional evidence confirming the double structure of the nanoemulsions.

Cryo-TEM microscopy was finally conducted on w1(p.)/O/W2 dialyzed samples to observe the double structure of the nanoemulsions. The results are shown in Fig. 4; the core shell structures are seen here with widths ranging from 10 nm up to 300 nm (black arrow). The inner parts of the objects present a low contrast due to the presence of water. In the background, many small objects are seen (white arrow). The latter could correspond to polymer particles without a core. The arrowheads correspond to the lacey carbon film. The picture clearly reveals a core–shell structure that is evidence of the presence of two different compositions on the same droplet, segregated in two different locations. The core/shell structure also indicates that the inner aqueous droplets underwent a potential agglomeration, such as flocculation/coalescence in the center of the double droplet. These observations appear to be of importance and corroborate the different hypotheses ventured above on the structure of the double nanodroplets.

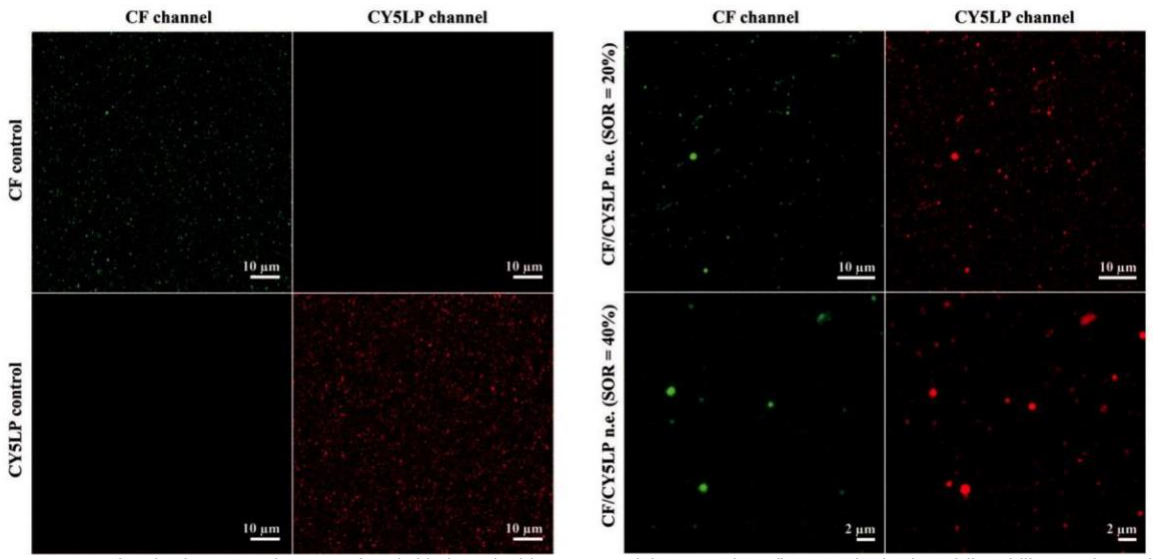

Fig. 3 Fluorescence confocal microscopy images of w1(p.)/O/W2 double nanoemulsions. Carboxyfluorescein (CF) and lipophilic cyanine 5 (CY5LP) are used as hydrophilic and lipophilic model dyes, respectively. The CF control is double nanoemulsions containing only CF in the aqueous core, and the CY5LP control is a nanoemulsion containing only CY5LP in the oil phase.

 This journal is © The Royal Society of Chemistry 2017

Published on 16 January 2017. Downloaded by Université de Strasbourg, Service Commun de la Documentation on 03/02/2017 03:53:38.

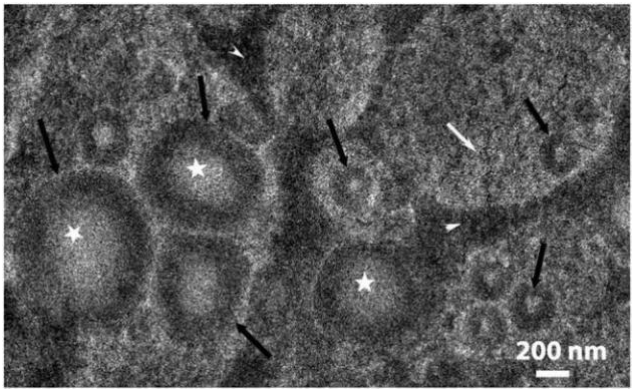

Fig. 4 Image of the double emulsion solutions after cryo preparation. Samples of w1(p.)/O/W2 double nanoemulsions were synthesized by formulation of the primary emulsions in entry 2 Table 2, and the SOR was fixed at 30 wt%. Cryo-TEM microscopy was finally conducted on w1(p.)/O/W2 dialyzed samples to observe the double structure of the nanoemulsions. The core shell structures are seen with widths ranging from 10 nm up to 300 nm (black arrow). The inner parts of the objects present a low contrast due to the presence of water (indicated by the white star). In the back-ground, many small objects are seen (white arrow). The latter could correspond to polymer particles without a core. The arrowheads corre-spond to the lacey carbon film.

Conclusion

The objective of this work was to create a double emulsion at the nanometric scale by a two-step process. The first primary nanoemulsion, the so-called reverse nanoemulsion, w1/O, was challenging to formulate and was achieved with a high-pressure homogenizer (Microfluidizer^{S}). The formulations of reverse nanoemulsions were shown to be mainly related to the composition of the system, namely to the concentration of the low-HLB surfactant (PGPR), which was soluble in oil (medium-chain triglyceride), and the quantity of maltodextrin in the aqueous phase, which impacted on the viscosity of the dispersed phase. We disclosed that a combination of $[PGPR]_{oil}$ 4 7% and $[MD]_{water}$ 4 50% is necessary to decrease the droplet size to below 100 nm, and a combination of $[PGPR]_{oil}$ 4 12% and $[MD]_{water}$ 4 50% reduces the size to below 50 nm. The second step of the process was the low-energy emulsification of this primary nanoemulsion, which gave rise to the double nanoemulsion, w1/O/W2, and this was characterized by the leakage of a small encapsulated hydro-philic molecule (CF). The results showed that the encapsula-tion efficiency (EE) can differ considerably depending on the formulation parameters, as with the final size of the double droplets (reducing the EE) or the polymerization of the inner aqueous phase (increasing the EE up to ca. 58%). Further cryo-TEM and fluorescence microscopy have been conducted on the most efficient formulations and these results corroborate the potential double structure, w1/O/W2. We can conclude that developing a formulation for a double nanoemulsion by a two-step approach is a significant challenge; this was pioneered by this work, which has opened the door to numerous formula-tions and applications.

Acknowledgements

The authors want to thank Dr Marc Schmutz for fruitful discussion. The EM facility of ICS is acknowledged for use of the instruments.

References

1 W. Seifriz, J. Phys. Chem., 1924, 29, 10.
2 G. J. Sperandio, J. Pharm. Sci., 1969, 54, 1227.
3 D.-S. Mahrhauser, C. Fischer and C. Valenta, Int. J. Pharm., 2016, 498, 130–133.
4 A. J. Garber, Arch. Intern. Med., 2003, 163, 1781–1782.
5 D. Lane, Nat. Biotechnol., 2006, 24, 163–164.
6 J. a. Kemp, M. S. Shim, C. Y. Heo and Y. J. Kwon, Adv. Drug Delivery Rev., 2016, 98, 3–18.
7 B. Rubinfeld, A. Upadhyay, S. L. Clark, S. E. Fong, V. Smith, H. Koeppen, S. Ross and P. Polakis, Nat. Biotechnol., 2006, 24, 205–209.
8 H. Gu, R. Zheng, X. Zhang and B. Xu, J. Am. Chem. Soc., 2004, 126, 5664–5665.
9 S. Santra, P. Zhang, K. Wang, R. Tapec and W. Tan, Anal. Chem., 2001, 73, 4988–4993.
10 A. Burns, H. Ow and U. Wiesner, Chem. Soc. Rev., 2006, 35, 1028–1042.
11 S.-H. Wu, Y. Hung and C.-Y. Mou, Chem. Mater., 2013, 25, 352–364.
12 C. Allen, D. Maysinger and A. Eisenberg, Colloids Surf., B, 1999, 16, 3–27.
13 R. H. Engel, S. J. Riggi and M. J. Fahrenbach, Nature, 1968, 219, 2.
14 A. J. Khopade, K. S. Nandakumar and N. K. Jainb, J. Drug Targeting, 1998, 6, 285–292.
15 R. Vermaj and T. N. Jaiswal, Vaccine, 1997, 15, 7.
16 A. T. Florence and D. Whitehill, Macro- and Microemulsions, American Chemical Society, 1985, ch. 23, vol. 272, pp. 359–380.
17 H. P. R. S. S. Davis and T. S. Purewal, J. Colloid Interface Sci., 1981, 80, 4.
18 M. F. Zambaux, F. Bonneaux, R. Gref, P. Maincent, E. Dellacherie, M. J. Alonso, P. Labrude and C. Vigneron, J. Controlled Release, 1998, 50, 31–40.
19 C. B. C. Jarrod, A. Hanson, S. M. Graves, Z. Li, T. G. Mason and T. J. Deming, Nature, 2008, 455, 5.
20 S. Y. Tang, M. Sivakumar, A. M.-H. Ng and P. Shridharan, Int. J. Pharm., 2012, 430, 299–306.
21 W. Seifriz, J. Phys. Chem., 1925, 29, 14.
22 M.-F. Ficheux, L. Bonakdar, F. Leal-Calderon and J. Bibette, Langmuir, 1998, 14, 5.
23 S. Matsumoto, Y. Kita and D. Yonezawa, J. Colloid Interface Sci., 1976, 57, 353–361.
24 N. Anton, J.-P. Benoit and P. Saulnier, J. Controlled Release, 2008, 128, 15.
25 N. Anton and T. F. Vandamme, Int. J. Pharm., 2009, 377, 6.
26 J. S. Komaiko and D. J. McClements, Compr. Rev. Food Sci. Food Saf., 2016, 15, 331–352.

Published on 16 January 2017. Downloaded by Université de Strasbourg, Service Commun de la Documentation on 03/02/2017 03:53:38.

27 R. Shay, in Source Book of Flavors, ed. G. Reineccius, Springer-Science+Business Media, 1994, ch. 11, p. 68.
28 S. M. Jafari, Y. He and B. Bhandari, Int. J. Food Prop., 2006, 9, 11.
29 Y.-F. Maa and C. C. Hsu, Pharm. Dev. Technol., 1999, 4, 8.
30 T. F. Vandamme and N. Anton, Int. J. Nanomed., 2010, 5, 7.
31 C. A. Miller, Colloids Surf., 1988, 29, 14.
32 A. Perazzo, V. Preziosi and S. Guido, Adv. Colloid Interface Sci., 2015, 222, 581–599.
33 S. Sajjadi, M. Zerfa and B. W. Brooks, Chem. Eng. Sci., 2002, 57, 663.
34 T. Ohtake, T. Hano, K. Takagi and F. Nakashio, J. Chem. Eng. Jpn., 1987, 20, 443.
35 G. I. Taylor, Proceedings of the Royal Society of London, Series A, Containing Papers of a Mathematical and Physical Character, 1934, vol. 145, p. 36.
36 J. K. Klahn, J. J. M. Janssen, G. E. J. Vaessen, R. de Swart and W. G. M. Agterof, Colloids Surf., A, 2002, 210, 167.
37 X. Li, N. Anton, G. Zuber, M. Zhao, N. Messaddeq, F. Hallouard, H. Fessi and T. F. Vandamme, Biomaterials, 2013, 34, 481–491.
38 F. Hallouard, S. Briançon, N. Anton, X. Li, T. Vandamme and H. Fessi, Eur. J. Pharm. Biopharm., 2013, 83, 54–62.
39 V. N. Kilin, H. Anton, N. Anton, E. Steed, J. Vermot, T. F. Vandamme, Y. Mely and A. S. Klymchenko, Biomaterials, 2014, 35, 4950–4957.
40 H. Schubert and H. Armbruster, Chem. Ing. Tech., 1989, 61, 701–711.
41 M. F. Attia, N. Anton, R. Akasov, M. Chiper, E. Markvicheva and T. F. Vandamme, Pharm. Res., 2015, 33, 12.
42 A. T. Florence and D. Whitehill, J. Pharm. Pharmacol., 1980, 32, 64.

CHAPTER 3

Toward the Formulation of Stable Micro and Nano Double Emulsions through a Silica Coating on Internal Water Droplets

LANGMUIR

Article

Cite This: Langmuir 2019, 35, 2313−2325 pubs.acs.org/Langmuir

Toward the Formulation of Stable Micro and Nano Double Emulsions through a Silica Coating on Internal Water Droplets

Salman Akram,[†] Xinyue Wang,[†] Thierry F. Vandamme,[†] Mayeul Collot,[‡] Asad Ur Rehman,[†] Nadia Messaddeq,[‡] Yves Mely,[§] and Nicolas Anton*[,†]

[†]CNRS, CAMB UMR 7199, [‡]CNRS, LBP UMR 7021, and [§]IGBMC, Inserm U964, CNRS UMR7104, Universite de Strasbourg, F-67000 Strasbourg, France

ABSTRACT: Delivery systems able to coencapsulate both hydrophilic and hydrophobic species are of great interest in both fundamental research and industrial applications. Water-in-oil-in-water (w1/O/W2) emulsions are interesting systems for this purpose, but they suffer from limited stability. In this study, we propose an innovative approach to stabilize double emulsions by the synthesis of a silica membrane at the water/oil interface of the primary emulsion (i.e., inner w1/O emulsion). This approach allows the formulation of stable double emulsions through a two-step process, enabling high encapsulation efficiencies of model hydrophilic dyes encapsulated in the internal droplets. This approach also decreases the scale of the double droplets up to the nanoscale, which is not possible without silica stabilization. Different formulation and processing parameters were explored in order to optimize the methodology. Physicochemical characterization was performed by dynamic light scattering, encapsulation efficiency measurements, release profiles, and optical and transmission electron microscopies.

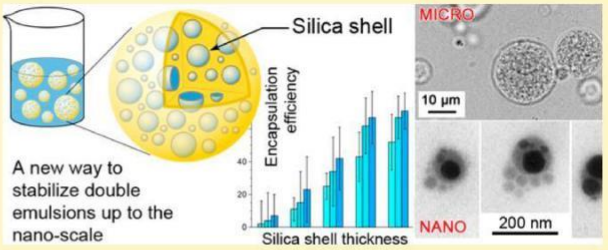

INTRODUCTION

Scientific challenges in the fields of agrofoods and cosmetic or pharmaceutical sciences have often found innovative solutions in the form of optimized delivery systems. With the unique properties to encapsulate hydrophilic molecules in lipid emulsions, the double emulsions have gained an important place in this research.[1] In the field of pharmaceuticals, double emulsions can be used as oral delivery systems for vaccines, drugs, and plant bioactives,[2,3] while in the food industry they can be used as carriers for probiotics, vitamins, seasoning agents, and extracts.[4−8] In the field of nanomedicine, nanoscale double emulsions could solve important challenges, like the targeted delivery of hydrophilic molecules.

When aiming for a globule dispersion in the aqueous continuous phase (e.g., in most pharmaceutical formulations), double emulsions are formulated to be in the water-in-oil-in-water type (w/O/W). These systems can be made through either a single-step[9,10] or a two-step process.[11,12] In the one-step method, internal and external water phases have the same composition. Moreover, this method may require an additional step of bulk purification (e.g., through a desalination column in the case of nanosized carriers). This method is not optimized for the encapsulation of high-added-value active compounds and for obtaining high encapsulation efficiencies. On the contrary, in the two-step processes (which we followed), the internal water may be different from the external water, which makes them more suited for optimizing the encapsulation efficiency.[13−15]

The primary w1/O emulsion must be very small, preferably a nanoemulsion stabilized by a low HLB surfactant. Reverse emulsion is generally obtained by a high-energy method, using a high-pressure homogenizer or ultrasound. For the second emulsification, several approaches can be used, but a low-energy method may be privileged in order to prevent the premature release of the hydrophilic material solubilized in the internal water droplets. Indeed, high-energy methods can destroy the primary emulsion, giving rise to simple O/W emulsions.[16]

For many years, double emulsions have been considered to be an emerging technology with high potential and high interest. Therefore, a huge research effort was undertaken to optimize double emulsions for industrial applications and scale-up. However, to date, only a few products based on these emulsions are on the market.[4] The main issue is that their limited stability (i.e., formulating robust double emulsions able to conserve its specifications with respect to storage time, appearance, texture, and taste) involves long-term physical and chemical stability. This stability is very difficult to control in double emulsions due to the difference in osmotic pressure between the inner and outer water phases that should be equalized, and the difference in Laplace hydrodynamic pressure that tends to vanish with time and modify the morphology of the double structure. These equilibration phenomena are also favored by the surfactants used for the first emulsification, which destabilize the thin liquid films between internal water droplets. As a result, the stability

Received: November 22, 2018
Revised: January 8, 2019
Published: January 10, 2019

ACS Publications © 2019 American Chemical Society

DOI: 10.1021/acs.langmuir.8b03919
Langmuir 2019, 35, 2313−2325

equation is complex and highly challenging. At this point, using a nanoemulsion as a primary w1/O emulsion can be an interesting option as a result of the strong stability of the nanodroplets.

On the other hand, stable double emulsions of nanometric size (<200 nm) are difficult to obtain because the second nanoemulsification process is very drastic in this case and the reduced dimensions of the oil film between internal droplets and the bulk can facilitate water transfer. Reducing the scale of the double emulsions should allow the nanoencapsulation of hydrophilic and lipophilic species in a single particle, compatible with parenteral and i.v. administration. For example, such a coencapsulation of drugs is critical for optimizing targeted therapies by the simultaneous codelivery of anticancer species with another complementary cytotoxic molecule, anti-inflammatory agent, or adjuvant. Double-emulsion formulations at the nanoscale have already been reported,[12−15,17,18] but always by turning one of the liquid phase (i.e., internal water or oil) into a polymerized matrix. Herein, we present for the first time a liquid/liquid/liquid system keeping all advantages of double emulsions in terms of encapsulation and release properties, along with the advantages of nanoemulsions that allow homogeneous dispersion and compatibility with parenteral administration and targeted drug delivery.

In this context, the objective of the present study was to understand the formation of double emulsions obtained with a reverse nanoemulsion as a primary w1/O emulsion and to explore how to improve their stability, keeping the liquid/ liquid/liquid morphology even on the nanoscale. To improve the double emulsion stability, the internal water/oil interface was reinforced by a silica-based membrane synthesized in situ.[19−28] It is noteworthy that silica material as well as silica nanomaterials are, in general, widely used in biomedical applications because they are considered to be biocompatible and safe.[29−31] In the first part, micrometric-scale double emulsions were formulated to understand the impact of the formulation parameters on the integrity of the droplets, as monitored by the encapsulation efficiency and leakage of a water-soluble dye (methylene blue). The second part of the study aimed to transpose the optimized formulation to the nanoscale, by modifying the secondary emulsification. Double nanoemulsions were characterized by dynamic light scattering (DLS) and transmission electron microscopy (TEM) as well as by measuring the encapsulation efficiencies (EE) and release profile of hydrophilic model species encapsulated in the internal aqueous droplets.

EXPERIMENTAL SECTION

Materials. Oil compatible with parenteral administration (Labrafac WL 1349) was obtained from GattefosséS.A., Saint-Priest, France. This is a mixture of capric and caprylic acids that we used throughout this study as the oil phase and thus as continuous phase in the primary w1/O nanoemulsion. Polyglycerol polyricinoleate (PGPR) was kindly gifted by Stearinerié Dubois (Boulogne-Billancourt, France), and served as a lipophilic surfactant (HLB around 1.5) for the preparation of a primary w1/O nanoemulsion. This emulsifier is largely used for human consumption, being approved for food formulation by the FDA (Food and Drug Administration) and the JECFA (Joint FAO/WHO Expert Committee on Food Additives). Kolliphor ELP (BASF, Ludwig-shafen, Germany) is a hydrophilic nonionic surfactant (HLB around 13) compatible with parenteral administration that was used as a hydrophilic surfactant for the second emulsification step in the formulation of double droplets. Methylene blue, tetra ethyl orthosilicate (TEOS), (3-aminopropyl) triethoxysilane (APTES), and sulforhodamine 101 were purchased from Sigma (St. Louis, MO, USA).

Methods. Formation of a Primary w1/O Nanoemulsion. The oil phase (4.8 g) consists of Labrafac WL 1349 containing PGPR (from 1 to 35 wt %) and the silica precursor (the quantity of TEOS ranging from 5 to 25 wt % or the quantity of APTES ranging from 2.5 to 10 wt %).

The oil phase was mixed with the aqueous phase w1 (1.2 g) made of distilled water containing $CaCl_2$ (5 wt %). This mixture was first vortex mixed for 1 min and then adjusted at 50 °C with gentle mixing at 100 rpm in a ThermoMixer C (Eppendorf) for 5 min. This choice of 50 °C simply comes from the experiment: compared to a similar experiment at room temperature, stirring the premix at 50 °C before the stage of nanoemulsification by ultrasonication is highly beneficial to the properties of the resulting dispersion. The size distribution is thinner, and the sample homogeneity and stability are improved. The reason could be linked to the modification of the phase viscosities lowered at higher temperature, impacting the phase viscosities ratio and thus impacting the critical Weber number (We_c) (cf., the classical so-called Grace curve). As a result, viscous forces may prevail over capillary forces, and the droplet fractionation is increased. Next, this coarse dispersion was nanoemulsified by ultrasonication (Bio block 75043, Sonics Materials, Newtown, MA, USA) operating at 400 W, 20 kHz, 3 mm sonotrode with total operating times of 5 to 20 min (cycles of 30 s carried out in a succession of 10 s of sonication and 20 s off).

Preparation of the Micrometric Double Emulsions w1/O/W2. The w1/O/W2 double emulsions of micrometric size were prepared by mixing the aqueous phase W2 (4.8 g) made of distilled water and Kolliphor ELP solubilized at concentrations ranging from 15 to 25 wt % with the primary emulsion w1/O (1.2 g) playing the role of the oil phase in the second emulsification. This mixture was vortex mixed for 30 s and emulsified with an UltraTurrax high-speed rotor/stator homogenizer (IKA T25 M Germany) operating at 15 000 rpm for 5 min.

Preparation of Nanometric Double Emulsions w1/O/W2. To formulate double emulsions in the nanometric range, the second emulsification step must be a nanoemulsification process. The oil phase is the primary emulsion w1/O (1.2 g) directly mixed with Kolliphor ELP at different surfactant-to-oil weight ratios (SORs) ranging from 25 to 45%. This mixture was vortex mixed for 30 s, and the second aqueous phase W2 (4.8 g of distilled water) was suddenly added before final vortex mixing (3 min). This immediately generates the double nanoemulsion according to the spontaneous emulsification method.[32−34]

Characterization of Primary Emulsions. All of the characterizations of primary and double emulsions, size, encapsulation efficiency, and release were carried out in triplicate on different formulations.

Hydrodynamic Diameter and PDI. The hydrodynamic diameter, size distribution, and PDI of the primary emulsions were determined by dynamic light scattering (Malvern ZS 90, Malvern Instruments, Orsay, France). Measurements were performed after a suitable dilution of the sample with oil, up to the point where the milky aspect of the sample becomes transparent, allowing the DLS measurement. In the case of primary emulsions, the diluent was exactly the same oil (medium-chain triglycerides, Labrafac WL 1349) used to prepare these primary w1/O nanoemulsions. In the second case, w1/O/W2, dilution was performed only with distilled water. The effect of dilution on the droplet size distributions was checked by different assays at different dilutions, and (data not shown) in both cases, the dilution does not affect the results. Each formulation and measurement was repeated three times.

Encapsulation Efficiency. The encapsulation efficiency of primary emulsions was measured to confirm that the methylene blue dyes are effectively encapsulated in the primary nanoemulsion and can be totally released. The primary emulsion is destabilized by mixing with a large amount of Kolliphor ELP (with a weight ratio of 50:50 with respect to the primary emulsion) and held at 90 °C for 1 h

DOI: 10.1021/acs.langmuir.8b03919
Langmuir 2019, 35, 2313−2325

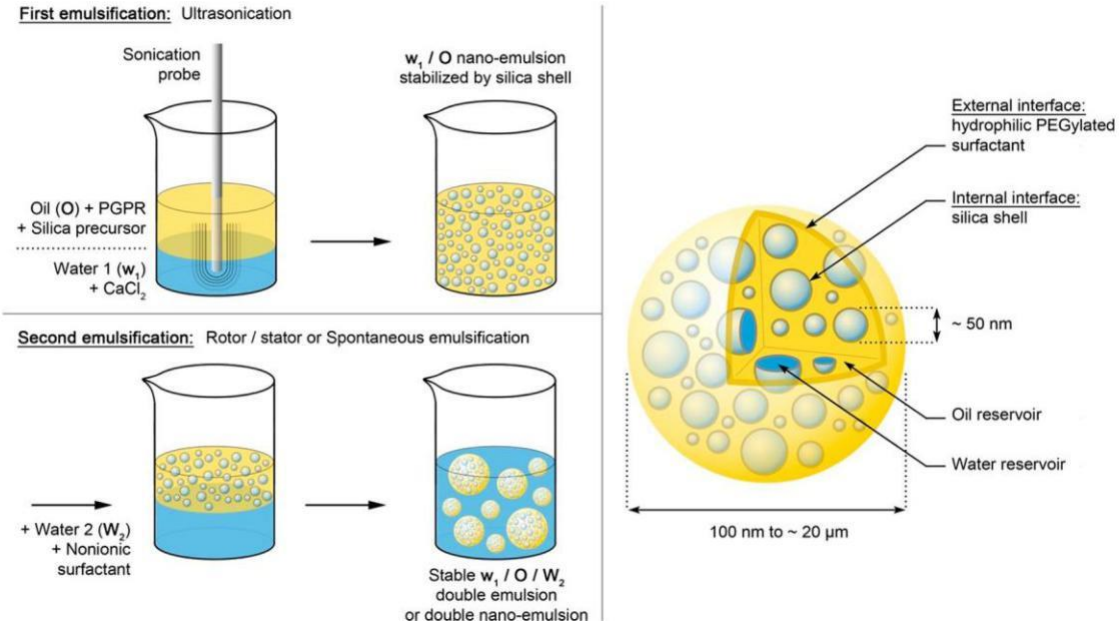

Figure 1. Formulation of the micrometric and nanometric double droplets stabilized by a silica shell. The first emulsification provides the primary reverse nanoemulsion by which the water/oil interface is stabilized by both PGPR and the silica shell. The second emulsification is performed either by a rotor/stator apparatus (Ultraturrax) for micrometric double emulsions or by spontaneous emulsification for double nanoemulsions.

(ThermoMixer C, Eppendorf). Then, the mixture is centrifuged for 30 min at 13 500 rpm to complete the destabilization of the w1/O nanoemulsion and induce a phase separation. This allows the collection of the aqueous phase at the bottom of the tube. The supernatant was removed, and the aqueous phase was washed with dichloromethane three times. Finally, dichloromethane was evaporated, and the methylene blue was dissolved in distilled water and quantified by absorption spectroscopy after a controlled dilution (plate reader Safas Xenius XM). The process was repeated three times, and averages of the encapsulation efficiency were reported as final values.

Characterization of Micrometric Double Emulsions. Optical Microscopy. The micrometric double emulsions were visually characterized by optical microscopy (AXIO Imager.A1, Carl Zeiss, Marly le-Roi, France). Different samples and controls were selected: emulsions without a primary emulsion, double emulsions without silica precursors, and double emulsions with silica precursors at 2.5 and 10 wt % in oil. (See the details in the text below.) A little drop of the suspension was deposited on the glass slide, covered with a coverslip, and observed at a magnification of 40× (recorded with an Axiocam camera). This optical characterization reveals the global morphology of the droplets (evidencing the double structure) and their size distribution through size analysis with ImageJ (done on around 100 droplets).

Encapsulation Efficiency Study. The ability of the double emulsions to encapsulate hydrophilic molecules was evaluated through the encapsulation efficiency (EE) value that was determined by comparing the dye encapsulated in the emulsions with the free dye in the bulk aqueous phase. To this end, 1 mL double emulsion samples were taken in Eppendorf tubes and centrifuged at 13 400 rpm for 30 min. As the size of these double droplets is micrometric, their separation is effective by a simple centrifugation. Bulk water was then collected with a syringe, filtered on 0.45 µm filters, diluted with distilled water, and analyzed by spectrophotometry.

Stability Studies at High Temperature. To evaluate their stability, the micrometric double emulsions were exposed to 90 °C (1 mL samples in Eppendorf tubes set in a boiler). Stability was assessed by following the EE loss for 30 min and 1 h, as described above.

Characterization of Nanometric Double Emulsions. Physicochemical Characterization. The hydrodynamic diameter and PDI were determined by dynamic light scattering (NanoZS, Malvern), as described above. In transmission electron microscopy, the double structure of the double emulsion shows a good contrast mainly because the silica capsules and the oil have two distinct electron attenuations and thus a distinct contrast. Samples were used without any staining agent and were diluted (1/10) with Milli-Q water. A drop of suspension was placed on a carbon grid (carbon type-A, 300 mesh, copper, Ted Pella Inc. Redding, PA, USA) and dried at 60 °C for 30 min. Observations were carried out using a Philips Morgagni 268D electron microscope operating at 70 kV. It is noteworthy that the operating conditions we used (70 kV) are very low compared to TEM experimental conditions generally followed in material science (e.g., 200 kV). This was chosen to minimally affect the samples.

Encapsulation Efficiency. As described above for micrometric double emulsions, EE values were determined by quantifying the dye concentration in the external bulk phase. However, as centrifugation is not efficient for separating such nanodroplets, they were separated from free dyes by size exclusion chromatography using a desalting column (PD-10 Sephadex G-25 M, GE Healthcare). One milliliter of sample was introduced into the prepacked column and then eluted using distilled water. (About 30 mL of distilled water was first introduced into the column for equilibration.) The elution showed that double nanodroplets came first and then a clear boundary was observed, finally eluting free dye. The free dye fractions were quantified by spectrophotometry. Each formulation and measurement was repeated three times.

Dye Release Studies. The release studies were performed by dialysis. One milliliter of sample was introduced into a dialysis tube (Spectrum Laboratories, 12−14 kDa) and dialyzed against distilled water at 37 °C, under gentle stirring at 500 rpm, in a volume of 500 mL. The samples were collected after 0.5, 1, 2, 4, and 6 h. EE values were determined by separating and quantifying free dyes (by spectrophotometry) and expressed as cumulative release as a function of time.

Spectroscopy. Emission spectra were recorded on a FluoroMax-4 spectrofluorometer (Horiba Jobin Yvon) equipped with a thermo-stated cell compartment. For the standard recording of fluorescence spectra, the emission was collected 10 nm after the excitation wavelength. All of the spectra were corrected from the wavelength-dependent response of the detector. Fluorescent behavior of SR101, in Milli-Q water, was recorded as a function of its concentration (data not shown) and exhibited linear behavior up to 10−20 µM, which was then attenuated at higher concentrations due to a partial quenching of

DOI: 10.1021/acs.langmuir.8b03919
Langmuir 2019, 35, 2313−2325

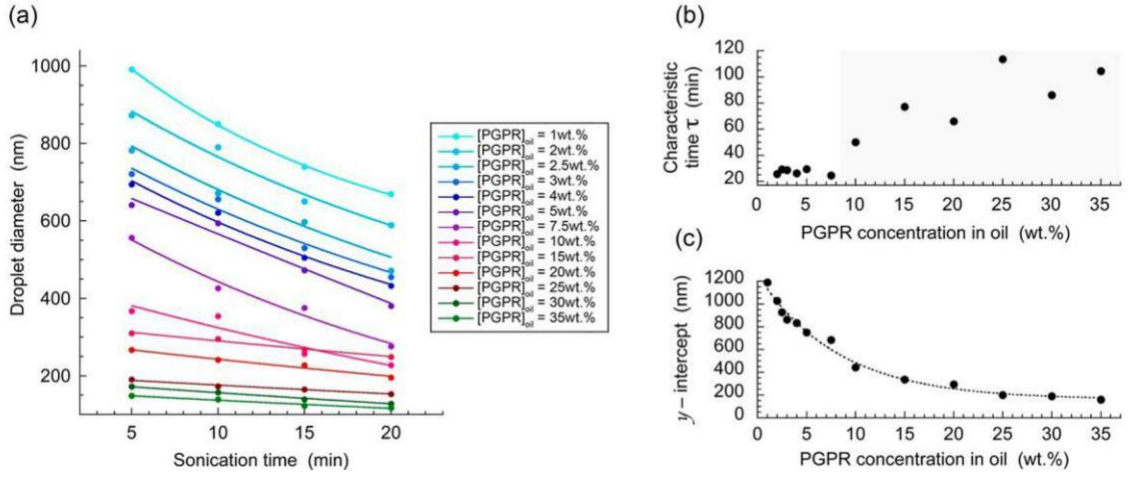

Figure 2. Dependence of the size of w1/O nanoemulsion as a function of time and concentration of surfactant (PGPR) in oil. (a) The curves of the dependence of the size of the w1/O nanoemulsion (ϕ^{water}_{V} = 20%) as a function of the sonication time were fitted by an exponential model (details in the text). (b) Characteristic time and (c) y intercept from the curve fits of (a) vs surfactant concentration.

SR101 induced by an ACQ (aggregation-caused quenching) effect. SR101 is included in the inner water at high concentration (100 μM in w1) to ensure the dye detectability for the different formulation stages that involve its dilution. On the other hand, to prove that SR101 is not soluble in oil, it was dispersed in Labrafac WL 1349 as follows: 2.3 mg of SR101 was mixed in 500 μL of Labrafac WL 1349, held at 60 °C for 1 h, and then slightly centrifugated to remove nondispersed crystals, collecting the supernatant for fluorescent measurement. Fluorescent spectra were recorded in triplicate on three different formulations, reporting the mean spectra in the figure.

RESULTS AND DISCUSSION

The great interest in double emulsions, even today, remains undeniable, probably due to the lack of appropriate solutions for encapsulating hydrophilic materials or for coencapsulating hydrophilic and lipophilic materials. However, because the double emulsions are of limited stability, the present study proposes a simple modification of the conventional two-step preparation process used to stabilize them by reinforcing the w1/O interface with a small silica membrane. This innovative methodology makes it possible not only to create stable micrometric double emulsions (of about 10 μm) but also to formulate double nanodroplets of <130 nm in diameter. The formulation process and the structure of the formulated double droplets are described in Figure 1.

For the formulation of the first emulsion, the oil phase, contains a lipophilic surfactant and a silica precursor. The energy supplied by the sonication process has two roles: (i) it allows the creation of the nanodroplets and (ii) it induces the polycondensation of the silica precursor[19−22,35] specifically at the water/oil interface. As a result, this first process produces aqueous nanodroplets in the form of silica nanocapsules.[36,37] Next, this primary emulsion is used as the oil phase for a second emulsification process in order to generate micrometric double droplets by using a mechanical method (rotor/stator, Ultraturrax), or nanometric double droplets by spontaneous emulsification.[32,38] In the following sections, we will investigate in depth the formulation of the primary emulsion and analyze the impact of the formulation parameters on its properties, and then we will characterize the macroscale and nanoscale double emulsions.

Primary w1/O Nanoemulsions and Silica Nanocapsules. The singularity of the nanoemulsification process based on ultrasonication lies in the amount of energy focused on a small volume. The high acoustic field leads to the gradual growth of cavitation bubbles, up to their implosion. This induces huge shearing forces that break up the aqueous droplets into smaller ones that are stabilized by the surfactants (PGPR). The average droplet size decreases as a function of the quantity of energy supplied.

To prevent the destruction of the double droplets during and after the second emulsification, the original approach proposed in this study resides in the stabilization of the water/ oil interface of the primary droplets by a silica membrane synthesized in situ to preserve the aqueous droplets and their encapsulation properties. On the basis of previous work,[19−22] the silica precursors were introduced into the oil phase, and the interfacial polycondensation was initiated through a sono-chemistry-mediated reaction. Two different silica precursors, TEOS and APTES, were studied. The growth of the silica chains occurs by the simultaneous presence of water and precursors solubilized in oil, and the silica shell is therefore formed and trapped at the water/oil interface.

Reverse Nanoemulsification. In this section, we will focus on the emulsification itself without silica and investigate the influence of the surfactant concentration and processing time on the size and polydispersity of the primary w1/O nanoemulsions. By monitoring the impact of the sonication time for different PGPR concentrations (ϕ^{water}_{V} = 20%), we observed, as expected,[39−42] a decrease in the droplet size (Figure 2a) according to a monoexponential decay $d = A\,e^{(-t/\tau)} + d\infty$ where d is the droplet diameter, A is a constant, $d\infty$ is the saturation diameter (diameter after stabilization of the monoexponential function), t is the sonication time, and τ is the characteristic time of the exponential. The choice of this monoexponential model was based on the literature, considered to be the more accurate description of the droplet size decrease, as a consequence of the droplet fractionation induced by ultrasonication.[39] The droplet fractionation directly results from the amount of energy supplied and gradually stabilizes up to a saturation size $d\infty$. The droplet size is clearly dependent on the surfactant concentration, with a decrease by about 800 nm between 1 and 35 wt %. Reporting the values of the characteristic time τ as a function of the sonication time (Figure 2b) revealed that the

DOI: 10.1021/acs.langmuir.8b03919
Langmuir 2019, 35, 2313−2325

time necessary to stabilize the droplet size showed first (up to 7.5 wt %) a plateau giving $\tau \approx 30$ min, indicating that the nanodroplets are rapidly stabilized independently of the PGPR concentration.[38,43,44] Then, a second regime appears (from 10 wt %) in which the τ values are much higher and gradually increase up to 100 min. This regime likely corresponds to a saturation regime in which the droplets are rapidly stabilized after their formation, followed by a further evolution of the size much more slowly. The threshold of 10 wt % PGPR is believed to correspond to the saturation regime that allows very small sizes to be achieved. When extrapolating the curve fits at $t = 0$ (Figure 2c), the sizes also show a stabilization for PGPR concentrations higher than 10−15 wt %. The y intercept reported in Figure 2c is an interesting parameter reflecting the whole behavior of the emulsification process, thus allowing a comparison between the different PGPR concentrations.

To formulate reverse nanoemulsions below 300 nm, our data pointed out that a PGPR concentration in oil of at least 10 wt % is required. However, a sonication time of 20 min is too long for a potential industrial application because it may destroy the encapsulated materials, increase the sample temperature, and release a large number of titanium nanoparticles from the sonication tip. An ideal sonication time should be no more than 5 min. In addition, to obtain double nanoemulsions based on this primary emulsion, the droplet size should be ideally decreased to 100 nm or less.[45,46]

Accordingly, the sonication time was fixed to 5 min, and the PGPR concentration was varied from 10 to 35 wt %. The results reported in Figure 3 confirmed the trend revealed in Figure 2, with a significant size decrease as a function of the surfactant concentration. At $[PGPR]_{oil} > 25$ wt %, sizes below 160 nm were observed. However, the variability of the results was quite high, likely related to the polydispersity of the nanoemulsions because PDI values ranged from 0.3 to 0.5 for all measurements with pure water as[44,47] reported in Figure 3. In line with previous reports showing that the emulsifying properties of PGPR can be improved when calcium chloride is added to the aqueous phase, the emulsification process was clearly more efficient in the presence of this additive (Figure 3, open symbols), providing droplets below 100 nm for [PGPR] ≥ 10 wt % and down to 50 nm for [PGPR] ≥ 30 wt %. Moreover, calcium chloride also improves the homogeneity and reproducibility (standard deviations are between 3 and 10 nm) of the results as well as the monodispersity (PDI values are equal to 0.16 ± 0.10 for [PGPR] = 10 wt % and to (0.06 ± 0.05) for [PGPR] ≥ 25 wt %).

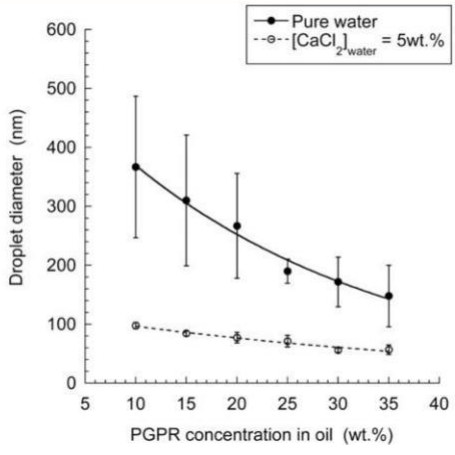

Figure 3. Effect of the PGPR concentration on the size of w1/O nanoemulsions at a fixed sonication time of 5 min and $\phi^{water}_V = 20\%$. The experiments were done with pure distilled water as the aqueous phase (pure water) and water-containing calcium chloride as an additive ($[CaCl_2]_{water} = 5$ wt %) ($n = 3$). Lines are drawn to guide the eye.

The strong effect of $CaCl_2$ on the emulsification process may be a consequence of the modification of PGPR activity. Indeed, $CaCl_2$ is a chaotropic salt[48] that affects the hydrogen bonding between the water and the PGPR molecules. As a result, the lipophilicity of the emulsifier may be increased and its HLB may be lowered. In addition, $CaCl_2$ can also directly affect the interfacial tension and improve the emulsification properties.[44,47,49] In these articles, the authors have shown that the addition of $CaCl_2$ to water can decrease the droplet size and improve the stability of the primary w1/O emulsion. This was explained by a specific action on the hydrophilic part of amphiphile-like PGPR through an increase in the surfactants' adsorption density, giving rise to decreasing interfacial tension along increasing interfacial elasticity and involving a reduction in the attractive forces between water droplets after their formation. Finally, all of these effects combined can strongly impact the emulsification process, lowering the rate of droplet recombination during sonication and thus decreasing the size, polydispersity, and variability of the results (i.e., lowering the standard deviation as it is presented in Figure 3). To conclude, in view of these results, the formulation with $[PGPR]_{oil} = 30$ wt % (giving a droplet size of (57 ± 4) nm and a PDI value equal to 0.06) was selected as the primary emulsion for the fabrication of the double emulsions.

Silica Nanocapsules. As described above, the silica shell is built at the water/oil interface of the reverse nanoemulsions through sonochemistry.[19−22,35] Two different silica precursors (TEOS and APTES) were solubilized in the oil phase. The silica precursors hydrolyze first and then undergo the condensation process. The hydrolysis of APTES and TEOS leads to the production of ethanol and trisilanols. The Si−C bond will not be hydrolyzed because this bond is hydrolytically stable, and thus the aminopropyl group will stay in the polymer structure. On the other hand, the transient silanol groups will condense with other silanols to produce the amino-function-alized network. Interestingly, the impact on the double emulsion of the alcohol formed during the chemical reaction cannot be specifically determined but will be included in the global determination of the encapsulation efficiency values, along with the other formulation and processing parameters. The emulsification process was performed under the same conditions as described above: $\phi^{water}_V = 20\%$, sonication time = 5 min, and $[PGPR]_{oil} = 30$ wt %. The sizes of the reverse nanodroplets (Figure 4) were compared for the APTES and TEOS precursors.

In both cases, the introduction of the silica precursor in oil before sonication increases the size of the water droplets, likely due to the formation of a silica shell around the droplets. Moreover, in both cases, the shell thickness is linearly related to the concentration of silica precursor in oil. Nevertheless, the slopes are different because, probably, part of the silica remains in the oil or has been expelled in water. It is important to note that we cannot prove that the water droplets do not increase when the amount of silica precursor is increased. However, we have thus assumed that because the formulation parameters were fixed ($\phi^{water}_V = 20\%$, sonication time = 5 min, $[PGPR]_{oil}$ =

DOI: 10.1021/acs.langmuir.8b03919
Langmuir 2019, 35, 2313−2325

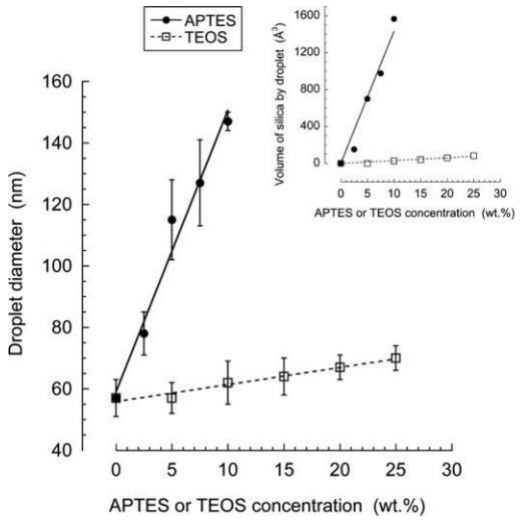

Figure 4. Effect of the concentration of the silica precursor (APTES or TEOS) on the size of the primary w1/O nanoemulsion (n = 3). (Inset) Dependence as a function of the silica precursor of the volume of the nanodroplets, calculated from their diameter.

30 wt %), the size of the water droplet core is considered to be constant and the silica shell gradually grows around it. In addition, the fact that the relationship between droplet size and silica precursor concentration is linear supports the assumption that the size of the water cavities should be the size of the initial aqueous droplets without silica (around 60 nm in the example shown in Figure 4), and the silica shells grow around it.

However, APTES appears to be much more efficient than TEOS for interfacial polycondensation. For example, at a concentration of 10 wt %, TEOS induced a shell thickness of about 3 nm, while it reached about 45 nm with APTES. On the basis of these data, the global volume of the silica shell can be estimated as a function of the precursor concentration (Figure 4, inset). The comparison of the growth rates (slopes of the linear fits, 3.0 and 143.2 $Å^3$ wt $\%^{-1}$ for TEOS and APTES, respectively) indicates that 50 times more material is synthesized at the interface with APTES than with TEOS.

The silica shell thus appears to be important in stabilizing the primary emulsion in order to formulate the double droplets, and these results demonstrated the feasibility of the in situ synthesis of the silica shell in the water/oil interface of the droplets. The linear relationship between the shell thickness and the concentration of the silica precursor indicates that the shell thickness can be adjusted very finely and thus controls the encapsulation and release properties of the double emulsions. The reason that APTES is more efficient than TEOS in the polycondensation process may be related to its chemical structure.[50] Unlike TEOS, the amphiphilic properties of APTES likely play an active role in their concentration at the water/oil interface. Indeed, because the pKa of APTES, $(CH_3{-}CH_2{-}O)_3{-}Si{-}(CH_2)_3{-}NH_2$, is around 8.5, and the aqueous phase containing $CaCl_2$ has a pH slightly below 7, the protonation of the amino function probably accelerates the migration of APTES (from oil) toward the interface, increasing the efficiency of the ultrasound-mediated interfacial polycondensation. In contrast, TEOS, lacking such a function, $(CH_3{-}CH_2{-}O)_4{-}Si$, may encounter the interface only because of molecular diffusion.

Micrometric Double Emulsions w1/O/W2. To prove that double droplets are stable when the inner droplet interface is reinforced by a silica membrane, the micrometric double emulsions formulated by a rotor/stator (Ultraturrax) device were characterized for their aspect, morphology, and size by optical microscopy (Figure 5). The microscopy images show the controls without primary emulsions O/W2 (Figure 5a), the double emulsions w1/O/W2 without silica precursor (Figure 5b), the double emulsions w1/O/W2 with 2.5 wt % APTES (Figure 5c), and the double emulsions w1/O/W2 with 10 wt % APTES (Figure 5d).

The double droplets and the control exhibit a quite homogeneous distribution. While in the control (a), the oil droplet core appears to be clear and transparent, and the primary emulsion is clearly visible as small "corrugations" within the double droplets in b−d. These corrugations are likely due to the light diffraction of the aqueous internal droplets and the limited resolution of the optical microscope around 300 nm. On the basis of these images, the double droplet size distribution was determined by a graphical analysis

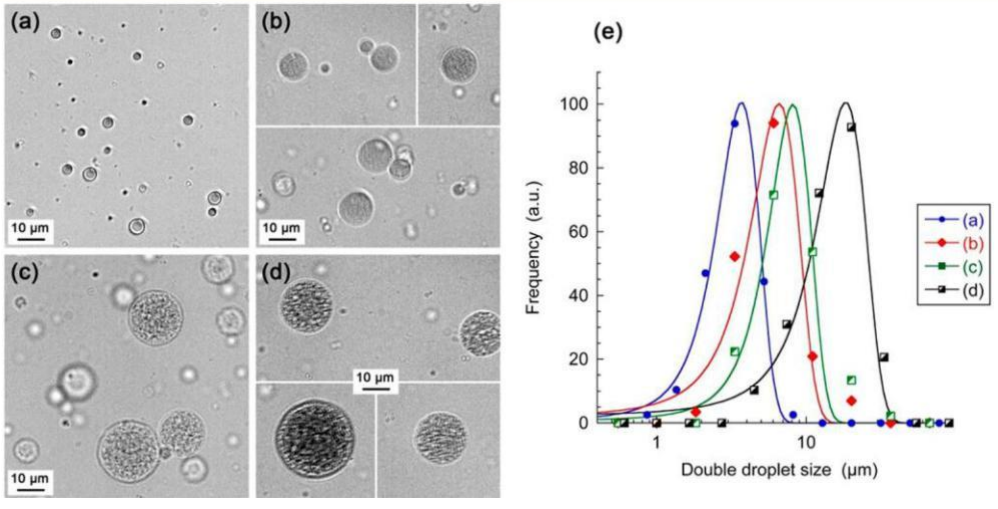

Figure 5. Optical microscopy of controls without primary emulsions O/W2 (a), double emulsions w1/O/W2 without the silica precursor (b), and double emulsions w1/O/W2 with 2.5 wt % APTES (c) and with 10 wt % APTES (d) ($\phi^{oil}_{V\ phase}$ = 20% and [Kolliphor ELP] = 25%). (e) Corresponding size distribution analysis of samples of 100 droplets fitted by a Gaussian function.

(Figure 5, right) for about 100 droplets each time. The experimental data were successfully fitted with a Gaussian equation, giving average sizes of 3.7, 6.6, 8.1, and 18.3 μm, respectively for a−d. As expected, the emulsification process is affected by the presence and size of the primary droplets. Indeed, because the size of these droplets playing the role of the template increases with increasing APTES concentration, the size of the double droplets increases as well.

To investigate the stability of these double emulsions in the formulation process, we monitored the leakage of methylene blue (MB) solubilized in the inner water w_1 toward the external water W_2. It is important to note that the EE values are those immediately after the second emulsification and thus describe the impact of the process itself on the structure of the double droplets, while the leakage of w_1 induced by storage will be studied and discussed in the following sections. Before discussing the EE values of double droplets, it is important to consider the preliminary controls regarding the full release of MB from the primary emulsion. In these control experiments performed on the primary emulsions (described in the Experimental Section) for APTES varying from 0 to 10 wt % and for TEOS varying from 0 to 25 wt %, values of total release are 99.6 ± 0.2 and 99.2 ± 0.4%, respectively. This clearly demonstrates that encapsulated materials can be released irrespective of the thickness of the silica shell.

The EE values for the double emulsions formulated with APTES and TEOS are reported in Figure 6 for different concentrations of the hydrophilic surfactant (Kolliphor ELP). The EE value for the formulation without silica is relatively weak (~25%) but increases rapidly with the silica concen-tration. In the case of APTES, the EE value increases rapidly to 80% for [APTES] = 0.25 wt % and reaches about 95% for [APTES] = 10 wt %. A similar trend is observed for TEOS, but higher TEOS concentrations are needed and EE values hardly exceed 60%. These results are in line with the respective efficiencies of APTES and TEOS in the fabrication of the silica shell (Figure 4). They indicate that even at very low concentrations APTES can efficiently reinforce the water/oil interface to stabilize the double emulsion against the second emulsification. The strong effect of low concentrations of APTES on the EE is outstanding and discloses the high potential of the technology to produce stable double emulsions compatible with the regulatory aspects imposed by industrial production and applications. The difference in EE between APTES and TEOS is likely related to the thickness and probably the density of the silica shell (Figure 4), which makes the silica shell more impermeable with APTES. In fact, in the Figure 4 inset, the "volume of silica by droplet" is represented as a function of the precursor concentration, revealing an important difference between APTES and TEOS, so a parallel can be drawn with the EE values correlating the results of Figure 6. Because of its high efficiency, we selected APTES for further stability studies and the formulation of double droplets at the nanoscale. It is noteworthy that the stability claimed herein and brought about by the reinforcement of interface by silica refers to the fact that the internal water droplets are much more robust compared to the ones without silica. The globules formed are much more robust toward changes in temperature, changes in osmotic pressure, and also the formulation processes (large differences in EE when we compare with and without silica). As a result, we can say that classical double emulsions are much more fragile compared to these new stabilized formulations. This is all the more confirmed by the accelerated aging experiment detailed below.

To further investigate the stability of the double droplets, we monitored their EE values at high temperature (90 °C) as a function of time and for several APTES concentrations (Figure 7). The idea here was to place the samples under very harsh conditions, such as those for accelerated aging procedures that are generally worked out (to a lesser extent). The results

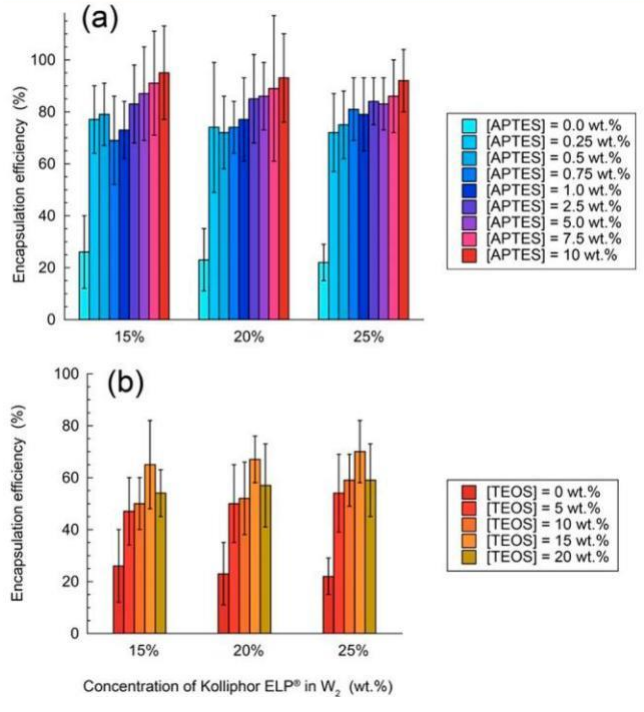

Figure 6. Encapsulation efficiency of MB solubilized in the inner water droplets of macroscopic double emulsions, immediately after the second emulsification. Effect of the concentration of the silica precursor in oil (APTES in a and TEOS in b) and for different concentrations of the hydrophilic surfactant (Kolliphor ELP) in W_2 (n = 3).

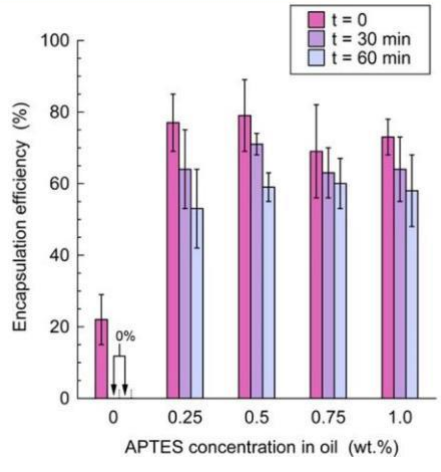

Figure 7. Encapsulation efficiency of MB solubilized in the inner water droplets of macroscopic double emulsions ($\phi^{oil}_{V\ phase}$ = 20% and [Kolliphor ELP] = 25%) immediately after the second emulsification (t = 0) or at high temperature (90 °C) for 30 or 60 min. The $[APTES]_{oil}$ = 0 wt % data point corresponds to the control without the silica precursor.

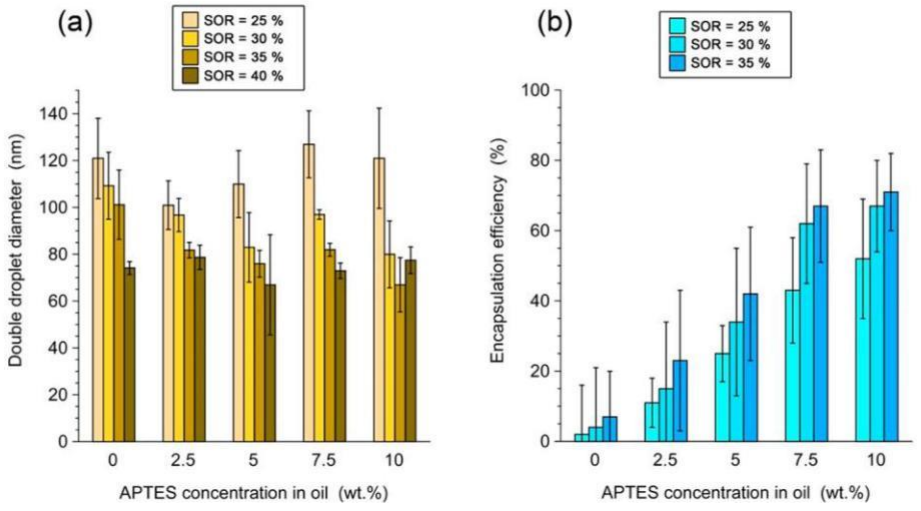

Figure 8. Diameter (a) and encapsulation efficiency (b) of double nanoemulsions for different concentrations of APTES and SOR. The nanoemulsions were obtained by spontaneous emulsification at room temperature. The encapsulation efficiencies were calculated from the concentration of methylene blue measured after the application of fresh samples on size exclusion chromatography columns.

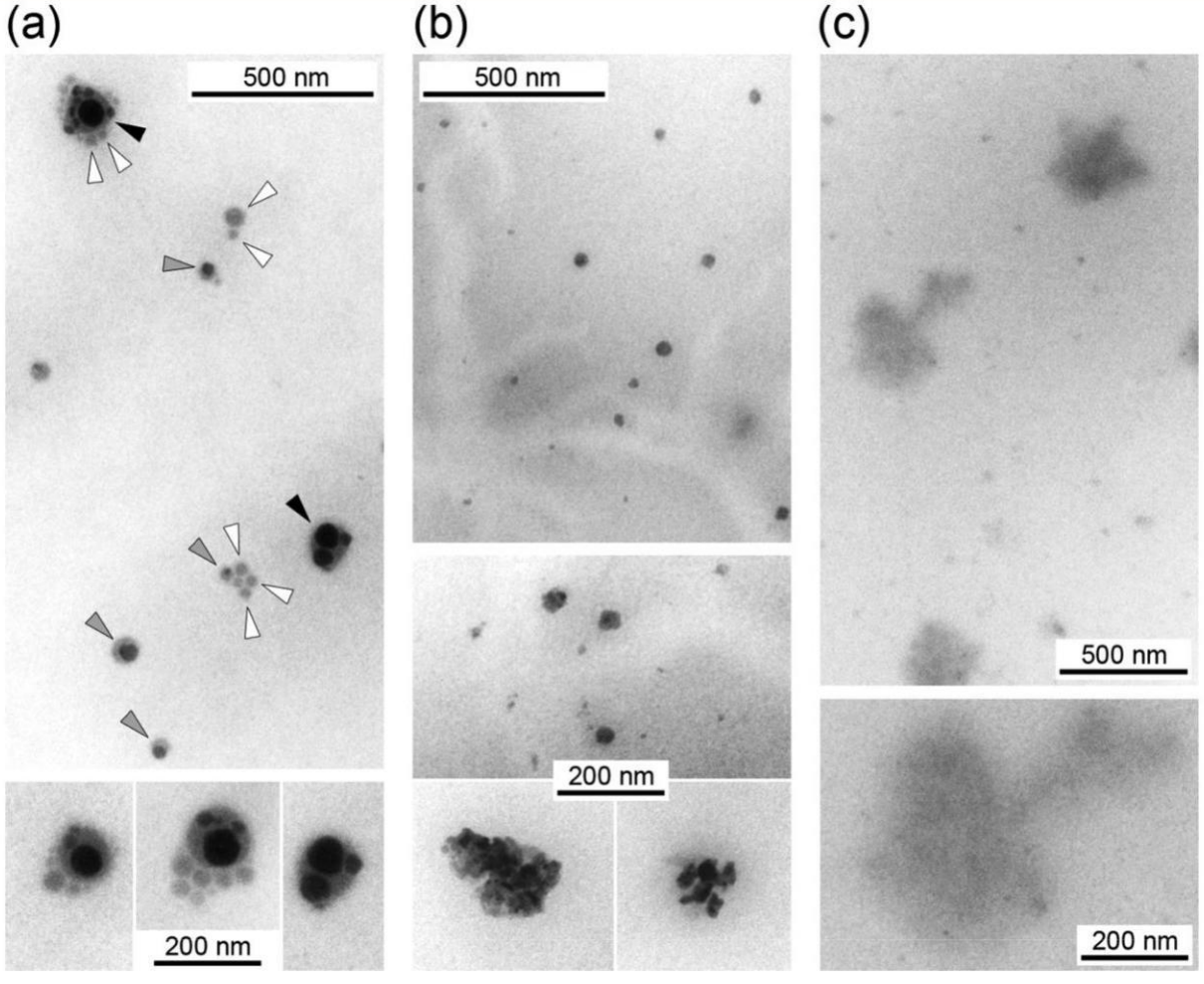

Figure 9. Transmission electron microscopy of double nanoemulsions for APTES concentrations of (a) 10 wt %, (b) 2.5 wt %, and (c) 0 wt %. Oil droplets can contain several (black arrowheads), one (gray arrowheads), or zero (white arrowheads) silica shells containing water droplets.

appear to be in line with our expectation, exhibiting a significant difference between control and silica-protected samples. A temperature of 90 °C was in fact chosen as the higher temperature before boiling to conduct such experiments under harsh temperature conditions. For the control (without APTES), the EE value starts at 23% and decreases to 0% after 30 min, indicating a very rapid release of the encapsulated compounds. In contrast, for [APTES] ≥ 0.25 wt %, the double

DOI: 10.1021/acs.langmuir.8b03919
Langmuir 2019, 35, 2313−2325

droplets appear to be much more resistant. A slow and regular release of dyes was observed, whatever the amount of silica. This observation confirmed the strengthening of the interface by the silica membrane, even at 0.25 wt % APTES, and the still possible release of encapsulated materials with time, as evidenced by the 20−30% decrease in the EE value after 60 min. After 1 h, the encapsulated MB became purple (the color of the crystalline form of this molecule) probably as a result of crystallization, which did not allow this experiment to be continued at 90 °C.

These results indicate that the silica shell formed by APTES is resistant to high temperature, which opens a number of applications. For example, in food applications, the double emulsions can ensure an efficient storage of hydrophilic materials such as flavors and then allow their controlled delivery during cooking.

Nanometric Double Emulsions $w_1/O/W_2$. In this last section, our goal was to transfer the best experimental conditions described for double micrometer emulsions to the formulation of double droplets smaller than 1 μm. For this purpose, the second emulsification has been adapted to be a nanoemulsification process capable of preserving the structure of the primary w_1/O nanoemulsions. Basically, nanoemulsification methods are divided into high-energy processes[51] (high-pressure homogenization or utrasonification) and low-energy processes based on spontaneous emulsification. To preserve the primary emulsion, we selected the gentlest process (i.e., the spontaneous emulsification). In this process, the hydrophilic surfactant in the oil phase (w_1/O nanoemulsion) is mixed at room temperature, and when homogenized, the second aqueous phase W_2 is added, producing spontaneous nanoemulsification.[52,53] Though it is a soft process, the droplets are formed as a result of the turbulent penetration of water in the network made of oil, primary droplets, and Kolliphor ELP. This turbulent droplet formation is less destructive than high-energy methods but is nevertheless aggressive for the small aqueous nanodroplets of the primary emulsion. This is confirmed by the data in Figure 8 correlating the size of the nanometric double emulsion (Figure 8a) with the encapsula-tion efficiency of MB (Figure 8b) as a function of the surfactant-to-oil weight ratio (SOR) and the APTES concentration (i.e., thickness of the silica shell). The global size of the double nanoemulsions is below 120 nm and, as expected, decreases as the quantity of surfactant increases, reaching 70 nm for SOR = 40%. The general behavior of the size decrease observed is similar whatever the concentration of APTES, indicating that the spontaneous emulsification is robust enough not to be affected by the modification of the oil composition. The EE values (Figure 8b) are strongly impacted by the silica shell. Indeed, without silica ([APTES] = 0 wt %), all of the MB leaks rapidly and the EE value is close to zero. Then, the EE values regularly grow as the APTES concentration in oil increases, reaching 60−70% for [APTES] = 10 wt %. Compared to macroscale double emulsions, the nanoemulsification process has a real destructive effect on the double nanodroplets and thus requires a higher shell thickness to provide efficient encapsulation (i.e., [APTES] = 7.5 wt % versus 0.25 wt % for macroscale double emulsions, see Figure 6a). Interestingly, for a given APTES concentration, the EE value depends on the SOR parameter. As a result, it is observed that the EE value and the size of the double nanodroplets are inversely correlated. This result is very important, even if the order of magnitude of the encapsulation efficiency is slightly below those of microscale double emulsions (discussed above Figure 6), and remains absolutely unprecedented regarding nanoscale double droplets.

To confirm the double structure of the nanoemulsions and further rationalize the data in Figure 8, transmission election microscopy was performed on representative samples (Figure 9).

The sizes of the double droplets correspond well to those in Figure 8a, being centered at about 90 nm for SOR = 30%. The silica shells allow the droplets to conserve their shape upon drying under extensive vacuum on the carbon grid (Figure 9a,b). In contrast, the drying process in the absence of APTES destroys the nanodroplets and results in oil puddles (Figure 9c), as previously reported.[54] For [APTES] = 10 wt % (Figure 9a), the ~45 nm thickness of the silica shell (given in Figure 4) appears to be strong enough to preserve the nanodroplet structure upon drying. The double nanostructure is clearly visible in this case, with the inner silica substructure in dark gray and the surrounding oil in light gray. Depending on their size, the double nanodroplets can include several (black arrowheads), one (gray arrowheads), or no (white arrow-heads) inner water droplets. The TEM pictures also reveal that the double droplets may be deformed by the primary droplets, showing their wettability by the oil (i.e., related to their good affinity for oil because they were not expelled from the oil phase). Once the bulk phase is removed, the capillary phenomenon should give the droplet their final shapes and strongly impacts the preservation of the droplet structure and shape. This is precisely what we observe, by comparing Figure 9a, for which the structure is preserved thanks to the silica shells inside, and Figure 9c, for which the oil spreads into the carbon support. Likewise, when several inner droplets are confined in one oil drop, they also seem deformed, forming a thin planar film in their contact region. These interdroplet interactions in the larger droplets can probably lead to their small degradation compared to smaller ones, explaining the difference in EE observed as a function of their size (Figure 8). The relatively dark aspect of the inner silica-stabilized droplets is likely attributed to the important thickness of the shell, as disclosed in Figure 4. Very comparable visual dark aspects were previously reported according to similar sonochemistry of APTES at the water/oil interface of (this time) direct O/W nanoemulsions.[55] This imagery seems related to the process and to the thickness of the silica shell formed. This large silica shell (in Figure 9a of around 45 nm) can also explain why the encapsulation efficiency is not very high compared to that expected in observing the double droplets by TEM: the water cavities are actually quite small. A remark can be made regarding the oil droplets containing or not containing internal particles. In fact, Figure 9a allows us to show that only larger droplets are able to have a double structure while smaller ones cannot. In fact, the spontaneous nanoemulsification gives rise to a log-normal size distribution, and logically, the inner silica shells can be distributed only in second droplets that are large enough to entrap them.

On the other hand, nanodroplets with [APTES] = 2.5 wt % (Figure 9b) appear to burst when water has escaped (during the sample drying), in line with their low EE values (Figure 8b) of around 15% as compared to 70% for nanodroplets obtained with [APTES] = 10 wt % (Figure 9a). The low EE value suggests that most of the inner water has escaped during the second nanoemulsification process. As a result, one can

DOI: 10.1021/acs.langmuir.8b03919
Langmuir 2019, 35, 2313−2325

observe oil droplets containing the remaining fragments of the shells. Noticeably, a good match is observed between the sizes measured by DLS (Figure 4) and the TEM diameters of 130 nm for [APTES] = 10% and 80 nm for [APTES] = 2.5%. (Even if the droplets are destroyed, the scale appears to be coherent.)

In addition to their encapsulation properties, an important feature of these new multifunctional nanocarriers is their ability to release and deliver an encapsulated material. To investigate this ability, we monitor the release of MB from double nanoemulsions incubated at 37 °C. The curves in Figure 10

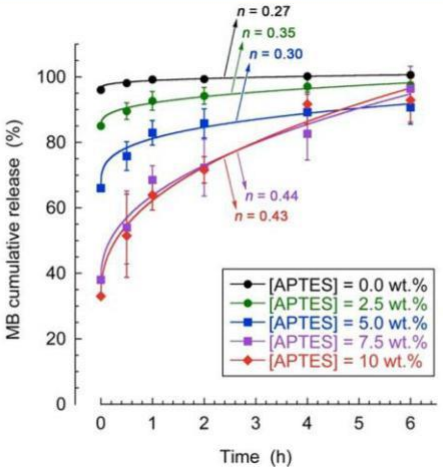

Figure 10. Release of methylene blue encapsulated in double nanoemulsions (SOR = 30%). The y-intercept value corresponds to the EE value after the second nanoemulsification. Experimental data are fitted using a Korsmeyer−Peppas equation giving the values of the release exponent n, as indicated.

represent the MB leakage into the external water phase (W_2) for up to 6 h after formulation. Because all of the samples have the same initial amount of MB (initially in w_1) but different EE values (Figure 8b), the initial offset corresponds to the MB that has already escaped during the second nanoemulsification. The release profiles are successfully fitted with a classical Korsmeyer−Peppas equation for spherical drug carriers,[56] $M_t/M_0 = K_m t^n$, where M_t/M_0 is the fraction of drug release at time t and K_m is a kinetic constant. The release exponent n allows us to identify the release regime.

For all samples, the encapsulated dye is effectively released (up to 100%), indicating that the double nanoemulsions are effective nanocarriers able to deliver the encapsulated materials. All values of the release exponent n (indicated in Figure 10) remain below the threshold of 0.5, indicating Fickian diffusion. However, a difference should exist between the samples with $n \approx 0.44$ ([APTES] = 7.5 and 10 wt %) indicative of a monodisperse Fickian drug release and the samples with $n \leq 0.35$ ([APTES] = 0, 2.5, and 5 wt %) indicative of a Fickian diffusion of a polydisperse sample.[56−58]

This difference likely arises from the fact that the double emulsions are more fragile for the lower APTES concentrations, as evidenced by the disruption and fusion of their inner droplets observed by TEM images (Figure 9). In contrast, the monodisperse Fickian drug release observed at higher APTES concentrations is in full line with the homogeneous population of internal droplets observed by TEM (Figure 9).

Proving the Presence of Water in the Inner Droplets of Micrometric and Nanometric Double Emulsions $w_1/O/W_2$.

To achieve the characterization of the double structure, beyond indirect ways such as EE measurements and TEM observations, and to dispel doubts about the presence of water inside the double micro- or nanodroplets, in this last paragraph we will use a water sensor to prove that inside the double droplets we still have liquid water. The water sensor is a fluorescent dye, sulforhodamine 101 (SR101), which presents a fluorescent signal only when it is solubilized in water. The general idea is to dissolve SR101 in the internal water (w_1, at 100 μM) right from the initial formulation stage and to show that its fluorescent signal is still present within the double micro- or nanodroplets after their separation from the continuous phase. The whole experiment, along with the spectrometric results are summarized in Figure 11, showing the fluorescent spectra at every stage of the experiment. In addition, the control without silica was also reported in parallel to compare the spectra with the double emulsion with APTES 10 wt %. First, the fluorescent signal of reverse nanoemulsions is presented in Figure 11a, showing a very important fluorescent signal with peaks at 606 and 607 nm.

At exactly the same concentration, the two signals with and without APTES show significantly different fluorescence (around 4.6×10^6 and 3.4×10^6 a.u., respectively), likely due to the change in composition that generally affects the environment of the dyes and can modify their fluorescence properties. On the other hand, when dispersed in oil at saturation (Figure 11b), SR101 displays a much lower fluorescence signal of a few orders of magnitude (around 6×10^3) that is not comparable to the former and, important for the discussion, slightly color-shifted around 10 at 596 nm. This huge difference between water and oil signals, compared to the fraction containing double droplets and free dyes, will indicate whether SR101 is still dissolved in water after the separation of the droplets from the bulk.

The formulation of microscale double emulsions is shown in Figure 11c,d before and after droplets separations, respectively. Before separation (Figure 11c), both signals are comparable (around 1.5×10^6 a.u.), in line with the curves of the primary emulsion (Figure 11a) diluted by the formulation process (with the difference between samples with and without silica still visible). Then, the droplet separation shows a much more important signal in the double droplets than in the bulk phase, greater than 1.5×10^6 and smaller than 6×10^3 a.u., respectively. The wavelength of the peak (λ_{max}= 604 and 605 nm) also corresponds to the signal of SR101 solubilized in water and not transferred to oil (see Figure 11a,b). This first result proves that SR101 is still and importantly solubilized in water within the microscale double droplets, thus in the internal water. Interestingly, the signal with and without silica exhibit different fluorescence intensities, higher in both cases corresponding to the samples without silica. This is due to the dye leakage from the double droplets without silica (EE is around 22%) when there is no leakage with silica (EE around 100%) (Figure 6a). This gives rise to the dequenching of SR101 inside the droplets (due to the ACQ effect as it is explained in the Experimental Section), along with an increase in the SR101 concentration in the bulk phase, thus increasing the fluorescence signal in both cases. In addition, a close study of the different fluorescence intensities discloses a decrease in the dye concentration inside the internal droplets, likely due to the dye escape. For example, with “micro-droplets with silica”,

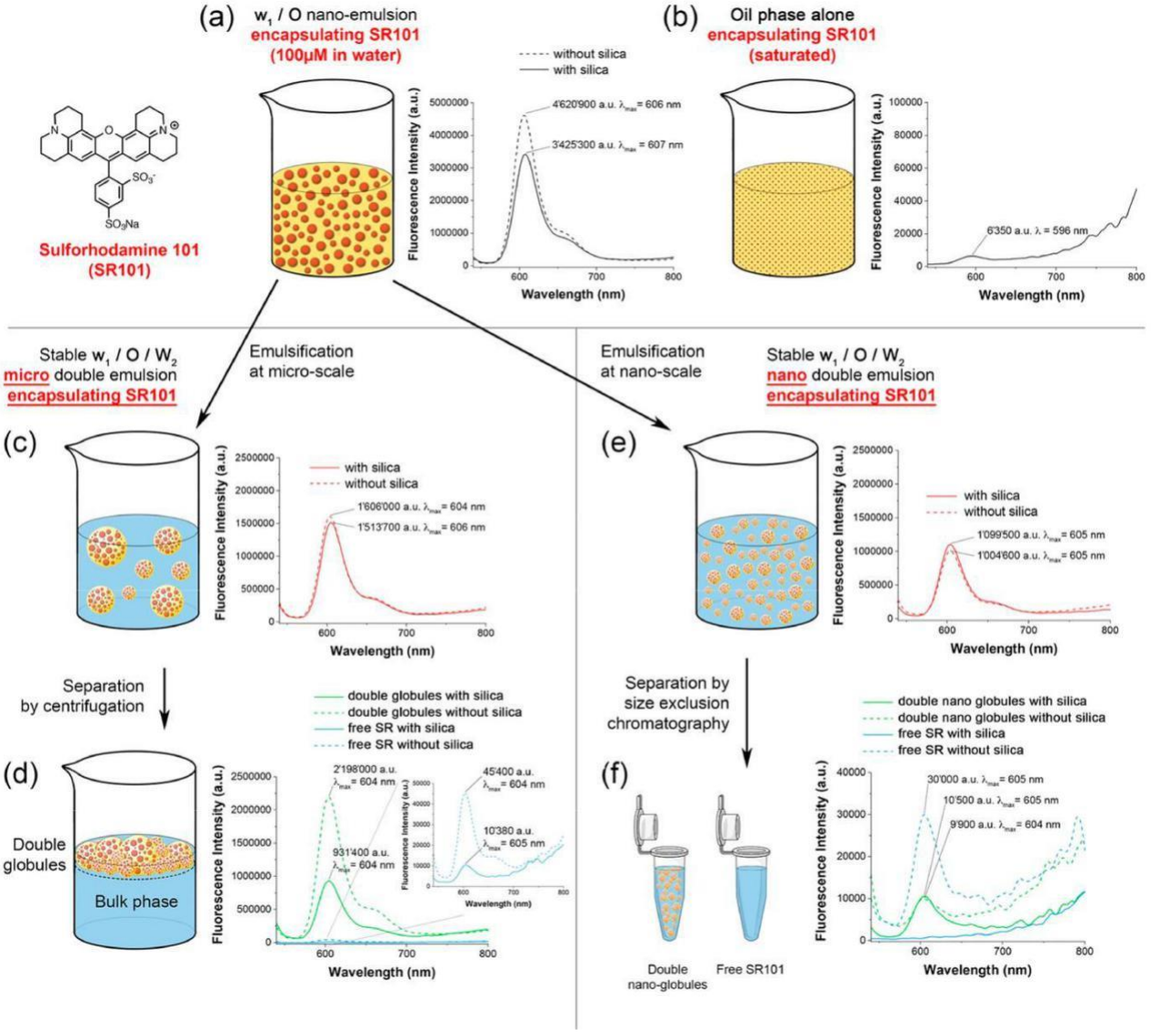

Figure 11. Schematic representation of the protocol followed to prove that liquid water is still present inside the micro and nano double droplets, along with the corresponding fluorescence spectra. Sulforhodamine (SR101) is (a) encapsulated in the w1/O nanoemulsions with and without silica (APTES 10% in oil), (b) dispersed at saturation in oil as a control, and then encapsulated in micro double droplets (c) before and (d) after separation by centrifugation or encapsulated in nano double droplets (e) before and (f) after separation by size exclusion chromatography.

the dilution factor inherent in the double droplet's formulation is 5 (1.2 mL of primary w1/O emulsions in 4.8 mL of W2), while the decrease in the resulting fluorescence signal is only around 2.2 (1.5×10^6 a.u./3.4×10^6 a.u.). This increase follows dye dequenching due to a concentration decrease (i.e., due to the dye release from the inner droplets, as observed with methylene blue).

On the other hand, in the case of nanodouble emulsions, the SR101 signal in double nanoemulsions is slightly more diluted around 1.5×10^6 a.u. (Figure 11e) as a result of the formulation method; however, this dilution is even further increased after the size exclusion chromatography separation (Figure 11f). The fluorescence signal in double nanodroplets with and without silica still appears to be measurable and significant (around 1.0×10^4 a.u.), and importantly, the peak maximums appear at 604 and 605 nm (not at 596 nm when the dye is dispersed in oil in Figure 11b). These two points confirm that SR101 is still solubilized in water, inside the double nanodroplets. Then, the signal of the free dyes appears to be important in the fraction without silica and nonexistent with silica, in line with the former EE results and conclusions established in the previous sections.

CONCLUSIONS

In this study, we formulate stable double emulsions from the micrometric to the nanometric scale, with their respective properties. This is achieved by simply reinforcing the water/oil interface of the primary internal water droplet with a silica membrane, resulting in efficient encapsulation of the hydrophilic materials in the internal water. We show that the modulation of the thickness of the silica membrane (by varying the formulation parameters) can modulate the encapsulation efficiency (up to 100% encapsulation), size, and release properties. Such a system paves the way for a large number of applications, from pharmaceuticals with the delivery of hydrophilic active principles to agrifood and cosmetics applications with the long-term storage and protection of fragile, unstable, or volatile compounds. Moreover, the double

DOI: 10.1021/acs.langmuir.8b03919
Langmuir 2019, 35, 2313−2325

emulsion morphology transposed to the nanoscale has never been reported and is a novel solution for the i.v. administration and targeted coadministration of hydrophilic and lipophilic agents.

AUTHOR INFORMATION

Corresponding Author

*Tel: + 33 3 68 85 42 51. Fax: + 33 3 68 85 43 06. E-mail: nanton@unistra.fr.

ORCID

Mayeul Collot: 0000-0002-8673-1730

Yves Mely: 0000-0001-7328-8269

Nicolas Anton: 0000-0002-7047-9657

Notes

The authors declare no competing financial interest.

ACKNOWLEDGMENTS

S.A. would like to acknowledge the Higher Education Commission of Pakistan for providing financial support for PhD scholar. X.W. would like to acknowledge the China Scholarship Council for her Ph.D. fellowship (Grant No. 201706240033 supported this work).

REFERENCES

(1) Lamba, H.; Sathish, K.; Sabikhi, L. Double Emulsions: Emerging Delivery System for Plant Bioactives. Food Bioprocess Technol. 2015, 8 (4), 709−728.

(2) Hearn, T. L.; Olsen, M.; Hunter, R. L. Multiple Emulsions Oral Vaccine Vehicles for Inducing Immunity or Tolerance. Ann. N. Y. Acad. Sci. 1996, 778 (1), 388−389.

(3) Okochi, H.; Nakano, M. Preparation and Evaluation of w/o/w Type Emulsions Containing Vancomycin. Adv. Drug Delivery Rev. 2000, 45 (1), 5−26.

(4) Muschiolik, G.; Dickinson, E. Double Emulsions Relevant to Food Systems: Preparation, Stability, and Applications. Compr. Rev. Food Sci. Food Saf. 2017, 16 (3), 532−555.

(5) Assadpour, E.; Maghsoudlou, Y.; Jafari, S.-M.; Ghorbani, M.; Aalami, M. Evaluation of Folic Acid Nano-Encapsulation by Double Emulsions. Food Bioprocess Technol. 2016, 9 (12), 2024−2032.

(6) Esfanjani, A. F.; Jafari, S. M.; Assadpoor, E.; Mohammadi, A. Nano-Encapsulation of Saffron Extract through Double-Layered Multiple Emulsions of Pectin and Whey Protein Concentrate. J. Food Eng. 2015, 165, 149−155.

(7) Esfanjani, A. F.; Jafari, S. M.; Assadpour, E. Preparation of a Multiple Emulsion Based on Pectin-Whey Protein Complex for Encapsulation of Saffron Extract Nanodroplets. Food Chem. 2017, 221, 1962−1969.

(8) Mohammadi, A.; Jafari, S. M.; Assadpour, E.; Esfanjani, A. F. Nano-Encapsulation of Olive Leaf Phenolic Compounds through WPC−Pectin Complexes and Evaluating Their Release Rate. Int. J. Biol. Macromol. 2016, 82, 816−822.

(9) Matsumoto, S. Development of W/O/W-Type Dispersion during Phase Inversion of Concentrated W/O Emulsions. J. Colloid Interface Sci. 1983, 94 (2), 362−368.

(10) Pradhan, M.; Rousseau, D. A One-Step Process for Oil-in-Water-in-Oil Double Emulsion Formation Using a Single Surfactant. J. Colloid Interface Sci. 2012, 386 (1), 398−404.

(11) O' Dwyer, S. P.; O' Beirne, D.; Ní Eidhin, D.; Hennessy, A. A.; O' Kennedy, B. T. Formation, Rheology and Susceptibility to Lipid Oxidation of Multiple Emulsions (O/W/O) in Table Spreads Containing Omega-3 Rich Oils. LWT - Food Sci. Technol. 2013, 51 (2), 484−491.

(12) Ding, S.; Anton, N.; Akram, S.; Er-Rafik, M.; Anton, H.; Klymchenko, A.; Yu, W.; Vandamme, T. F. T. F.; Serra, C. A. C. A. A New Method for the Formulation of Double Nanoemulsions. Soft Matter 2017, 13 (8), 1660−1669.

(13) Zhang, M.; Corona, P. T.; Ruocco, N.; Alvarez, D.; Malo de Molina, P.; Mitragotri, S.; Helgeson, M. E. Controlling Complex Nanoemulsion Morphology Using Asymmetric Cosurfactants for the Preparation of Polymer Nanocapsules. Langmuir 2018, 34 (3), 978− 990.

(14) Malo de Molina, P.; Zhang, M.; Bayles, A. V.; Helgeson, M. E. Oil-in-Water-in-Oil Multinanoemulsions for Templating Complex Nanoparticles. Nano Lett. 2016, 16 (12), 7325−7332.

(15) Zhang, M.; Nowak, M.; Malo de Molina, P.; Abramovitch, M.; Santizo, K.; Mitragotri, S.; Helgeson, M. E. Synthesis of Oil-Laden Poly(Ethylene Glycol) Diacrylate Hydrogel Nanocapsules from Double Nanoemulsions. Langmuir 2017, 33 (24), 6116−6126.

(16) Florence, A. T.; Whitehill, D. The Formulation and Stability of Multiple Emulsions. Int. J. Pharm. 1982, 11 (4), 277−308.

(17) Hanson, J. A.; Chang, C. B.; Graves, S. M.; Li, Z.; Mason, T. G.; Deming, T. J. Nanoscale Double Emulsions Stabilized by Single-Component Block Copolypeptides. Nature 2008, 455 (7209), 85−88.

(18) Mehrnia, M.-A.; Jafari, S.-M.; Makhmal-Zadeh, B. S.; Maghsoudlou, Y. Rheological and Release Properties of Double Nano-Emulsions Containing Crocin Prepared with Angum Gum, Arabic Gum and Whey Protein. Food Hydrocolloids 2017, 66, 259− 267.

(19) Zhao, Y.; Zhang, J.; Li, W.; Zhang, C.; Han, B. Synthesis of Uniform Hollow Silica Spheres with Ordered Mesoporous Shells in a CO2 Induced Nanoemulsion. Chem. Commun. 2009, No. 17, 2365− 2367.

(20) Wu, S.-H.; Hung, Y.; Mou, C.-Y. Compartmentalized Hollow Silica Nanospheres Templated from Nanoemulsions. Chem. Mater. 2013, 25 (3), 352−364.

(21) Spernath, L.; Magdassi, S. Formation of Silica Nanocapsules from Nanoemulsions Obtained by the Phase Inversion Temperature Method. Micro Nano Lett. 2010, 5 (1), 28−36.

(22) Attia, M. F.; Anton, N.; Bouchaala, R.; Didier, P.; Arntz, Y.; Messaddeq, N.; Klymchenko, A. S.; Mely, Y.; Vandamme, T. F. Functionalization of Nano-Emulsions with an Amino-Silica Shell at the Oil−Water Interface. RSC Adv. 2015, 5, 74353−74361.

(23) Hu, Y.; Zou, S.; Chen, W.; Tong, Z.; Wang, C. Mineralization and Drug Release of Hydroxyapatite/Poly(l-Lactic Acid) Nano-composite Scaffolds Prepared by Pickering Emulsion Templating. Colloids Surf., B 2014, 122, 559−565.

(24) Nebogina, N. A.; Prozorova, I. V.; Yudina, N. V. Effect of Mineralization of Aqueous Phase and Watering on the Composition of the Interphase Layer of Water-Oil Emulsions. Chem. Sust. Dev. 2009, 17, 207−212.

(25) Fornasieri, G.; Badaire, S.; Backov, R. V.; Poulin, P.; Zakri, C.; Mondain-Monval, O. Mineralization of Water-in-Oil Emulsions Droplets. MRS Online Proc. Libr. 2004, 847 (1−6). DOI: 10.1557/ PROC-847-EE3.5

(26) Kresge, C. T.; Loenowicz, M. E.; Roth, W. J.; Vartulli, J. C.; Beck, J. S. Ordered Mesoporous Molecular Sieves Synthesized by a Liquid-Crystal Template Mechanism. Nature 1992, 359, 710−712.

(27) Cacace, D. N.; Rowland, A. T.; Stapleton, J. J.; Dewey, D. C.; Keating, C. D. Aqueous Emulsion Droplets Stabilized by Lipid Vesicles as Microcompartments for Biomimetic Mineralization. Langmuir 2015, 31 (41), 11329−11338.

(28) Jutz, G.; Böker, A. Bio-Inorganic Microcapsules from Templating Protein- and Bionanoparticle-Stabilized Pickering Emul-sions. J. Mater. Chem. 2010, 20 (21), 4299−4304.

(29) Liberman, A.; Mendez, N.; Trogler, W. C.; Kumme, A. C. Synthesis and Surface Functionalization of Silica Nanoparticles for Nanomedicine. Surf. Sci. Rep. 2014, 69 (2−3), 132−158.

(30) Jaganathan, H.; Godin, B. Biocompatibility Assessment of Si-Based Nano- and Micro-Particles. Adv. Drug Delivery Rev. 2012, 64 (15), 1800−1819.

(31) Foglia, S.; Ledda, M.; Fioretti, D.; Iucci, G.; Papi, M.; Capellini, G.; Lolli, M. G.; Grimaldi, S.; Rinaldi, M.; Lisi, A. In Vitro Biocompatibility Study of Sub-5 Nm Silica-Coated Magnetic Iron Oxide Fluorescent Nanoparticles for Potential Biomedical Applica-tion. Sci. Rep. 2017, 7, 46513.

(32) Anton, N.; Vandamme, T. F. T. F. The Universality of Low-Energy Nano-Emulsification. Int. J. Pharm. 2009, 377 (1), 142−147.
(33) Anton, N.; Benoit, J.-P.; Saulnier, P. Design and Production of Nanoparticles Formulated from Nano-Emulsion Templates-A Review. J. Controlled Release 2008, 128 (3), 185.
(34) Anton, N.; Vandamme, T. F. Nano-Emulsions and Micro-Emulsions: Clarifications of the Critical Differences. Pharm. Res. 2011, 28 (5), 978−985.
(35) Ocotlán-Flores, J.; Saniger, J. M. Catalyst-Free SiO2 Sonogels. J. Sol-Gel Sci. Technol. 2006, 39 (3), 235−240.
(36) Kentish, S.; Wooster, T. J.; Ashokkumar, M.; Balachandran, S.; Mawson, R.; Simons, L. The Use of Ultrasonics for Nanoemulsion Preparation. Innovative Food Sci. Emerging Technol. 2008, 9 (2), 170− 175.
(37) Mahdi Jafari, S.; He, Y.; Bhandari, B. Nano-Emulsion Production by Sonication and Microfluidization A Comparison. Int. J. Food Prop. 2006, 9 (3), 475−485.
(38) Anton, N.; Benoit, J.-P.; Saulnier, P. Design and Production of Nanoparticles Formulated from Nano-Emulsion Templates A Review. J. Controlled Release 2008, 128 (3), 185−199.
(39) Delmas, T.; Piraux, H.; Couffin, A.-C.; Texier, I.; Vinet, F.; Poulin, P.; Cates, M. E.; Bibette, J. How To Prepare and Stabilize Very Small Nanoemulsions. Langmuir 2011, 27 (5), 1683−1692.
(40) Tang, S. Y.; Shridharan, P.; Sivakumar, M. Impact of Process Parameters in the Generation of Novel Aspirin Nanoemulsions − Comparative Studies between Ultrasound Cavitation and Micro-fluidizer. Ultrason. Sonochem. 2013, 20 (1), 485−497.
(41) Gaikwad, S. G.; Pandit, A. B. Ultrasound Emulsification: Effect of Ultrasonic and Physicochemical Properties on Dispersed Phase Volume and Droplet Size. Ultrason. Sonochem. 2008, 15 (4), 554− 563.
(42) Manchun, S.; Dass, C. R.; Sriamornsak, P. Designing Nanoemulsion Templates for Fabrication of Dextrin Nanoparticles via Emulsion Cross-Linking Technique. Carbohydr. Polym. 2014, 101, 650−655.
(43) Abismaïl, B.; Canselier, J. P.; Wilhelm, A. M.; Delmas, H.; Gourdon, C. Emulsification by Ultrasound: Drop Size Distribution and Stability. Ultrason. Sonochem. 1999, 6 (1−2), 75−83.
(44) Marquez, A. L.; Wagner, J. R. Rheology of Double (W/O/W) Emulsions Prepared with Soybean Milk and Fortified with Calcium. J. Texture Stud. 2010, 41 (5), 651−671.
(45) Gupta, A.; Eral, H. B.; Hattona, T. A.; Doyle, P. S. Controlling and Predicting Droplet Size of Nanoemulsions: Scaling Relations with Experimental Validation. Soft Matter 2016, 12, 1452−1458.
(46) Gupta, A.; Eral, H. B.; Hatton, T. A.; Doyle, P. S. Nanoemulsions: Formation, Properties and Applications. Soft Matter 2016, 12 (11), 2826−2841.
(47) Marquez,́A. L.; Medrano, A.; Panizzolo, L. A.; Wagner, J. R. Effect of Calcium Salts and Surfactant Concentration on the Stability of Water-in-Oil (w/o) Emulsions Prepared with Polyglycerol Polyricinoleate. J. Colloid Interface Sci. 2010, 341 (1), 101−108.
(48) Luo, H.; Macapagal, N.; Newell, K.; Man, A.; Parupudi, A.; Li, Y.; Li, Y. Effects of Salt-Induced Reversible Self-Association on the Elution Behavior of a Monoclonal Antibody in Cation Exchange Chromatography. J. Chromatogr A 2014, 1362, 186−193.
(49) Lee, L.; Hancocks, R.; Noble, I.; Norton, I. T. Production of Water-in-Oil Nanoemulsions Using High Pressure Homogenisation: A Study on Droplet Break-Up. J. Food Eng. 2014, 131, 33−37.
(50) Wibowo, D.; Zhao, C. X.; Middelberg, A. P. Emulsion-Templated Silica Nanocapsules Formed Using Bio-Inspired Silicifica-tion. Chem. Commun. 2014, 50 (77), 11325−11328.
(51) Jakhmola, A.; Vecchione, R.; Guarnieri, D.; Belli, V.; Calabria, D.; Netti, P. A. Bioinspired Oil Core/Silica Shell Nanocarriers with Tunable and Multimodal Functionalities. Adv. Healthcare Mater. 2015, 4 (17), 2688−2698.
(52) Saberi, A. H.; Fang, Y.; McClements, D. J. Fabrication of Vitamin E-Enriched Nanoemulsions: Factors Affecting Particle Size Using Spontaneous Emulsification. J. Colloid Interface Sci. 2013, 391, 95−102.
(53) Guttoff, M.; Saberi, A. H.; McClements, D. J. Formation of Vitamin D Nanoemulsion-Based Delivery Systems by Spontaneous Emulsification: Factors Affecting Particle Size and Stability. Food Chem. 2015, 171, 117−122.
(54) Attia, M. F.; Anton, N.; Akasov, R.; Chiper, M.; Markvicheva, E.; Vandamme, T. F. Biodistribution and Toxicity of X-Ray Iodinated Contrast Agent in Nano-Emulsions in Function of Their Size. Pharm. Res. 2016, 33 (3), 603−614.
(55) Attia, M. F.; Anton, N.; Bouchaala, R.; Didier, P.; Arntz, Y.; Messaddeq, N.; Klymchenko, A. S.; Mely,́Y.; Vandamme, T. F. Functionalization of Nano-Emulsions with an Amino-Silica Shell at the Oil-Water Interface. RSC Adv. 2015, 5 (91), 74353.
(56) Ritger, P. L.; Peppas, N. A. A Simple Equation for Description of Solute Release I. Fickian and Non-Fickian Release from Non-Swellable Devices in the Form of Slabs, Spheres, Cylinders or Discs. J. Controlled Release 1987, 5, 23−36.
(57) Gupta, A.; Badruddoza, Z.; Doyle, P. S. A General Route for Nanoemulsion Synthesis Using Low Energy Methods at Constant Temperature. Langmuir 2017, 33 (29), 7118−7123.
(58) Badruddoza, A. Z.; Gupta, A.; Myerson, A. S.; Trout, B. L.; Doyle, P. S. Low Energy Nanoemulsions as Templates for the Formulation of Hydrophobic Drugs. Adv. Ther. 2018, 1, 1700020.

SECTION 2

Transitional Nanoemulsification Methods and Synthesis of W/O Nanoemulsions

Executive Summary:

This section is divided into the two chapters. The chapter 4 is book chapter that was published by Academic Press in book on Nano-emulsions. It gives a detailed account of principle governing behind the popular transitional nano-emulsification methods. The section provides a conceptual foundation about role of non-ionic surfactants and their role in transitional nano-emulsification methods. Phase inversion method and spontaneous emulsification method are two most popular low energy methods exploited for the nano-emulsification. In literature it is generally believed that the principle behind these two methods is different. However, we have shown in this section that the principle behind these two nano-emulsification methods is the same. At last, it also highlights some of the common misconceptions in literature that confuse the readers between the two totally different systems i.e. nano-emulsions and microemulsions by providing clarity regarding their thermodynamic and kinetic stability.

The section 5 provides results finding from our research project about the W/O nano-emulsification by two different methods of the spontaneous emulsification and added in the form of research article. In this study, we have investigated in detail about the different factors that affect the particle size by the spontaneous emulsification methods. The variable we tested for checking their effect on the particle size in both methods were surfactant concentration, type of surfactant, mixture of surfactant, phase ratio and type of oils. The studies clearly showed that among all the variables surfactant concentration was most important factor in determining the particle size of nano-emulsions.

Chapter 4

Transitional Nanoemulsification Methods

Chapter 4

Transitional Nanoemulsification Methods

Nicolas Anton, Salman Akram and Thierry F. Vandamme
University of Strasbourg, Strasbourg, France

Chapter Outline

4.1 INTRODUCTION

Nanoemulsions have emerged in the last decade as an important tool in the for-mulation of pharmaceuticals, for applications as nanomedicines and/or as probes for biomedical imaging. Nanoemulsions offer new possibilities for dis-persing lipophilic therapeutics or biomedical imaging agents in aqueous phases, such as isotonic aqueous buffer solutions compatible with parenteral adminis-tration (Anton et al., 2008a; Attia et al., 2014; Kilin et al., 2014; Li et al., 2013). These lipophilic active pharmaceutical ingredients (API) can be solubilized at high concentrations in the oily core of the nanoemulsion droplets, thereby lead-ing to a uniform distribution throughout the whole system. Nanoemulsions are generally considered as nontoxic nanocarriers with the same potential as lipo-somes or polymeric systems, with, of course, different encapsulation properties. The composition and structure of nanoemulsions can be optimized to obtain

good encapsulation properties, high physicochemical stability, and targeting to specific sites in vivo. Moreover, another fundamental advantage of nanoemulsions lies in the simplicity and robustness of the formulation methods. This chapter focuses on low-energy transitional emulsification methods that are particularly simple to perform and that are robust in the sense that a wide range of oil compositions can be utilized, for example, including drugs solubi-lized, even at high concentration, without impacting significantly on the process as will be discussed below.

Let us focus now on the formulation processes of emulsions. In general, the terminology emulsion refers to macroemulsions, typically with droplet diame-ters ranging from a micrometer to several tens of micrometers (Leal-Calderon et al., 2007a). The formulation of macroemulsions is relatively simple, requir-ing widely used and relatively inexpensive mechanical methods such as rotor-stator devices. However, macroemulsions are usually highly unstable due to physical destabilization mechanisms such as gravitational separation, floccula-tion, and coalescence (Leal-Calderon et al., 2007b). For this reason, macroe-mulsions are usually homogenized again using another mechanical method that aims at decreasing the droplet size and polydispersity. The resulting nanoe-mulsions contain droplets with diameters in the nanometer range, that is, typ-ically from about 30 to 300 nm.

The thermodynamic instability of emulsions and nanoemulsions is due to the fact that the free energy G_f associated with their formation is greater than zero. This free energy change is mainly due to the increase in contact between the two immiscible liquids: $G_f = A\gamma$, where A is the increase in interfacial area and γ is the interfacial tension. Thus, the interfacial area has a tendency to spontaneously decrease, thereby favoring droplet flocculation and coalescence. On the other hand, once formed, nanoemulsions tend to have very good kinetic stability because their small droplet size reduces the rate of gravitational separation and droplet aggregation. Nevertheless, nanoemulsions are still prone to droplet growth through a phenomenon known as Ostwald ripening, which is the growth of large droplets at the expense of small droplets due to diffusion of oil molecules through the intervening aqueous phase (Leal-Calderon et al., 2007b; Tadros et al., 2004; Anton et al., 2008b). Nanoemulsions must therefore be carefully formulated to avoid Ostwald ripening, for example, by adding ripening inhibitors or ensuring a narrow particle size distribution (Tadros et al., 2004).

This brief overview on the formulation of emulsions and nanoemulsions highlights the potential advantages of emulsification methods that produce small droplets with narrow distributions. In addition, emulsification efficiency depends on the composition, chemical nature of the phases and stabilizing agents, viscosity ratios of the phases, temperature and time of processing, shear rate, cooling time, type of emulsification apparatus, and energy supplied. Rotor/stator apparatuses provide high shearing along with an efficient recirculation of the liquid, thereby giving rise to a premix emulsion between 10 and 100 μm. They induce a strong shearing that favors the breaking up of the drops, but do not permit decreasing the droplet size below about 1 μm, due to the massive

dissipation of the mechanical energy in the form of heat. Specially designed mechanical devices capable of supplying huge amounts of energy are necessary to increase A and decrease the droplet size despite heat dissipation. These methods, so-called high-energy methods, are performed by the homogenization of the premix mainly not only with high-pressure homogenization but also with ultrasound-based methods.

These high-energy methods have a number of advantages that have led them to be widely used in industrial processes, such as their versatility and high throughput. However, they also have a number of limitations of high-energy methods: (i) The process typically involves several steps, including dispersion, premixing, and homogenization; (ii) there are high-energy needs; (iii) there is a potential risk of degradation or denaturation of fragile molecules in the formulation; and (iv) there are high costs associated with purchasing, maintaining, and running the equipment. Consequently, there has been interest in alternative emulsification methods, such as low-energy methods, that allow the formulation of very small and monodisperse nanoemulsions without the need for any specialized equipment. These low-energy methods have emerged as highly robust and adaptive emulsification methods that have many potential applications. For example, they can be used to produce nanomedicines that are nontoxic and stable carriers for different sorts of lipophilic active ingredients at the same time.

The purpose of the present chapter is to present an overview of these low-energy methods, mainly related to the concept of transitional methods. The term "transitional" comes from the transitional emulsion phase inversion, a phe-nomenon traditionally induced by a change in temperature. These systems were first reported in 1969 by Shinoda and Saito (1969). In Section 4.2, a discussion of the underlying principles of the transitional emulsification method is given, with an emphasis on the thermodynamic properties of nonionic surfactants, which play a key role in these processes. In Section 4.3, we focus on the con-sequences of the transitional phenomena applied to low-energy emulsification. Different low-energy emulsification methods are reviewed, and the impact of nonionic surfactant phase behavior on the process is stressed, including a dis-cussion of the role of ternary phase diagrams of the water/nonionic surfactant/ oil system. In addition, differences between transitional nanoemulsions and microemulsions are highlighted, from the formation and formulation processes to the thermodynamic and physicochemical properties of these dispersions. Section 4.4 then deals with the robustness of the transitional nanoemulsification processes, due to the modification of the composition related to the encapsula-tion of active ingredients in the droplet's core.

4.2 THE ROLE OF PEGYLATED NONIONIC SURFACTANTS ON TRANSITIONAL EMULSIFICATION METHODS

Low-energy emulsification methods are almost exclusively based on the use of surfactants for which the polar head is a poly(ethylene glycol) chain (PEG and

PEGylated surfactants), which are a particular form of nonionic surfactant. Representative examples of nonionic surfactants typically used in the formation of nanoemulsions by low-energy emulsification are presented in Fig. 4.1:

(A) PEG-4 dodecyl ether (Rao and McClements, 2010; Astaraki, 2016; Izquierdo et al., 2004), with a total number of ethylene glycols of 4 and a molec-ular weight of the PEG moiety of 176 g/mol (Brij 30); (B) PEG-20 sorbitan monooleate (Mei et al., 2011; Rao and McClements, 2011), with 20 ethylene glycol units and a molecular weight of the PEG moiety of 880 g/mol (Tween 80); (C) PEG-15 stearate (Klassen et al., 2014), with 15 ethylene glycol units and a molecular weight of the PEG moiety of 660 g/mol (Kolliphor HS15); and

(D) PEG-35 ricinoleate (Attia et al., 2014; Li et al., 2013; Anton and Vandamme, 2009), with 35 ethylene glycol units and a molecular weight of the PEG moiety of 1540 g/mol (Kolliphor ELP).

These surfactants all have a relatively high total number of ethylene glycol units, or PEG chain length, with values in a comparable size range (15–35 per lipid chain). Moreover, these surfactants all have hydrophilic-lipophilic balance (HLB) values around 13–15, which is related to the relative sizes of the polar

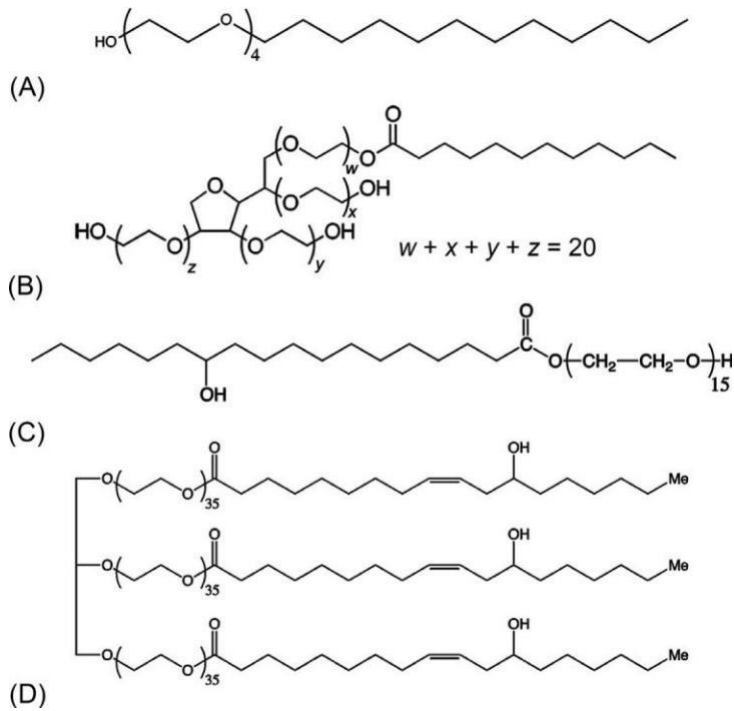

FIG. 4.1 Some representative nonionic surfactant used in transitional emulsification: (A) Brij 30 (PEG-4 dodecyl ether), (B) Tween 80 (PEG-20 sorbitan monooleate), (C) Kolliphor HS15 (PEG-660 stearate), and (D) Kolliphor ELP (PEG-35 ricinoleate).

head and nonpolar chain. Shorter or much longer PEG chains will induce a loss in water solubility or surface activity, respectively. In general, the solubility of PEGylated surfactants is induced not only by interactions between the PEG chain and the bulk water through the formation of hydrogen bounds (Goldstein, 1984; Wartewig et al., 1990) but also by the conformation of the PEG chain that can create a localized dipole moment (in the cis conformation), which enhances the dipole-dipole interactions with the bulk water (Karlstrom, 1985) and thus solubility. Another phenomenon that tends to reduce PEG sol-ubility comes from the structuration of water molecules associated by hydrogen bonds into flickering clusters (so-called linked water) that wraps the PEGylated polar heads. The presence of flickering clusters has been shown to exhibit a buffer or shielding effect that increases with water structuration, that is, with cluster size. In fact, the hydration state of the PEG chains is an important param-eter that can be considered as an intrinsic property of the nonionic surfactant, which is strongly related to the thermodynamic environment and composition of the aqueous phase in which it is solubilized. Indeed, temperature, surfactant concentration (Schottand and Han, 1976a), and electrolyte concentration in water induce salting-in or salting-out effects of PEGylated surfactants (Schottand and Han, 1976a; Schick, 1962a; Maclay, 1956; Schott, 1973, 1997, 2001; Schott and Han, 1975; Schottand and

Royce, 1984; Schott et al., 1984), thereby shifting the equilibrium $nH_2O > (H_2O)_n$ toward the left or the right, respectively, in function of the type of ion. Consequently, the size of the flickering clusters affects the phase diagrams and macroscopic properties of nonionic surfactants, such as the critical micelle concentration (CMC) (Hsiao et al., 1956; Schick, 1962b, 1964; Schottand and Han, 1976b; Rayand and Nemethy, 1971; Malikand and Jhamb, 1970; Malikand and Saleem, 1968; Arai, 1967) and cloud point (cp) (Schick, 1962b; Arai, 1967; Dorenand and Goldfarb, 1970; Shinodaand and Takeda, 1970; Gu et al., 1989).

To summarize, the solubility of nonionic surfactants is primarily determined by interactions between the PEG groups and water and is modified by the size of the flickering clusters. Thus, water solubility is highly dependent on tempera-ture, strongly decreasing with heating because the thermal excitation of the water molecules reduces their interactions with the ethylene oxide groups. This phenomenon is at the origin of the cloud point and nonionic surfactant demixing phenomena (giving rise to a surfactant-rich phase in equilibrium with an aque-ous one with surfactant concentration close to the CMC) and at the center of the emulsion phase inversion phenomenon.

A large variety of PEGylated surfactants have been used in phase inversion temperature (PIT), spontaneous emulsification, and self-emulsifying drug delivery system methods, but their global behavior and their role in these emul-sification processes follow a universal mechanism. However, if the use of non-ionic surfactants is usually necessary to obtain low-energy emulsification, the choice of oil phase is also very important for the success of the process. Indeed, as discussed later, the transitional emulsification methods used to produce

nanoemulsions are based on changes in the relative interactions of PEGylated surfactants with the oil and water phases and particularly on the possibility of modifying these interactions using thermodynamic variables. To illustrate these considerations, it is interesting to consider the general phase diagram, reported in Fig. 4.2, of nonionic surfactants with respect to water and oil phases.

At constant composition, it appears that the nonionic surfactants are not fully soluble in the aqueous and oil phases and that this solubility behavior is linked to temperature. Electrolyte concentration influences the location of the phase frontiers (see earlier), while the temperature has a direct incidence on the solubility of the surfactants. The phase diagram shows two demixing two-phase regions: (i) for the binary system surfactant/water for which a key parameter is the cloud point in water

(cpβ) and (ii) in oil for the binary system surfactant/oil for which a key parameter

is the cloud point in oil (cpα). The phase behavior of nonionic surfactant in water has a crucial role and is principally at the origin of low-energy emulsification processes. More precisely, emulsifica-tion comes from the sudden change of the nonionic surfactant solubility, rapidly crossing the boundary of the phase diagram, from the two-phase region to the one-phase region. Let us consider the physicochemical behavior adopted by the nonionic surfactants during the low-energy emulsification or transitional pro-cesses, through the binary phase diagram surfactant/water in Fig. 4.2. As an example, point A corresponds to the thermodynamic conditions and composi-tion in which the surfactants are before emulsification, and points B, C, and D correspond to possible points compatible with the emulsification process. Indeed, the process is driven by the transition from a state where the nonionic surfactants are nonsoluble in water to a state where they are fully soluble. Emul-sification is therefore possibly performed by a number of routes: (i) pathway A-B, which involves dilution with water at constant temperature;

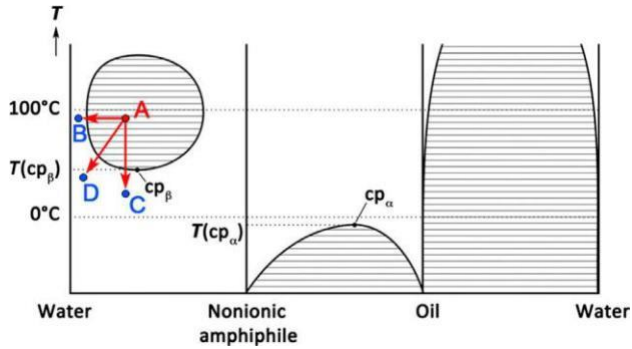

FIG. 4.2 General binary phase diagrams between water, nonionic surfactant, and oil. The cloud points are represented in water cpβ and in oil cpα. The signification of the pathways A-B, A-C, and A-D is dis-cussed in the text. (Reproduced with permission from Kahlweit, M., Strey, R., Firman, P., Haase, D., Jen, J., Schomaecker, R., 1988. General patterns of the phase behavior of mixtures of water, nonpolar solvents, amphiphiles, and electrolytes. Langmuir 4, 499–511; Anton, N., Vandamme, T.F., 2011. Nano-emulsions and micro-emulsions: clarifications of the critical differences. Pharm. Res. 28, 978–985.)

(ii) pathway A-C, which corresponds to sudden cooling of the system at constant composition; and (iii) pathway A-D, which combines both dilution and cooling (e.g., adding cold water). Pathway A-C occurs at constant composition and may therefore be reversible process, while the other two pathways involve changes in composition and are therefore irreversible. Traditionally, the PIT method was considered to be the only transitional method for producing nanoemulsions. However, the term transitional more generally refers to the change in solubility of the nonionic surfactants whatever the pathway (e.g., A-B, A-C, or A-D) and can therefore be used more broadly.

In addition, Fig. 4.2 shows that the nonionic surfactant seems freely soluble in the oil phase whatever the temperature, but below cpβ, the surfactant shows good affinity for both the water and oil phases. This temperature-dependent change in relative solubility of surfactants around cpβ plays a major role in the emulsification process.

4.3 TRANSITIONAL EMULSIFICATION METHODS, EMULSION PHASE INVERSION, SPONTANEOUS EMULSIFICATION, AND UNIVERSALITY OF THE PROCESS

Let us focus now on the fabrication of nanoemulsions using low-energy emulsification methods based on these transitional phenomena. The formation of nanoemulsions by these methods is a dynamic and irreversible process, thereby establishing a direct relationship between ternary phase diagrams (at equilibrium) and emulsification processes (dynamic) that is only justified to emphasize the physicochemical interactions (and their modification with temperature and composition) between the nonionic surfactant and the water and oil phases. Traditionally, the two most important transitional emulsification methods are the PIT and spontaneous emulsification methods. In the following sections, the main prin-ciples driving these processes are presented, and it is shown that they are based on a universal mechanism related to the behavior of nonionic surfactants.

4.3.1 PIT Method

The particular feature of the PIT method is the presence of all the components (oil, water, and surfactant) from the start of the process. In the PIT method, the ternary system is constantly and mechanically homogenized (e.g., under gentle magnetic stirring), and the temperature is monitored and gradually changed to force the nonionic surfactant to cross the boundary shown in Fig. 4.2. Under these dynamic conditions, the mechanical energy supplied constantly creates new droplets and new interfaces that counterbalance any droplet coalescence that occurs. The droplets formed are stabilized by the nonionic surfactant, and for an equilibrated water-to-oil ratio of around 50 wt%, the type of the emulsion formed (O/W or W/O) is driven by the affinity of the nonionic surfac-tant for the water or oil phases, respectively. The general principle of the PIT method is summarized in Fig. 4.3, which shows the link between the binary

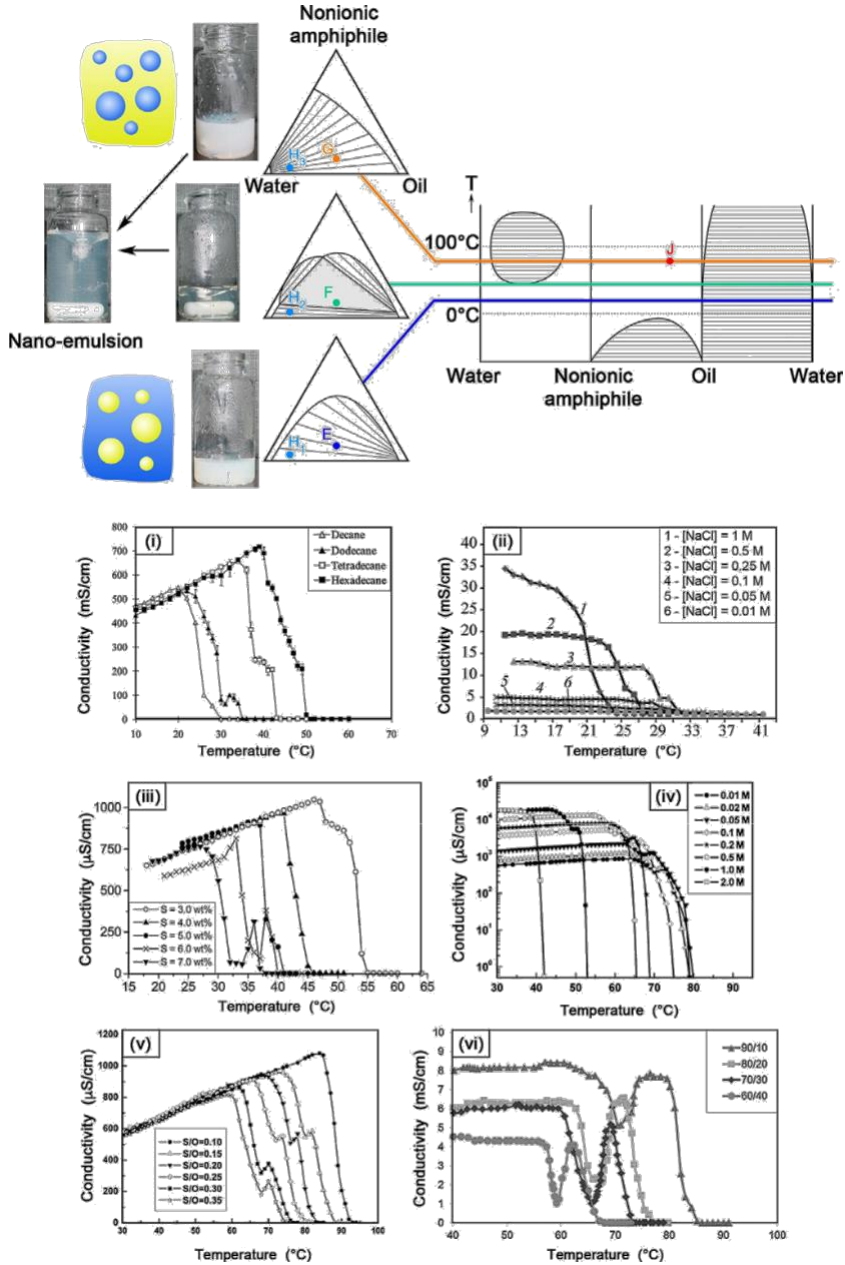

FIG. 4.3 (Top) Schematic presentation of the phase behavior of ternary systems (water/nonionic surfactant/oil) as a function of temperature, below (lower line, point E), equal (middle line, point F), and above (upper line, point G) the phase inversion temperature. The pictures show the dif-ferent states of the corresponding emulsion during phase inversion (made with MilliQ water/Kolliphor HS15/Labrafac WL) and the resulting nanoemulsion (on the left, point $H_{1, 2, or 3}$). The graphs from (i) to (vi) show emulsion phase inverting with Brij 30 as surfactant in (i) (Rao and McClements, 2010), (ii) (Astaraki, 2016), and (iii) (Izquierdo et al., 2004); Tween 80 in (iv) and (v) (Mei et al., 2011); and Kolliphor HS15/Igepal CO-210 in (iv) (Klassen et al., 2014). The different examples show the influ-ence of (i) the nature of the oil, (ii) and (iv) electrolyte concentration, (iii) and (v) surfactant concentration, and (vi) different nonionic surfactant composition (see details in the text).

diagrams discussed earlier and the ternary diagrams corresponding to the three-component systems studied. Three different characteristic temperatures are emphasized, below (lower curve), equal to (middle curve), and above (upper curve) the cloud point cpβ. A model ternary system (45 wt% water, 45 wt% oil, and 10 wt% nonionic surfactant) is represented as a function of temperature with E, F, and G, along with the pictures showing the nature of the different dispersions.

Ternary phase diagrams clearly show the change of affinities of the surfac-tants for the water and oil phases through the orientation of the phase lines, as a function of temperature. At point E, the ternary diagram corresponds to a Winsor I system, the surfactant shows a better solubility toward the aqueous phase, and the emulsion formed is the oil-in-water (O/W) one; at point G, a Winsor II is formed, in which the surfactant is mostly soluble in the oil phase, and the emulsion formed is a water-in-oil (W/O) one; finally, point F corre-sponds to the intermediate configuration, Winsor III, where the nonionic surfactants present similar affinities for the two phases forming a translucent microemulsion (see the picture). The temperature marking the frontier between O/W and W/O emulsions is called PIT, which is intrinsically close to the cloud point (cpβ) but possibly shifted depending on the nature of the oil (for which the surfactant solubility in oil can vary).

Beyond the surfactant behavior and phase diagram, let us consider the emulsification method based on the phase inversion process, for which the determination of the PIT location is crucial. The characterization of the PIT is performed by monitoring the electric conductivity χ of the emulsion, for which an electrolyte is added in water (keeping in mind that the electrolyte can also influence the PIT). This allows the characterization of the emulsion phase inversion and characterization of the parameters that can influence its value. This method is based on the fact that the electric conductivity of the system is much higher when water is the continuous phase (χ of the order of millisiemens per centimeter) than when oil is the continuous phase (χ close to zero). With increasing temperature, the conductivity decreases continuously in the phase inversion region, with conductivity peaks sometimes being observed (attributed to mesostructures and liquid crystals (1)). Overall, the PIT is taken to be located at the middle of the transitional region. Representative examples are reported in Fig. 4.3 (i)–(vi).

The graphs (i), (ii), and (iii) show the emulsion phase inversion obtained with Brij 30 (Fig. 4.1A) and the potential impact of the formulation and com-position parameters on the PIT location. In graph (i), the nature of oil is changed by varying the length of the saturated aliphatic chains (C_nH_{2n+2} with n ¼10, 12, 14, or 16). The PIT clearly increases as the oil chain length increases, showing a loss of Brij 30/oil affinity when the oil phase becomes more lipophilic. In graph (ii), the electrolyte concentration in water is decreased from 1 to 0.01 M, and as a result, the water solubility of the surfactant is increased (due to the decrease in the size of the flickering cluster of water molecules around the polar head group; see Section 4.2) increasing the PIT. Also for Brij 30, in graph (iii), the total surfactant concentration is increased, which decreases their global solubility

(as the water volume is constant) and thereby decreases the PIT. This comparison is interesting to see the potential influence of these formulation parameters on the PIT value, but the PIT shifts remain relatively limited, with the location for Brij 30 remaining around 30–50°C. However, for different surfactants with longer PEG chains (e.g., 20 units for Tween 80), the PIT can be up to 80°C, and the effects of NaCl concentration in the water phase (graph (iv)) or of the total surfactant concentration (graph (v)) are much more important. The last example with Kolliphor HS15/Igepal CO-210 (graph (vi)) highlights this observation; the figure shows emulsion phase inversion with a mixture of different surfactants used at different ratios. Kolliphor HS15 is largely hydrophilic, and Igepal CO-210 is largely lipophilic with 15 and 2 ethylene gly-col units, respectively. This difference has a major impact on the PIT location: the higher the Kolliphor HS15 proportion, the higher the PIT value. It is noteworthy that other approaches can be used to monitor the emulsion phase inversion process, such as turbidity measurements that are based on a change in the optical properties resulting from alterations in the dimensions of the particles in O/W emulsions, microemulsions, and W/O emulsions (Rao and McClements, 2011; McClements, 2011).

The characterization of the phase diagram and of the phase inversion process is important for the success and optimization of the emulsification using the transitional approach. However, the formation of nanoemulsions is an irrevers-ible process that involves a specific mechanism (Anton and Vandamme, 2009). The principle is summarized in Fig. 4.4A in which the emulsion and location of the nonionic surfactants are schematically represented during the emulsion

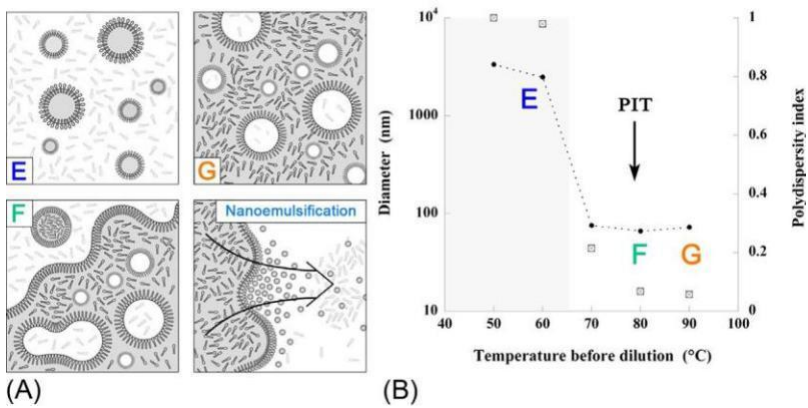

FIG. 4.4 (A) Schematic illustration of the formation of nanoemulsions by the PIT method. The different points E, F, and G correspond to the compositions shown in Fig. 4.3, and the nanoemulsi-fication to the process is described in the text after dilution or rapid cooling of the system.
(B) Diameter of the nanoemulsion formed after dilution of the ternary system at the temperatures indicated in the abscissa. (Reproduced with permission from Anton, N., Vandamme, T.F., 2009. The universality of low-energy nano-emulsification. Int. J. Pharm. 377, 142–147.)

phase inversion process and linked to the compositions indicated in the relevant phase diagrams (Fig. 4.3). At point E, the majority of nonionic surfactant is sol-ubilized in the aqueous phase, thereby stabilizing O/W emulsions; however, at point G, the surfactants are primarily solubilized in the oil, thereby stabilizing W/O emulsions. Within the PIT zone, at point F, there is a partition of surfactant between both phases, leading to the formation of a nanoscale microemulsion, leading to a transparent appearance of the overall system. If we draw a parallel with the composition pathways presented in Fig. 4.2 (A-B, A-C, or A-D) pass-ing from a

lipophilic to a hydrophilic state, herein (see Fig. 4.3), the correspon-dence is G-H_3,

G-E, and G-H_1, respectively. The general pathways gather the dilution and/or cooling (Rao and McClements, 2011; Anton and Vandamme, 2009) and thus can

be extended to G-H_3, G-H_2, G-H_1, G-E, F-H_2, and F-H_1. The irreversible emulsification process comes from the rapid change of the water solubility of the nonionic surfactants from a state where they are fully (point G) or partially (point F) located in the oil to a state where they are primarily solubilized in water (points

E and $H_{1,2,3}$). As a result, the water phase penetrates very fast into the oil/surfactant mixture, breaking up the oil into the form of nanosized particles, following a spinodal decomposition. The nanodroplets formed are then immedi-ately stabilized by the surfactants present in the water phase, thereby forming a stable dispersion of nanoemulsions (see Fig. 4.4A).

The impact of initial temperature before the nanoemulsification step is shown in Fig. 4.4B (Anton and Vandamme, 2009). The system selected is Kol-liphor HS15/Labrafil M1944CS, with a surfactant-to-oil weight ratio (SOR) fixed at 30% and a water-to-oil weight ratio (WOR) fixed at 70%, with a PIT around 80°C. The nanoemulsification process is performed with water dilu-tion at room temperature (a different experiment for each point). The results show that the nanoemulsion droplet size and polydispersity drastically decrease when the system temperature approaches the PIT and then stabilizes above the PIT. Therefore, this corroborates the mechanism proposed and emphasizes the crucial importance of this parameter in the transitional nanoemulsification process.

The last remark on the PIT nanoemulsification method will concern the size of the droplets formed in the nanoemulsion. As seen in Fig. 4.4B, at T PIT, the droplet diameter does not depend strongly on temperature, and so, this param-eter does not strongly impact the final size of the droplets in the nanoemulsions formed. However, one fundamental parameter is the concentration of nonionic surfactants used, as shown in Fig. 4.5, for increasing concentrations of Tween 80 (increasing surfactant-to-oil ratio) that the mean size of droplets in the nanoemulsions gradually decreases. Fig. 4.5A shows the size distribution giving an image of the polydispersity, and Fig. 4.5B only reports the mean size with the surfactant concentration. It appears that the value of the mean size is strongly impacted by the surfactant concentration used, from around 95 nm to around 45 nm, and from the shape of the distribution, which becomes more monodis-perse. This was expected since the nanoemulsification mechanism is directly

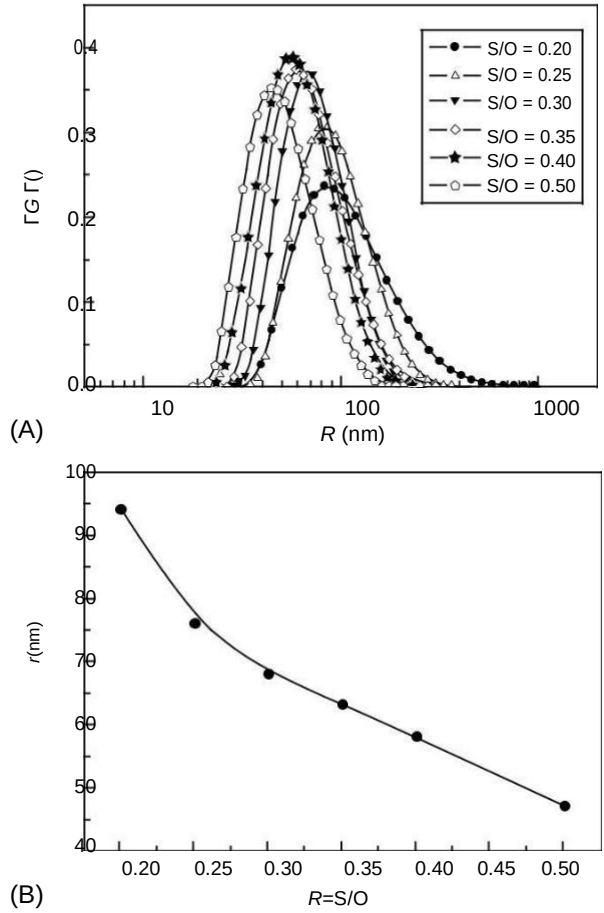

FIG. 4.5 With the ternary system (paraffin oil/water/nonionic surfactant (a mixture of Tween 80 and Span 80)). (A) Size distribution and (B) mean radius, as a function of the surfactant-to-oil ratio (S/O) after nanoemulsification by the PIT method. (Reproduced with permission from Mei, Z., Xu, J., Sun, D., 2011. O/W nano-emulsions with tunable PIT induced by inorganic salts. Colloids Surf. A Physicochem. Eng. Asp. 375, 102–108.)

linked to the behavior and displacement of the nonionic surfactants: the higher the nonionic surfactant concentration, the higher the disorder induced in the oil phase during emulsification and the smaller the droplets produced.

4.3.2 Spontaneous Emulsification and the Universality of Transitional Emulsification

The term spontaneous emulsification comes from the simplicity of the emulsification process: the nanoemulsions are generated only by gently mixing two

liquid phases. This method is in general considered and classified as a different method than the PIT emulsification method, but in fact, they are very close and based on the same mechanism. As a consequence, compared with the PIT method, the spontaneous emulsification could appear for the formu-lator as a preferred methodology for forming emulsions by giving the same result with a much higher simplicity. On the other hand, to understand the sim-ilarities between these two approaches, it is important to understand the mechanisms driving the PIT method and the transitional processes described earlier.

As illustrated in Fig. 4.6A and B point J (and in Fig. 4.3) and largely sup-ported by the literature (Anton and Vandamme, 2009, 2011; McClements, 2012; Lee et al., 2014), the starting point of the process is a simple oil/surfac-tant system, set at a temperature for which the surfactant has the best affinity for the oil phase, that is, above the cloud point or PIT. Then, the mixture J is suddenly mixed with the aqueous phase, at temperature lower than PIT (toward

H_1) for the best efficiency, but in some cases, the nanoemulsification process is

more efficient at higher temperatures (H_2 or H_3) depending on the system, for example, with the oil phase sensitive to temperature (solid lipid, wax, or very viscous oils), and in that case, the water dilution is sufficient to modify the surfactant solubility and induce nanoemulsification. Once the oil/ surfactant mixture is in contact with water, changing suddenly the thermody-namic condition to make surfactants more soluble in the aqueous phase than the oily

one, Fig. 6A(i) (system composition is, e.g., H_1, H_2, or H_3), the water phase rapidly penetrates the oil/surfactant mixture (Fig. 6A(ii)), break-ing up the oil in the form of nanodroplets (Fig. 6A(iii)). In addition, in function of the surfactant-to-oil initial ratio, that is, location of J on the surfactant/oil axis (see Fig. 6B), the size of the resulting nanoemulsion droplets is strongly modified, like in the example reported in Fig. 6C for a system prepared from Kolliphor HS15/Labrafil M1944CS, where the size follows a monotonous decrease according to a power law. Similar results were obtained with a mix-ture of Tween 80/Span 80, showing similar trends and also emphasizing the strong impact of the temperature of the system before dilution (Tong et al., 2016).

This mechanism is very close to the one described above for the PIT method (Fig. 4.4). It is not surprising because the systems are quite similar, but this is very interesting since it can simplify the nanoemulsification pro-cesses. In the literature, the PIT method is often considered quite distinct from the spontaneous emulsification method. However, the above discussion high-lights that both methods are actually based on the same physicochemical phe-nomena and can therefore be considered to be very similar. Therefore, these considerations define the concept of universality for the formation of nanoe-mulsions using low-energy emulsification, which originates from the very specific behavior of nonionic PEGylated surfactants. One experimental obser-vation that supports the fact that the same behavior of nonionic surfactants

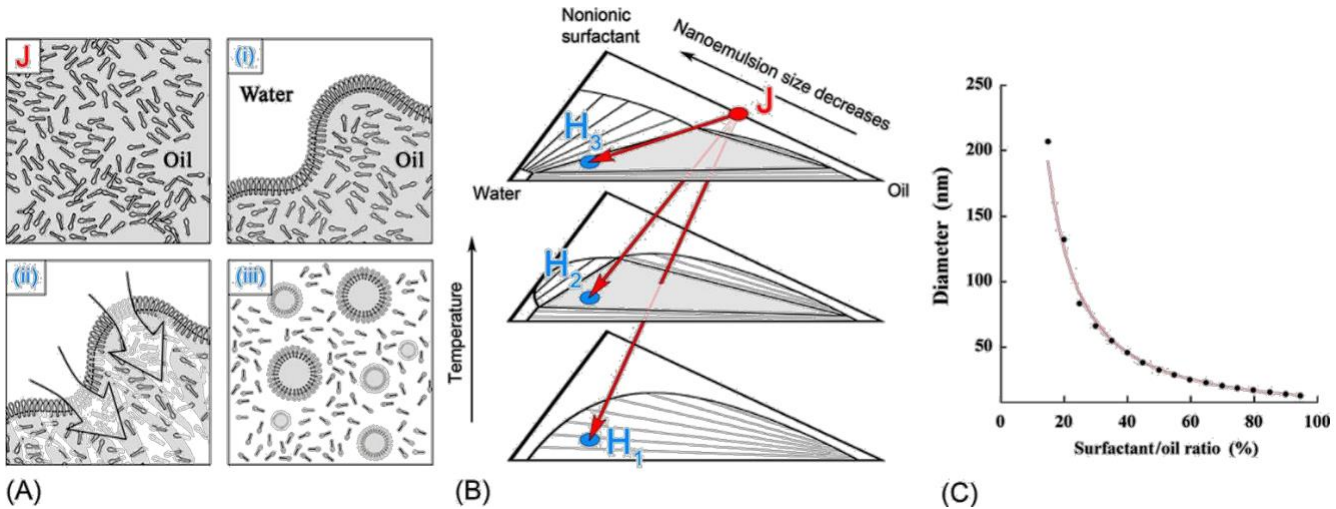

FIG. 4.6 (A) Schematic illustration of nanoemulsion formation using the spontaneous emulsification process. Point J corresponds to the compositions shown in Fig. 4.3, and the schemes (i), (ii), and (iii) show the nanoemulsification mechanism in chronological order after dilution of the oil/surfactant mixture with water. (B) Shown is the thermodynamic configuration of the system, before (J) and after the spontaneous emulsification process, dilution at the same temperature T > PIT (H3), at T ¼ PIT (H2), and at T < PIT (H1). (C) Nanoemulsion diameters are shown as a function of the surfactant content, after nanoemulsification by the spontaneous emulsification method (surfactant ¼ Kolliphor HS15, oil ¼ Labrafil M1944CS (oleoyl macrogolglycerides), and aqueous phase ¼ MilliQ water; curve fit is a power law, to guide the eye). (Reproduced with permission from Anton, N., Vandamme, T.F., 2009. The universality of low-energy nano-emulsification. Int. J. Pharm. 377, 142–147.)

drives the nanoemulsification mechanism and thus the concept of universality is the effect of the surfactant-to-oil ratio on the nanoemulsion droplet size, which follows the same trend whatever the method. The results shown in Fig. 4.5 illustrate this fact for the PIT method, and the ones shown in Fig. 4.6C for the spontaneous emulsification method. To further support this idea of universality, the PIT and the spontaneous emulsification methods are compared now with the same system (Kolliphor HS15/Labrafil M1944CS), on the one hand following the spontaneous emulsification procedure for different SOR and, on the other hand, following the PIT method over the same SOR range and also with different WOR.

The results reported in Fig. 4.7 show the direct correspondence between the two methods. In both cases, the droplet size of the nanoemulsions depends neither on the method (at least for SOR 30%) nor on the WOR value, but only on the surfactant concentration (SOR value), corroborating the predominant role of the nonionic surfactant in the process and its governing role in the universal nanoemulsification process.

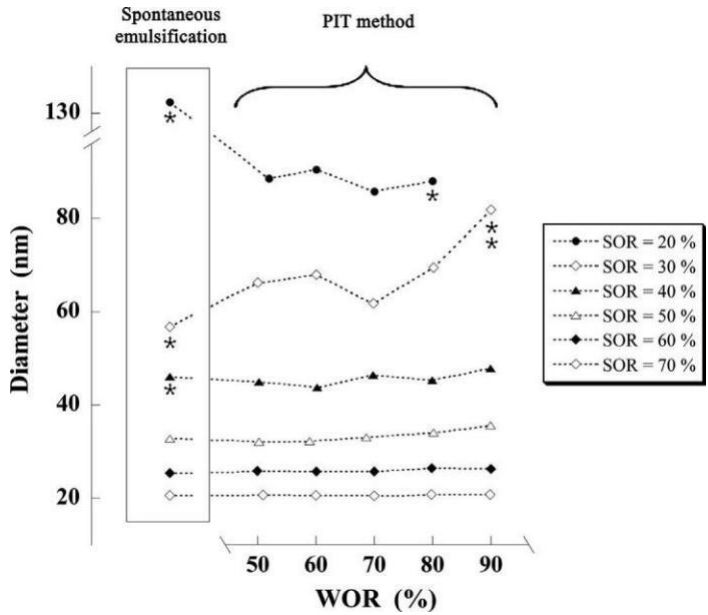

FIG. 4.7 Size of nanoemulsions obtained from the spontaneous emulsification and PIT methods, for different surfactant (SOR) and water (WOR) contents. Surfactant ¼ Kolliphor HS15, oil ¼ Labrafil M1944CS, and aqueous phase, MilliQ water. Two stars ¼ PDI >c0.2; one star ¼0.1 < PDI < 0.2, and no star ¼ PDI <0.1. (Reproduced with permission from Anton, N., Vandamme, T.F., 2009. The univer-sality of low-energy nano-emulsification. Int. J. Pharm. 377, 142–147.)

4.3.3 Critical Difference Between Spontaneous Nanoemulsions and Microemulsions

In a chapter on low-energy nanoemulsification, it appears important to emphasize a confusion that is often made between nanoemulsions and microemulsions (Anton and Vandamme, 2011; McClements, 2012). In fact, in some cases, the structure and morphology of microemulsions can be very close to the one of nanoemulsions, that is, in the form of spherical swollen micelles. On the other hand, as we have seen in the previous section, the formation of nanoemulsions by spontaneous emulsification can be very close to the methodology used to fabricate microemulsions. These two factors have led to some of the confusion between nanoemulsions and microemulsions, with undeniable impact on their potential applications.

The first comment concerns the stability of nanoemulsions. Like almost all emulsified systems, they exist in a metastable thermodynamic state, rather than in the state with the lowest free energy. However, due to the small droplet size (which reduces gravitational separation and droplet aggregation), the main pro-cess inducing their destabilization is Ostwald ripening. This factor results in sta-bility of nanoemulsions for months and even higher if specific additives (ripening inhibitors) slow down interdroplet oil transfer. On the other hand, microemulsions are stable systems from a thermodynamic point of view. They are formed as a result of the equilibrium between oil, water, and surfactants, namely, all the phases are mixed homogeneously, whatever the order of intro-duction, and the mixture is sealed and set at constant temperature until equilib-rium is reached. However, the structure of microemulsions can change considerably when the composition, temperature, and other parameters (such as electrolyte, cosurfactant, or cosolvent concentration) are varied. Let us con-sider a phase diagram (Fig. 4.8), showing some particular structures of micro-emulsions formed at a temperature below the cloud point (T

<T(cpβ)). The point K1 is the extreme case of a microemulsion (i.e., without oil), which occurs when the surfactants are at a level above the CMC. Under these conditions, the surfactants spontaneously form aggregates (typically containing tens or hun-dreds of molecules) that have diameters below about and are in equilibrium with water (which contains surfactant monomers at a concentration close to the CMC). Now, if we add to this system a small amount of oil but keep the system in

the one-phase region (point K2), oil molecules are naturally entrapped inside the micelles, forming swollen micelles. These swollen micelles show spherical nanodomains dispersed in water and potentially have diameters between about 30 and 100 nm, which actually present a structure very close to the one of nanoemulsions with the fundamental difference in their stability and formula-tion method. If further oils are added to the systems, making it crossing the phase

boundary to a WOR ¼ 50% (point K3, two-phase region), the micelles cannot "absorb" such a quantity of oil, and the excess oil appears at the top of the flask. If the content of surfactant is further increased, the system will cross

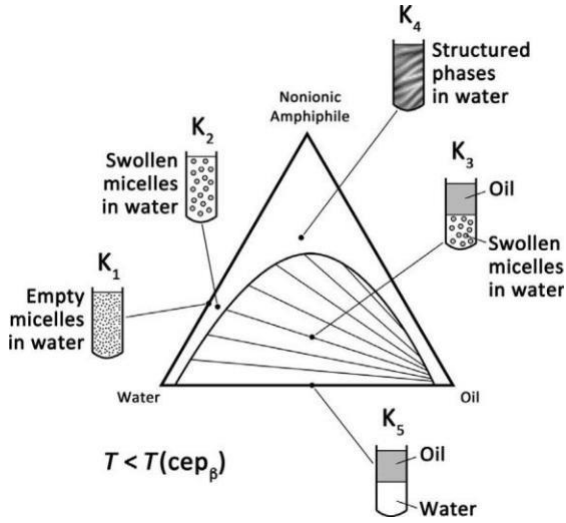

FIG. 4.8 Ternary diagram showing schematically the location of microemulsions and their structures (see details in the text). (Reproduced with permission from Anton, N., Vandamme, T.F., 2011. Nano-emulsions and micro-emulsions: clarifications of the critical differences. Pharm. Res. 28, 978–985.)

again the phase boundary (point K5), and a one-phase bicontinuous microemulsion is generated. Point K5 simply shows the corresponding system with no surfactant, oil, and water at equilibrium.

This schematic representation lets us understand that, for a certain compo-sition corresponding to K2, the particles in a microemulsion are morphologi-cally very close to the ones in a nanoemulsion. In addition, the method of forming nanoemulsions by spontaneous emulsification appears very close to the method used to form microemulsions (describe above), with the main dif-ference being that the order of mixing and introduction of the different com-pounds matters a lot. It is important to clarify this point, because the formulation methodologies for nanoemulsions and microemulsions could appear very similar, but the behaviors of these two colloidal dispersions are quite different. However, even if the formulation of microemulsions seems very simple and more convenient, the intrinsic properties of microemulsions are less compatible with the applications as drug delivery systems. The first reason is the limited concentration of droplets; the feasibility domain of spherical micro-emulsions shown in Fig. 4.8 is quite small, meaning that the possible WOR values are only high; thus, oil concentration is low, as opposed to nanoemul-sions where oil amount can easily increase higher than 20% of the nanoemul-sion (Anton and Vandamme, 2009). The second reason is the stability: even if microemulsions are thermodynamically stable, unlike the nanoemulsions, they are not stable against the modification of thermodynamic conditions like tem-perature or dilution that could correspond to a parenteral administration.

For instance, the dilution of a microemulsion with water makes the system move toward the water corner, which can potentially change the structure and size of the particles and potentially cause precipitation of an encapsulated drug.

4.4 APPLICATIONS OF TRANSITIONAL NANOEMULSIONS FOR ENCAPSULATION OF ACTIVE PRINCIPLE INGREDIENTS

This last section will detail some potential applications of spontaneous emulsification for forming nanoemulsion-based systems. These potential applica-tions include the homogeneous and stable dispersion in water of lipophilic molecules, drugs, contrast agents, imaging probes, and polymers. Therefore, the question we address here deals with the potential influence of the encap-sulation of such API on the emulsification process itself. The examples pre-sented in this work support the idea that the chemical nature of the compounds used matters a lot. Due to differences in the specific affinities of nonionic sur-factants for different oil and water phases, it may be possible to form a nanoe-mulsion with one type of oil, but not with another type of oil, using the same procedures. This signifies the fact that a modification of the composition of the oil, for the same surfactant and the same proportions, can have significant consequences on the nanoemulsion droplet size and polydispersity. This effect may also be important when lipophilic API are solubilized in the oil phase and depend on the chemical characteristics and concentrations used. Some exam-ples are reported in Fig. 4.9, showing the impact of the nature of the oil, sol-ubilization of drug, and chemical modification of the oil, on the nanoemulsification process. Fig. 4.9A shows typical size-SOR graphs for nanoemulsions generated by spontaneous emulsification (Anton and Vandamme, 2009) performed with the same surfactant (Kolliphor HS15) and the same protocol (temperature of dilution at 90°C) and different oils: Labrafac WL (medium-chain triglycerides) and Labrafil M1944CS (oleoyl macrogolglycerides). These results clearly illustrate the discussion above; the chemical nature of the oil phase is a key parameter driving the efficiency of spontaneous emulsification, revealed by a difference in the droplet sizes obtained, which can be, for example, around 100 nm for SOR ¼40%. Inter-estingly, the two curves meet each other for the highest surfactant concentra-tions, in accordance with the fact that nonionic surfactants override the effects of oil, for example, at SOR >80%.

The two other examples presented in Fig. 4.9(B1) and (B2) show the nanoe-mulsification processes (Vandamme and Anton, 2010) still performed using the same conditions, for Kolliphor ELP/Labrafil M1944CS and Kolliphor HS15/Labrafac WL, respectively. These two sets of results compare the nanoemulsions encapsulating a lipophilic drug (diclofenac at 1 wt% in oil, diclofenac-loaded nanoemulsions) with the empty nanodroplets (drug-free nanoemulsions), and the results give very close curves, whatever the surfactant

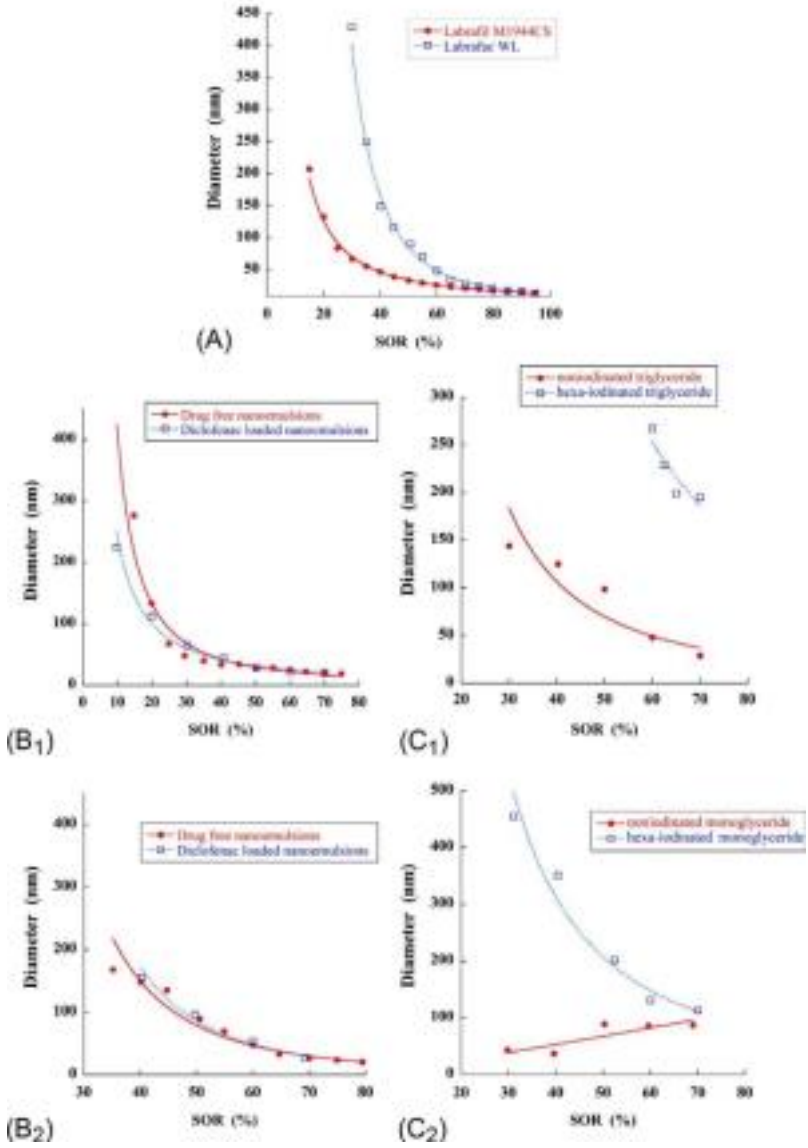

FIG. 4.9 Nanoemulsions formed by spontaneous emulsification, presenting the effect of the surfactant content (SOR) on the mean droplet size of the dispersion: (A) comparing the nature of oil; (B) comparing the presence and absence of lipophilic drugs at 1 wt% in the oil core; and (C) comparing the chemical modification of oils (see the text for details on the compositions for each case). (Reproduced with permission from (A) Anton, N., Vandamme, T.F., 2009. The univer-sality of low-energy nano-emulsification. Int. J. Pharm. 377, 142–147; (B) Vandamme, T.F., Anton, N., 2010. Low-energy nano-emulsification to design veterinary controlled drug delivery devices. Int. J. Nanomedicine 5, 867–873); (C) Attia, M., Anton, N., Chiper, M., Akasov, R., Anton, H., Messaddeq, N., Fournel, S., Klymchenko, A., Mely, Y., Vandamme, T.F., 2014. Biodistribution of X-ray iodinated contrast agent in nano-emulsions is controlled by the chemical nature of the oily core. ACS Nano 8, 10537–10550.)

oil system. Even if the curves are not exactly superimposed, in that case, the presence of drug solubilized at 1 wt% does not affect this robust process. On the other hand, if the oil is chemically modified to graft iodinated com-pounds (two triiodobenzene function per oil molecules) for imaging applica-tions, the process is seriously affected. This is the case shown in Fig. 4.9C1 and C2 (Attia et al., 2014), for triglycerides and monoglycerides, respectively, where the noniodinated molecules are presented with the filled circles (plain lines) and the iodinated compounds with empty squares (dashed lines). The difference between these two curves is important, and in fact, the molecule iodination results in a decrease of the efficiency of the process, either significantly increase the droplet size or simply not allow the emulsification to occur as in Fig. 4.9C1 for SOR values below 60%. This is likely due to an increase of the lipophilicity of the oily molecules after iodination that probably reduces the solubility of nonionic surfactants. This result supports the first observation shown in Fig. 4.9A that the nature of the oil importantly matters. To conclude, this section reports representative examples of nanoemul-sification produced by spontaneous emulsification, comparing different oils with the same nonionic surfactant, or encapsulating a lipophilic drug. It appears that the process is robust enough for keeping the same efficiency with including an API solubilized at 1 wt%. Other examples in the literature (Kilin et al., 2014) show that the efficiency of the process is conserved up to 8% (of lipophilic near-infrared dyes in oil). However, it is drastically influ-enced by the nature of the oil and notably by a change of the lipophilic properties of oils.

As a last remark, it should be noted that spontaneous nanoemulsification has also been adapted to the encapsulation of hydrophilic pharmaceutical ingredi-ents using various formulation strategies. The first strategy was to incorporate hydrophilic species directly into the oil phase using reverse micelles (Vrignaud et al., 2011; Anton et al., 2010), following exactly the same formulation proce-dure as described above (PIT method) with oils containing model hydrophilic dyes like fluorescein sodium salt or doxorubicin hydrochloride. The second strategy involved adapting the spontaneous emulsification method for the for-mulation or reverse nanoemulsions, that is, W/O nanoemulsions. This proce-dure has been described by several research groups (Vrignaud et al., 2013; Anton et al., 2009; Assadpour et al., 2016a,b; Assadpourand and Jafari, 2017; Mohammadi et al., 2016a,b; Esfanjani et al., 2015, 2017; Mehrnia et al., 2016, 2017) and allowed the fabrication of W/O/W nanoemulsions by carrying out a second emulsification of the primary W/O nanoemulsion. These studies allowed the encapsulation of model hydrophilic dyes (methylene blue); proteins (bovine serum albumin) (Vrignaud et al., 2013; Anton et al., 2009); and other bioactive compounds like folic acid, crocin, olive leaf phenolics, and saf-fron extract (Assadpour et al., 2016a,b; Assadpourand and Jafari, 2017; Mohammadi et al., 2016a,b; Esfanjani et al., 2015, 2017; Mehrnia et al., 2016, 2017).

4.5 CONCLUSION

In this chapter, the principles of nanoemulsion formation by low-energy tran-sitional methods were presented. At first, we presented the main phenomenon driving the low-energy emulsification methods, which is based on the physico-chemical behavior of nonionic surfactants. We discussed not only this behavior in terms of the interactions between the PEG moiety and water phase and the role of temperature causing the cloud point but also other factors like the type and level of electrolytes in water, impacting directly on the location of the phase boundary. Then, the link between the physicochemical behavior of nonionic surfactants and nanoemulsification was developed, through a discussion of the PIT and spontaneous emulsification methods. The different ways to perform these nanoemulsification methods, the impact of composition and temperature, and their limitations were presented and critically assessed. A link between phase diagrams (reflecting surfactant behavior) and the nanoemulsification pro-cess (due to temperature and/or composition changes) was highlighted. Through the nanoemulsion properties, mainly size and polydispersity, the PIT and spontaneous emulsification methods were compared. We emphasized a universality of the emulsification mechanism based on the behavior of non-ionic surfactants. The critical difference between microemulsions and nanoe-mulsions was highlighted. Finally, the impact of including active ingredients or changing the nature of the oil phase on the formation of nanoemulsions by the transitional emulsification method was presented, because this has important implications for the practical application of this technology.

REFERENCES

Anton, N., Vandamme, T.F., 2009. The universality of low-energy nano-emulsification. Int. J. Pharm. 377, 142–147.

Anton, N., Vandamme, T.F., 2011. Nano-emulsions and micro-emulsions: clarifications of the critical differences. Pharm. Res. 28, 978–985.

Anton, N., Benoit, J.P., Saulnier, P., 2008a. Particular conductive behaviors of emulsions phase inverting. J. Drug Delivery Sci. Tech. 18, 95–99.

Anton, N., Benoit, J.P., Saulnier, P., 2008b. Design and production of nanoparticles formulated from nano-emulsion templates—a review. J. Control. Release 128, 185–199.

Anton, N., Saulnier, P., Gaillard, C., Porcher, E., Vrignaud, S., Benoit, J.P., 2009. Aqueous-core lipid nanocapsules for encapsulating fragile hydrophilic and/or lipophilic molecules. Langmuir 25, 11413–11419.

Anton, N., Mojzisova, H., Porcher, E., Benoit, J.P., Saulnier, P., 2010. Reverse micelles-loaded lipid nano-emulsions: a new technology for the nano-encapsulation of hydrophilic materials. Int. J. Pharm. 398, 204–209.

Arai, H., 1967. Relation between the cloud points and the properties of micelles of nonionic detergents. J. Colloid Interface Sci. 23, 348–351.

Assadpour, E., Maghsoudlou, Y., Jafari, S.M., Ghorbani, M., Aalami, M., 2016a. Optimization of folic acid nano-emulsification and encapsulation by maltodextrin-whey protein double emulsions. Int. J. Biol. Macromol. 86, 197–207.

Assadpour, E., Jafari, S.M., Maghsoudlou, Y., 2016b. Evaluation of folic acid release from spray dried powder particles of pectin-whey protein nano-capsules. Int. J. Biol. Macromol. 95, 238–247.

Assadpour, E., Jafari, S.M., 2017. Spray drying of folic acid within nano-emulsions: optimization by Taguchi approach. Drying Technol. 35 (9), 1152–1160.

Astaraki, A.M., 2016. The effect of concentration of surfactant and electrolyte on the PIT and droplet sizes nanoemulsions of n-dodecane in water. Russ. J. Appl. Chem. 89, 84–89.

Attia, M., Anton, N., Chiper, M., Akasov, R., Anton, H., Messaddeq, N., Fournel, S., Klymchenko, A., Mely, Y., Vandamme, T.F., 2014. Biodistribution of X-ray iodinated contrast agent in nanoemulsions is controlled by the chemical nature of the oily core. ACS Nano 8, 10537–10550.

Dorenand, A., Goldfarb, J., 1970. Electrolyte effects on micellar solutions of nonionic detergents. J. Colloid Interface Sci. 32, 67–72.

Esfanjani, A.F., Jafari, S.M., Assadpour, E., Mohammadi, A., 2015. Nano-encapsulation of saffron extract through double-layered multiple emulsions of pectin and whey protein concentrate. J. Food Eng. 165, 149–155.

Esfanjani, A.F., Jafari, S.M., Assadpour, E., 2017. Preparation of a multiple emulsion based on pectin-whey protein complex for encapsulation of saffron extract nanodroplets. Food Chem. 221, 1962–1969.

Goldstein, R.E., 1984. On the theory of lower critical solution points in hydrogen-bonded mixtures. J. Phys. Chem. 80, 5340–5341.

Gu, T., Qin, S., Ma, C., 1989. The effect of electrolytes on the cloud point of mixed solutions of ionic and nonionic surfactants. J. Colloid Interface Sci. 127, 586–588.

Hsiao, L., Dunning, H.N., Lorenz, P.B., 1956. Critical micelle concentrations of polyoxyethylated non-ionic detergents. J. Phys. Chem. 60, 657–660.

Izquierdo, P., Esquena, J., Tadros, T.F., Dederen, J.C., Feng, J., Garcia-Celma, M.J., Azemar, N., Solans, C., 2004. Phase behavior and nano-emulsion formation by the phase inversion temperature method. Langmuir 20, 6594–6598.

Karlstrom, G.J., 1985. A new model for upper and lower critical solution temperatures in poly(ethylene oxide) solutions. J. Phys. Chem. 89, 4862–4964.

Kilin, V., Anton, H., Anton, N., Steed, E., Vermot, J., Vandamme, T.F., Mely, Y., Klymchenko, A.S., 2014. Counterion-enhanced cyanine dye loading into lipid nano-droplets for single particle tracking in zebrafish. Biomaterials 35, 4950–4957.

Klassen, P.L., George, Z., Warwick, J., Georgiadou, S., 2014. PIT tuning effects of hydrophobic co-surfactants and drugs. Colloids Surf. A Physicochem. Eng. Asp. 455, 1–10.

Leal-Calderon, F., Scfmitt, V., Bibette, J., 2007a. Emulsification. In: Emulsion Science, Basic principles. Springer, New York, pp. 5–40 (Chapter 1).

Leal-Calderon, F., Scfmitt, V., Bibette, J., 2007b. Stability of concentrated emulsions. In: Emulsion Sciences, Basic Principles. Springer, New York, pp. 143–168 (Chapter 5).

Lee, H.S., Morrison, E.D., Frethem, C.D., Zasadzinski, J.A., McCormick, A.V., 2014. Cryogenic electron microscopy study of nanoemulsion formation from microemulsions. Langmuir 30, 10826–10833.

Li, X., Anton, N., Zuber, G., Zhao, M., Messaddeq, N., Hallouard, F., Fessi, H., Vandamme, T.F., 2013. Iodinated alpha-tocopherol nano-emulsions as non-toxic contrast agents for preclinical X-ray imaging. Biomaterials 34, 481–491.

Maclay, W.N., 1956. Factors affecting the solubility of nonionic emulsifiers. J. Colloid Sci. 11, 172–185.

Malikand, W.U., Jhamb, O.P., 1970. Critical micelle concentration of polyoxyethylated nonionic surfactants and the effect of additives. Kolloid Z. Z. Polym. 242, 1209–1211.

Malikand, W.U., Saleem, S.M., 1968. Effect of additives on the critical micelle concentration of some polyethoxylated nonionic detergents. J. Am. Oil Chem. Soc. 45, 670–672.

McClements, D.J., 2011. Edible nanoemulsions: fabrication, properties, and functional performance. Soft Matter 7, 2297–2316.

McClements, D.J., 2012. Nanoemulsions versus microemulsions: terminology, differences, and similarities. Soft Matter 8, 1719–1729.

Mehrnia, M.A., Jafari, S.M., Makhmal-Zadeh, B.S., Maghsoudlou, Y., 2016. Crocin loaded nanoemulsions: factors affecting emulsion properties in spontaneous emulsification. Int. J. Biol. Macromol. 84, 261–267.

Mehrnia, M.A., Jafari, S.M., Makhmal-Zadeh, B.S., Maghsoudlou, Y., 2017. Rheological and release properties of double nano-emulsions containing crocin prepared with Angum gum, Arabic gum and whey protein. Food Hydrocoll. 66, 259–267.

Mei, Z., Xu, J., Sun, D., 2011. O/W nano-emulsions with tunable PIT induced by inorganic salts. Colloids Surf. A Physicochem. Eng. Asp. 375, 102–108.

Mohammadi, A., Jafari, S.M., Assadpour, E., Esfanjani, A.F., 2016a. Nano-encapsulation of olive leaf phenolic compounds through WPC-pectin complexes and evaluating their release rate. Int. J. Biol. Macromol. 82, 816–822.

Mohammadi, A., Jafari, S.M., Esfanjani, A.F., Akhavan, S., 2016b. Application of nano-encapsulated olive leaf extract in controlling the oxidative stability of soybean oil. Food Chem. 190, 513–519.

Rao, J., McClements, D.J., 2010. Stabilization of phase inversion temperature nanoemulsions by surfactant displacement. J. Agric. Food Chem. 58, 7059–7066.

Rao, J., McClements, D.J., 2011. Formation of flavor oil microemulsions, nanoemulsions and emul-sions: influence of composition and preparation method. J. Agric. Food Chem. 59, 5026–5035.

Rayand, A., Nemethy, G., 1971. Effects of ionic protein denaturants on micelle formation by nonionic detergents. J. Am. Chem. Soc. 93, 6787–6793.

Schick, M.J., 1962a. Surface films of nonionic detergents. I. Surface tension study. J. Colloid Interface Sci. 17, 801–813.

Schick, M.J., 1962b. Surface films of nonionic detergents. I. Surface tension study. J. Colloid Sci. 17, 801–813.

Schick, M.J., 1964. Effect of electrolyte and urea on micelle formation. J. Phys. Chem. 68, 3585–3592.

Schott, H., 1973. Salting in of nonionic surfactants by complexation with inorganic salts. J. Colloid Interface Sci. 43, 150–155.

Schott, H., 1997. Effect of inorganic additives on solutions of nonionic surfactants. XIV. Effect of chaotropic anions on the cloud point of octoxynol 9 (Triton X-100). J. Colloid Interface Sci. 189, 117–122.

Schott, H., 2001. Effect of inorganic additives on solutions of nonionic surfactants—XVI. Limiting cloud points of highly polyoxyethylated surfactants. Colloids Surf. A Physicochem. Eng. Asp. 186, 129–136.

Schott, H., Han, S.K., 1975. Effect of inorganic additives on solutions of nonionic surfactants. II. J. Pharm. Sci. 64, 658–664.

Schott, H., Royce, A.E., Han, S.K., 1984. Effect of inorganic additives on solutions of nonionic surfactants. VII. Cloud point shift values of individual ions. J. Colloid Interface Sci. 98, 196–201.

Schottand, H., Han, S.K., 1976a. Effect of inorganic additives on solutions of nonionic surfactants. IV: Krafft points. J. Pharm. Sci. 65, 979–981.

Schottand, H., Han, S.K., 1976b. Effect of inorganic additives on solutions of nonionic surfactants. III: CMC's and surface properties. J. Pharm. Sci. 65, 975–978.

Schottand, H., Royce, A.E., 1984. Effect of inorganic additives on solutions of nonionic surfactants. VI: further cloud point relations. J. Pharm. Sci. 73, 793–799.

Shinoda, K., Saito, H., 1969. The stability of O/W type emulsions as functions of temperature and the HLB of emulsifiers: the emulsification by PIT-method. J. Colloid Interface Sci. 30, 258–263.

Shinodaand, K., Takeda, H., 1970. Effect of added salts in water on the hydrophile-lipophile balance of nonionic surfactants: effect of added salts on the phase inversion temperature of emulsions. J. Colloid Interface Sci. 32, 642–646.

Tadros, T.F., Izquierdo, P., Esquena, J., Solans, C., 2004. Formation and stability of nano-emulsions. Adv. Colloid Interf. Sci. 108-109, 303–318.

Tong, K., Zhao, C., Suna, D., 2016. Formation of nanoemulsion with long chain oil by W/O micro-emulsion dilution method. Colloids Surf. A Physicochem. Eng. Asp. 497, 101–108.

Vandamme, T.F., Anton, N., 2010. Low-energy nano-emulsification to design veterinary controlled drug delivery devices. Int. J. Nanomedicine 5, 867–873.

Vrignaud, S., Anton, N., Gayet, P., Benoit, J.P., Saulnier, P., 2011. Reverse micelle-loaded lipid nanocarriers: a novel drug delivery system for the sustained release of doxorubicin hydrochloride. Eur. J. Pharm. Biopharm. 79, 197–204.

Vrignaud, S., Anton, N., Passirani, C., Benoit, J.P., Saulnier, P., 2013. Aqueous core nanocapsules: a new solution for encapsulating doxorubicin hydrochloride. Drug Dev. Ind. Pharm. 39, 1706–1711.

Wartewig, S., Alig, I., Hergeth, W.D., Lange, J., Lochmann, I., Scherzed, T., 1990. Spectroscopic investigations on aqueous solution of poly(oxyethylene)-poly(oxypropylene)-poly(oxyethylene) triblockcopolymers. J. Mol. Struct. 219, 365–370.

FURTHER READING

Kahlweit, M., Strey, R., Firman, P., Haase, D., Jen, J., Schomaecker, R., 1988. General patterns of the phase behavior of mixtures of water, nonpolar solvents, amphiphiles, and electrolytes. Langmuir 4, 499–511.

Chapter 5

Synthesis of W/O nano-emulsion by spontaneous emulsification

Synthesis and Physicochemical Characterization of Water in Oil Nano-Emulsion Prepared by Spontaneous Emulsification

Salman Akram, † Thierry Vandamme, Nicolas Anton†

† Université de Strasbourg, CNRS, CAMB UMR 7199, F-67000 Strasbourg, France

Abstract

Spontaneous emulsification is an interesting method for generating nano-emulsions because of simplicity of the process. Experimental procedure does not involve use of any specialized instrument or external energy for creating nano-droplets. In our study, we have exploited spontaneous emulsification to produce water-in-oil nano-emulsions. The water-in-oil nano-emulsions are a system able to encapsulate hydrophilic molecules. It can offer an alternative to liposomes and double emulsions for hydrophilic drug delivery. In our study, we have investigated the spontaneous emulsification processes to produce water-in-oil nano-emulsions, by two different methods. We have shown that by changing surfactant concentration, surfactant type, phase ratio and oil type, the particle size and polydispersity of the nano-emulsions can be controlled. Irrespective of the method, surfactant type, phase ratio and oil type, increasing the surfactant to oil ratio always lead to decrease in the particle size. The study offers new horizon for hydrophilic drug encapsulation and drug delivery.

Keywords: Spontaneous emulsification; nano-emulsification; surfactants; water-in-oil nano-emulsion.

1. Introduction

Nanomedicine has emerged an important field of research from the past few decades due to number of advantages over conventional therapeutic option [1, 2]. Nano-emulsions are one of the most important drug vehicles in nanomedicine which offer the possibility of carrying both hydrophilic
[3] or lipophilic drugs [4] or both at the same time in form of double nano-emulsions [5, 6]. Nano-emulsions have certain advantages such as low toxicity, high physical stability, high absorption value, improved bioavailability of drugs, helps to mask taste [7, 8]. An important consideration about nano-emulsions is that they are thermodynamically unstable and kinetically stable [9]. Their thermodynamic instability is mainly because their free energy is greater than zero. The free energy depends upon interfacial area and surface tension and upon mixing of two different phases these two factors leads to free energy greater than zero and hence in thermodynamic instability of nano-emulsions [10]. On the other hand, gravitational separation and droplet aggregation is very small due to very small size of nano droplets and hence it makes these systems kinetically stable [11]. The main mechanism of their breakdown is Ostwald ripening [12], that is growth in formation of large droplets favored by diffusion of oil molecules through the aqueous phase. Therefore, we prefer nano-emulsions with narrow particle size distribution and addition of ripening inhibitors to reduce Ostwald ripening [13].

Nano-emulsions can be formed by several ways that are mainly divided into the high energy and low energy methods [10, 14]. The most popular high energy methods are high speed homogenization, Micro fluidization and Ultrasonication [10] . The low energy methods [15] also known as transitional nano-emulsification methods are mainly divided in literature as phase inversion and spontaneous emulsification methods. In this project, we have made our nano emulsion by a low energy method known as spontaneous emulsification method. So, we will investigate the detail of this method,

mechanism of formation of nano-droplets and some of the most important factors that influence the formation of nano particles by this method.

Spontaneous emulsification simply involves gentle mixing of two different liquid phases into each other in a way that intrinsic physico-chemical properties of surfactants are exploited to create the nano droplets [8]. One of the main advantages of spontaneous emulsification is that they offer the formation of nano-emulsions without the use of any specialized instrument with robustness [16]. They can be used for the formulation of sensitive components that are prone to degradation by high energy methods such as some sensitive proteins. Spontaneous emulsification process is mainly driven by the properties of surfactant and surfactant to oil ratio (SOR) entering in the formulation composition [17]. High SOR leads to smaller droplet size as compared to low SOR, which is mainly because the high surfactant amount leads to greater disorder in the system and more turbulent flow inside the system as compared to low surfactant amount upon addition of other liquid phase in which surfactant is normally more soluble. This greater disorder leads to more powerful turbulent flow and hence decrease in particle size [8, 10, 17].

Spontaneous emulsification is mainly used for the encapsulation of lipophilic drugs by making O/W nano-emulsions [10]. However, in our paper we have used it for the encapsulation of hydrophilic materials by making W/O nano emulsions. We have introduced two very novel methods to create W/O nano-emulsion, following the same principle of spontaneous emulsification. We have shown that both these methods are compatible with a range of phase ratios between oil and aqueous phase, different surfactants and mixtures of surfactants, types of oil and other such variables.

2. Materials and Methodology

a) Materials

Model parenteral oil compatible with parenteral administration (Labrafac® WL 1349) was obtained from Gattefossé S.A., Saint-Priest, France. This is a mixture of capric acid and caprylic acid. Whereas peanut oil, mineral oil, olive oil, soya bean oil, sesame oil, span 80 and span 85 were purchased from Sigma Aldrich (Merck), France. Polyglycerol polyricinoleate (PGPR) was kindly gifted by Stéarinerie Dubois (Boulogne-Billancourt, France), This emulsifier is largely used for human consumption, and, e.g. approved for their used in food formulation by the FDA (Food and Drug administration) and the JECFA (Joint FAO/WHO Expert Committee on Food Additives).

b) Methodology

The Inverse nanoemulsions are made by two unique methods mentioned here as Method A and Method B.

Method A

In method A, nano-emulsions were prepared by spontaneous emulsification by the controlled addition of the aqueous phase in the oil plus surfactant mixture. The experiments were conducted in a 100 mL beaker at room temperature (20°C). In all the experiments, final nano-emulsion always have a total volume of 10 mL. Initially, oily phase was prepared by mixing oil and lipophilic surfactants, and then gently mixed using them magnetic stirrer (at a fixed velocity, varied in function of the experiments). for 5 minutes. Aqueous phase was added at a predetermined constant rate to the oily phase by a peristaltic pump over a definite predetermined time. Then the W/O nano-emulsion formed and was further homogenized for five more minutes. Important to note that the further

homogenization did not lead to any improvement in the formulation regarding particle size and dispersity.

Method B

In the method B, nano-emulsions were prepared by another method of spontaneous emulsification & involves gentle mixing of oil to mixture of lipophilic surfactant and water. The experiments were conducted in 4 mL glass vial at room temperature. In all the experiments, final nano-emulsion always have a total volume of 2 mL. Initially, lipophilic surfactant was mixed with water & homogenized by magnetic stirrer at 500 rpm for five minutes. Then oil was added instantaneously by disposable pipette and the mixture was homogenized by vortex mixing for 5 minutes.

c) Physico-chemical Characterization and Variables tested

Particle Size and Dispersity value was determined by zeta sizer (Malvern (Malvern ZS 90) for all the different formulations of primary emulsions. The reverse nano-emulsions, formerly opaque (since concentrated) were diluted with the continuous oil phase till they become totally transparent. Then, one more little drop of nano-emulsions was added into the dilution to make the translucent sample ready to be characterized. For each formulation three readings were taken by the instrument. As each formulation was repeated three times, so the final value reported was average of total nine readings.

For method A, a variable (i.e. effect of different process parameters) on particle size and dispersity was noted. Then for both methods, three different additional variables were tested (i.e., effect of surfactant nature and surfactant mixture, effect of phase ratio and effect of oil nature).

Effect of process parameters

For method A exclusively (since not applicable to method B), influence of process parameters such as aqueous phase addition rate and homogenization speed was noted on the particle size at fixed SOR of 20 % and Phase ratio of Oil / Aqueous phase of 80 : 20. Aqueous phase addition rates of 0.1, 0.2, 0.4, 0.8 and 1 mL/min were explored whereas homogenization speed of 100, 300, 500, 700 and 1000 rpm were investigated. For these set of experiments, oil phase was containing PGPR and Labrafac in oil phase where aqueous phase contains simple distilled water.

Effect of surfactant nature and surfactant mixture at different surfactant to oil ratios

In the next set of experiments, the influence of surfactant to oil ratios and surfactant type on particle size was investigated. In these set of experiments phase ratio of oil/aqueous was set at 90:10 and SOR was varied from 5 % to 25 %. Three different surfactants PGPR, Span 80 and Span 85 was tested with Labrafac oil in the oil phase separately. Aqueous phase simply consisted of distilled water and for the method A it was added at rate of 0.4ml/minute for these set of experiments.

In addition, when pure surfactants were used above, different surfactant mixtures in different ratios of 1:3, 1:1 and 3:1 were investigated, and their effect on the particle size and dispersity. The SOR was set at 20 % and phase ratio of oil and aqueous phase was 90:10.

Effect of phase ratio at different surfactant to oil ratios

Then nano-emulsions were prepared at different phase ratios of oil/aqueous phase are 70:30, 80:20 & 90:10 at different surfactant to oil ratios. For these set of experiments the oil phase was made up of PGPR and Labrafac and aqueous phase made up of simple distilled water.

Effect of oil type

The influence of oil type was investigated by changing the oil nature into the oil phase. For these set of experiments, surfactant to oil ratio SOR = 20 % and surfactant PGPR was used.

3. Results and Discussion

a) Effect of process parameters

For the Method A, first the effect of different process parameters such as effect of aqueous phase addition rate and stirring speed was noted on particle size and dispersity. The results are shown in figure 1. It is shown that an optimum range of both of parameters is needed to produce nano-emulsion with an optimum particle size.

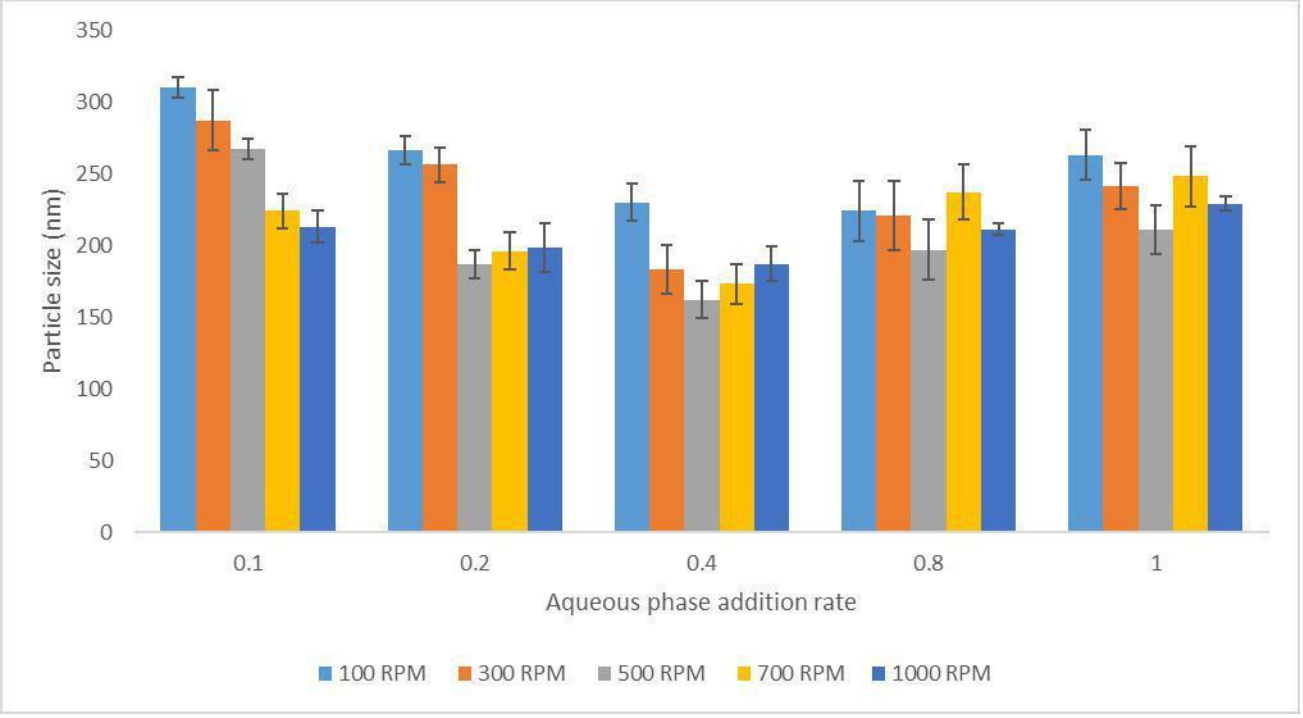

Figure 1 : Influence of process parameters i.e. stirring speed and aqueous phase addition rate on the particle size (nm)

It is reported in literature that stirring does not have any influence on the spontaneous behavior of nano-emulsion but it can increase the rate of emulsification [10]. The procedure doest not require

any external energy like in case of high-pressure homogenization and sonication but stirring always helps to speed up the process. During the procedure, the formation of new droplets is favored by stirring and literature generally mentions that increasing the homogenization speed can lead to decrease in the particle size [18]. In our procedure, this system follows the same trend from 100 to 500 rpm but above 500 rpm the particle size is again increased. This increase in this particle size is generally believed to be by re coalescence of few particles to form bigger droplets. Obviously one can predict that at a very high speed of stirring the rate of formation of new droplets is so high that newly formed surfaces does not get any surfactant molecules to stabilize them and hence coalescence happens which lead to formation of bigger droplets. This behavior for W/O nano-emulsion is well reported in literature and hence our system follows the same trend [19].

The rate of addition of water also follows the same trend as of stirring speed. By increasing the addition rate beyond 0.4 mL the nano-emulsion droplet size increases. This is explained by the fact in the dilution pathway when high amount of water is added in short time. This leads to nucleation growth and leads to increase the particle size.

b) Effect of Surfactant to oil ratio, nature of surfactants and mixture of surfactants Method A

The results of nano-emulsion droplets produced by both methods is given in the figure 2 and 3. The results clearly show that surfactant to oil ratios and surfactant type has an influence over the particle size of nano-emulsions. But before going further into the detail of this impact of surfactant on particle size, we will provide a brief overview of mechanism involved in the spontaneous emulsification by this method.

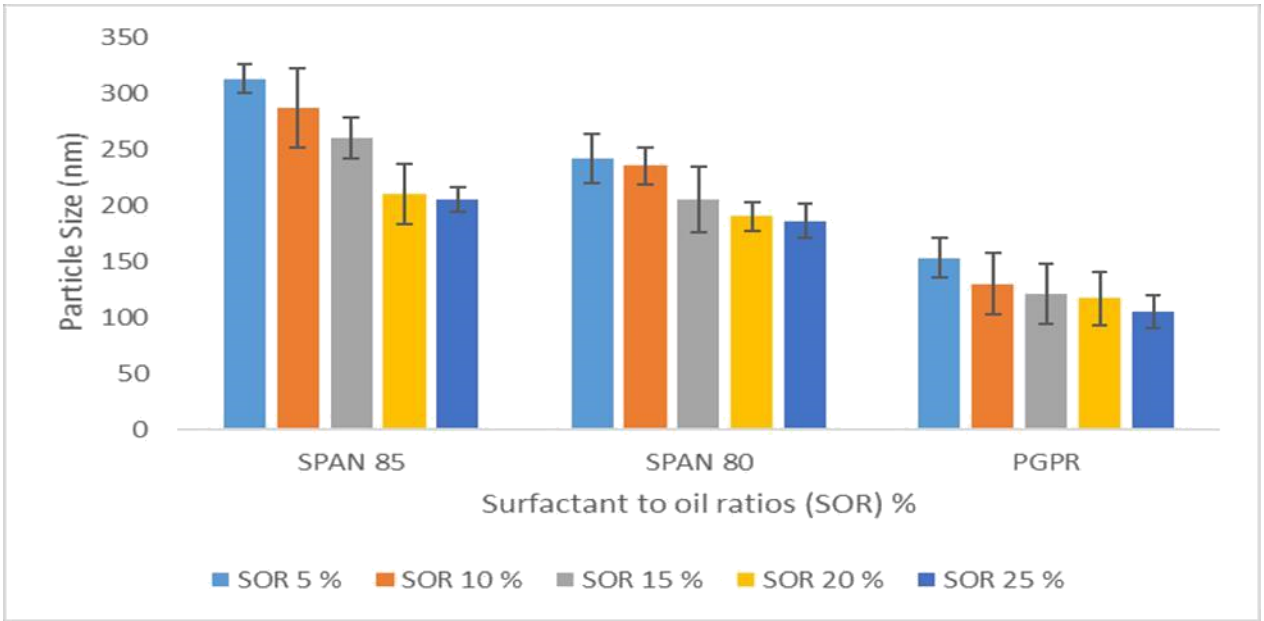

Figure 2: Influence of surfactant concentration and surfactant type on the particle size by (a) Method A and (b) Method B

In method A, nano-emulsification is done by a method known as emulsion phase inversion point method [10]. In case of W/O nano-emulsions, first microemulsion or liquid crystals are generated that are thermodynamically stable and then dilution by water molecules leads to formation thermodynamically unstable but kinetically stable nano-droplets. In our method, we progressively changed the concentration of water by adding it at a continuous rate into the oil and lipophilic surfactant. This addition leads to change the affinity of the surfactants for water and oil phases and hence creates instabilities in the phases. The oil / water interaction is weakened by this and interfacial fluctuations take place in the system, giving rise to the formation of nano-emulsion droplets.

The newly formed nano-emulsion droplets are not so stable and coalescence can happen. This will lead to formation of bigger droplets, again and so an optimum amount of surfactant is needed to cover the newly formed interfaces. The results show that the higher the concentration of surfactant, the lower is the particle size produced [20]. This is explained by the above mechanism that higher

amount of surfactant leads to stabilization of nano-emulsion droplets and prevents them from coalescence.

In the next step, different surfactant mixtures were also studied to determine the impact of the surfactant type and surfactant mixture in the particle size as shown in figure 3.

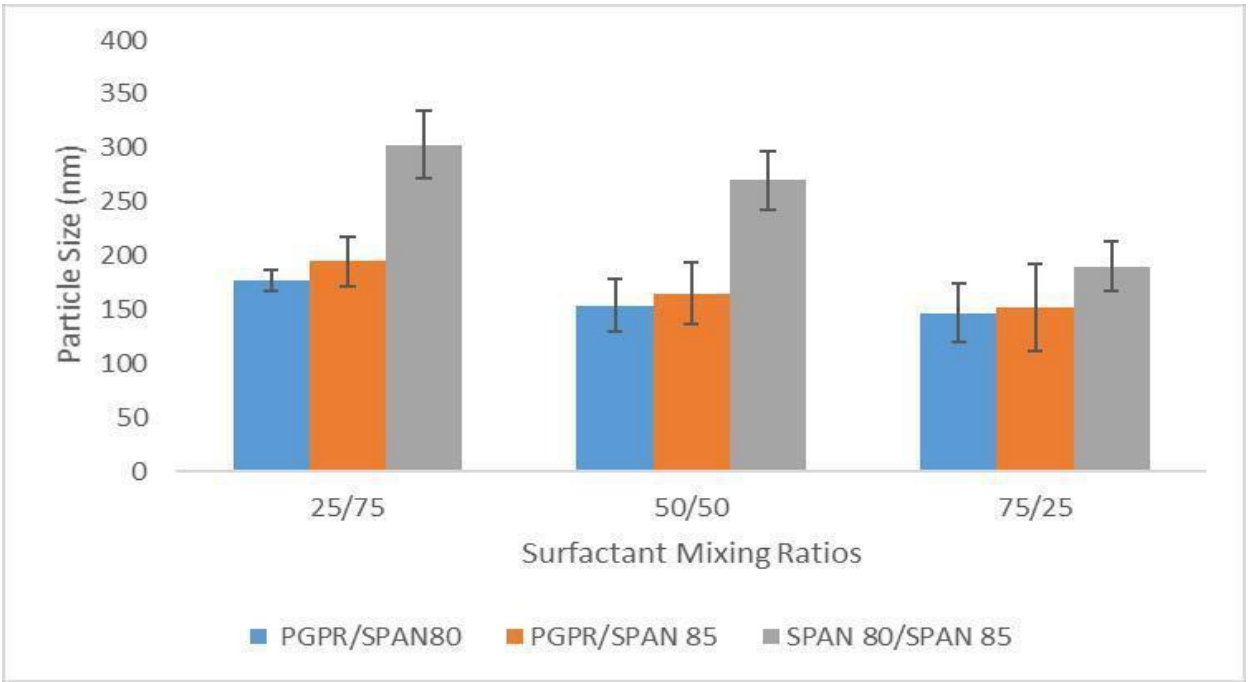

Figure 3: Influence of Surfactant Mixture on Particle Size

It I swell known that in function of the oil type, the HLB *required* will define the optimum formulation, and thus the interfacial efficiency of surfactants depends on the surfactant mixture [21, 22]. Herein we studied different mixtures made with Span 80 (HLB = 4.3), Span 85 (HLB = 1.8) and PGPR (HLB = 1.5). So, we have exploited three different lipophilic surfactants with very low HLB value for production of nano-emulsions. The higher lipophilicity of the surfactant decreases the mass transfer inside the droplets and deceases the nucleolus growth and hence leads to decrease in particle size [22].

Our results show that the particle size is affected by nature of the surfactant and follows the trend of decreasing particle size as span 85 > span 80 > PGPR. Indeed, particle size is least with the PGPR and highest with Span 85. This shows that HLB value is not the sole criteria, and the trend is not always same as some studies report not following this trend [20].

It is now believed that surfactant geometrical configuration also plays an important part in determining the final size of the nano-emulsion droplets [23]. The molecular geometry of the surfactant effects the packing parameters of the surfactant. This packing parameter have an influence on the interfacial tension and rheology of surfactant and hence can impact the spontaneous emulsification process. Another method suggests that presence of double bonds in nonpolar structure of nonionic surfactant leads to reduction in particle size of nano-emulsions [24]. This shows that surfactant HLB is not the final parameter in determining the particle size of nano-emulsions.

Method B

In method B, the results follow the same trend as we saw in the Method A as reported in Figure 4.

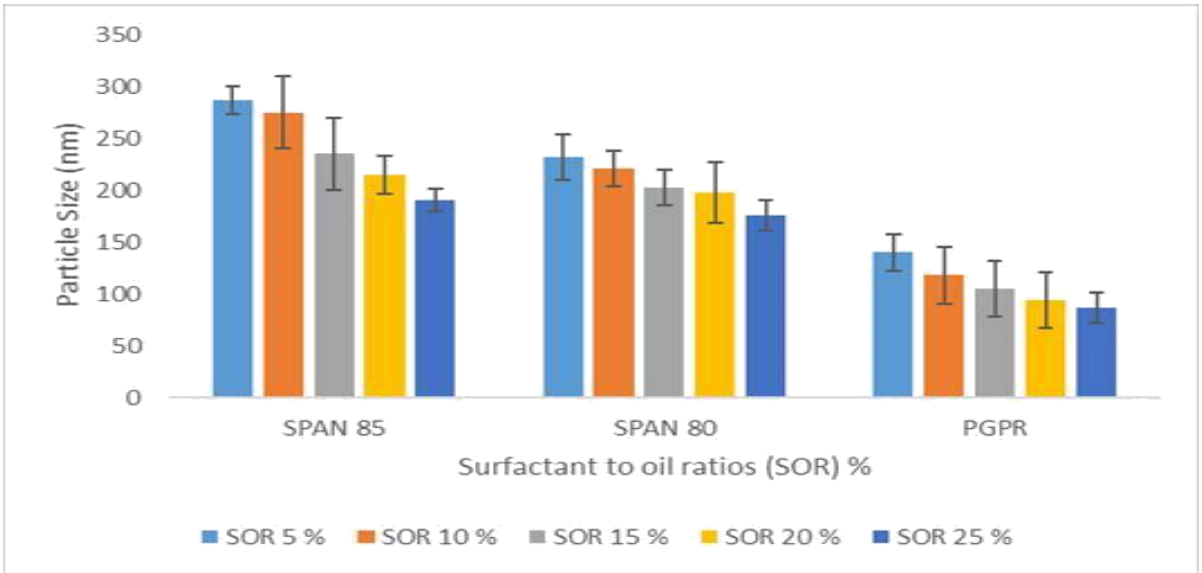

Figure 4: Influence of surfactant concentration and surfactant type on particle size (Method B)

In this method, spontaneous phenomenon simply arises from the fact that nonequilibrium states arise when two different immiscible phases are brought into contact with each other without stirring. Spontaneous emulsification only occurs under specific conditions and in a very rare case nano-emulsion droplets are produced. The surfactant is normally first added into the phase in which it is generally less soluble. Upon introduction of the second phase the surfactant diffuses into second phase because of its preferential solubility into the two phases. The emulsification is promoted by diffusion of this surfactant into the opposite phase in which it becomes more soluble after their mixing. By monitoring the diffusion pathway, we can predict the spontaneous emulsification phenomenon. The energy of spontaneous emulsification comes from the interfacial turbulence produced by the diffusion of the surfactant between two different phases. The sufficiently large interfacial turbulence leads to droplet breakup in to nano-emulsion region. Through this sight, the higher the amount of the surfactant initially in the system, the greater is interfacial turbulence produced and hence smaller is the particle size produced. This is the reason that increasing the surfactant concentration can lead to decrease in the particle size of nano-emulsions. The stirring has no influence on the intrinsic phenomenon of spontaneous emulsification, but it can increase the rate of emulsification by increasing the interfacial area [10].

PGPR produced nano-emulsions with the smaller particle size. In the next step, different surfactant mixtures ware prepared but as shown in the method A, PGPR was alone best regarding producing small particles. Moreover, higher the amount of PGPR in the mixture smallest is the particle size produced as shown in figure 5.

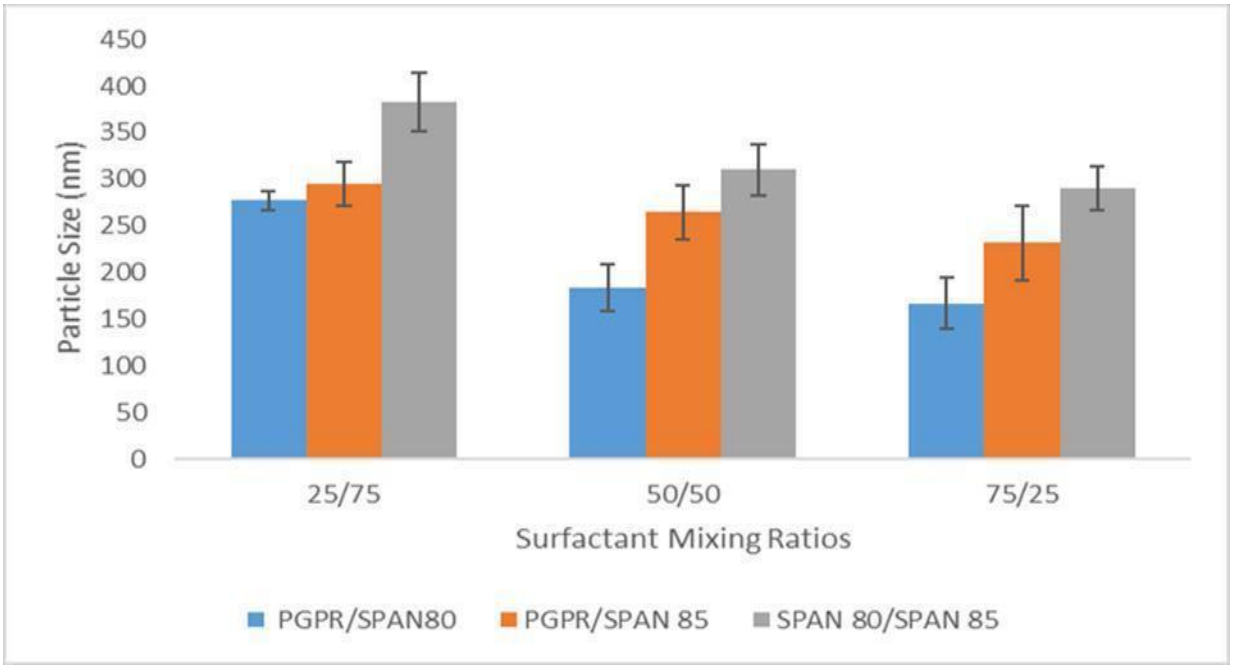

Figure 5: Influence of Surfactant Mixture on particle size (Method B)

c) Effect of Phase Ratio at different Surfactant to Oil

Ratios Method A

The particle size and PDI of different formulation is affected by changing the SOWR or phase ratio from Oil: Aqueous Phase from 70:30 to 90:10. The W/O emulsion was prepared at aqueous phase addition rate of 0.4ml/min, Homogenization Speed of 500 RPM. The oil phase contains PGPR and Labrafac whereas aqueous phase just contains distilled water.

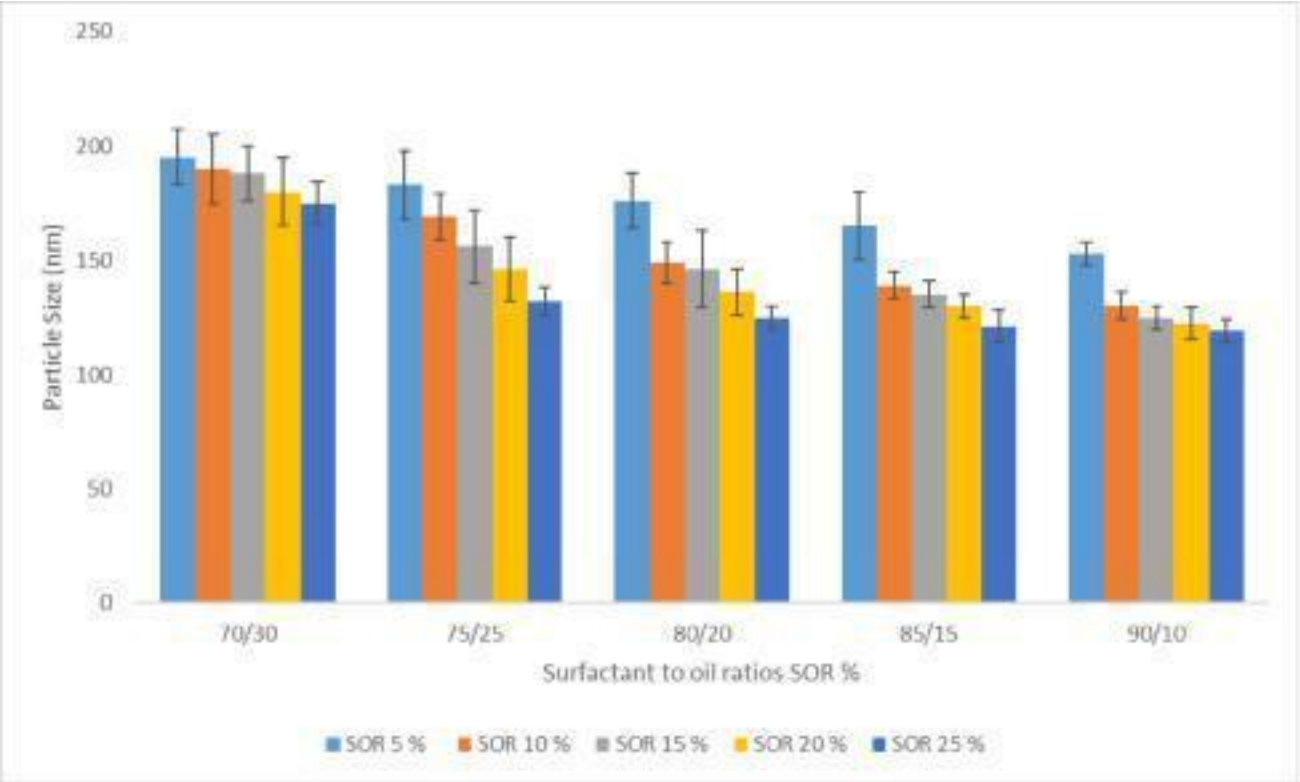

Figure 6: Influence of phase ratio or SOWR % at different Surfactant to oil ratios, Method A.

At higher SOWR of 90 %, the particle size is least dropping to 119 nm. First, as shown in the figure at every SOWR %, increasing the surfactant to oil ratios leads to decrease in the particle size. The principle behind this phenomenon is explained in the section below. When we start titrating our mixture of surfactant and oil, the microemulsion network loses its thermodynamic stability and system is favored in the nano-emulsion range. Some of the experiment have been done at SOWR 5 %, but at that phase only microemulsion lose network has been observed. When add further little water the system turns into liquid crystal phase before changing into the transparent nano-emulsion system. If we keep on adding water and go from water concentration from 10 % to 30 % the nano-

emulsion turn into the milky appearance and particle size is increased. The same phenomenon have been observed and reported before and have been reported quite frequently in literature [25, 26].

Method B

The particle size and PDI of different formulation is affected by changing the SOWR % or phase ratio as shown in Figure 7. The oil phase contains PGPR and Labrafac whereas aqueous phase just contains distilled water.

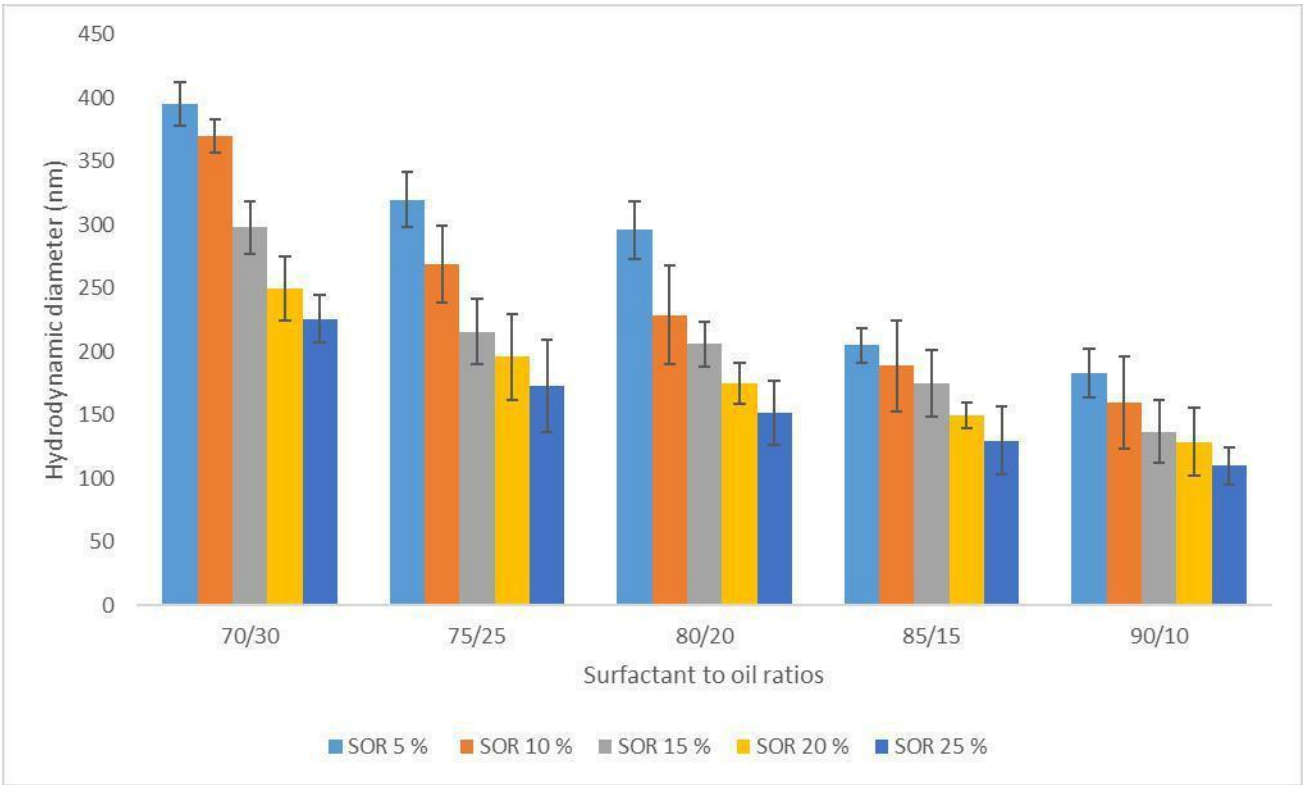

Figure 7: Influence of SOWR % on particle size at different surfactant to oil ratios, Method B.

As with Method A, method B also produced nano-emulsions of comparable particle size and dispersity values. As compared to Method A, the method B produces the particle size with smaller particle size. This is mainly because that this method exploits the intrinsic energy of the nano-emulsion component in better way. The rapid transfer of lipophilic surfactant from aqueous phase to oil leads to turbulent flow in the system and this turbulent flow leads to drop in particle size. The

higher the amount of surfactant, the higher the amount of turbulence force produced. This leads to formation of smaller particle size. Although, particle size produced is small as compared to Method A, but the dispersity is high in Method B ranging from 0.2 to 0.35.

d) Effect of oil type

Method A

The effect of different kind of different oils can have impact on the particle size of nano-emulsions. The nano-emulsion composed of PGPR, Labrafac and Distilled water and was prepared at phase ratio of oil/water 90:10 and SOR 20 %. The results are shown in the figure 8.

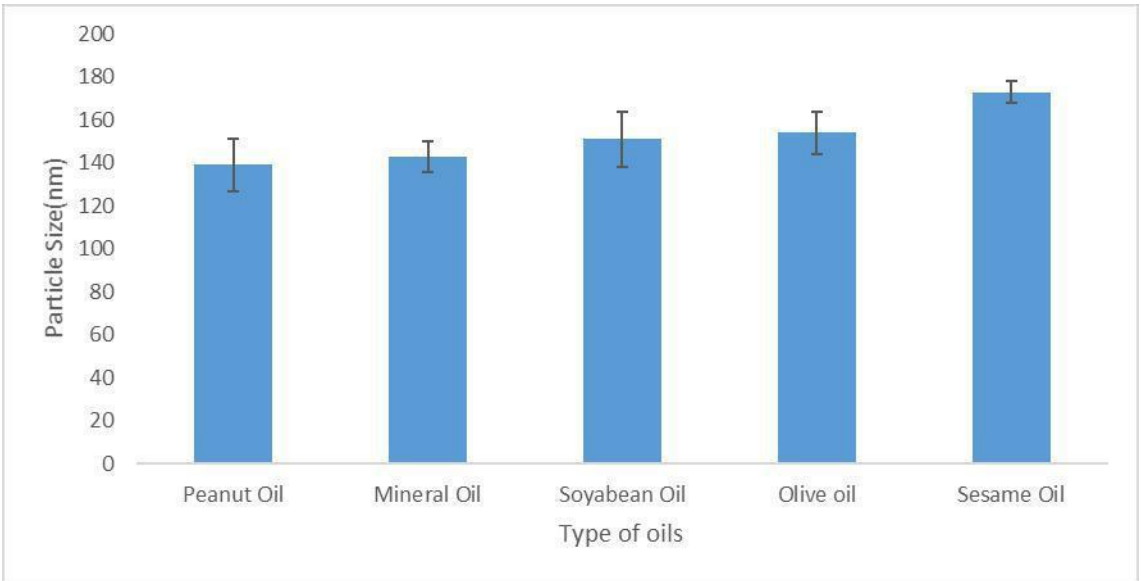

Figure 8: Impact of type of oil on particle size (nm)

The physicochemical properties of oil can have influence on the particle size of nano-emulsions. Different literature reports have proposed that viscosity can have impact on the particle size of nano-emulsions, as affecting by the critical Weber number. Increasing the oil viscosity impacts on the ratio of viscosity between dispersed and continuous phase, and thus on the break-up of the droplets during the emulsification process [8]. Accordingly, the viscosity of the oil taken alone cannot be predictive a dn in some increasing the oil viscosity leads to increase the droplet size [11, 27].

When we change the nature of oils and their impact on the droplet size, the effect is weak. The result show that the nature of oil has a limited influence on the particle size.

Method B

Similar results were found through the method B, nano-emulsions of comparable particle size was produced as shown in figure 9. There was no correlation found between the physicochemical properties of oil and particle size produced.

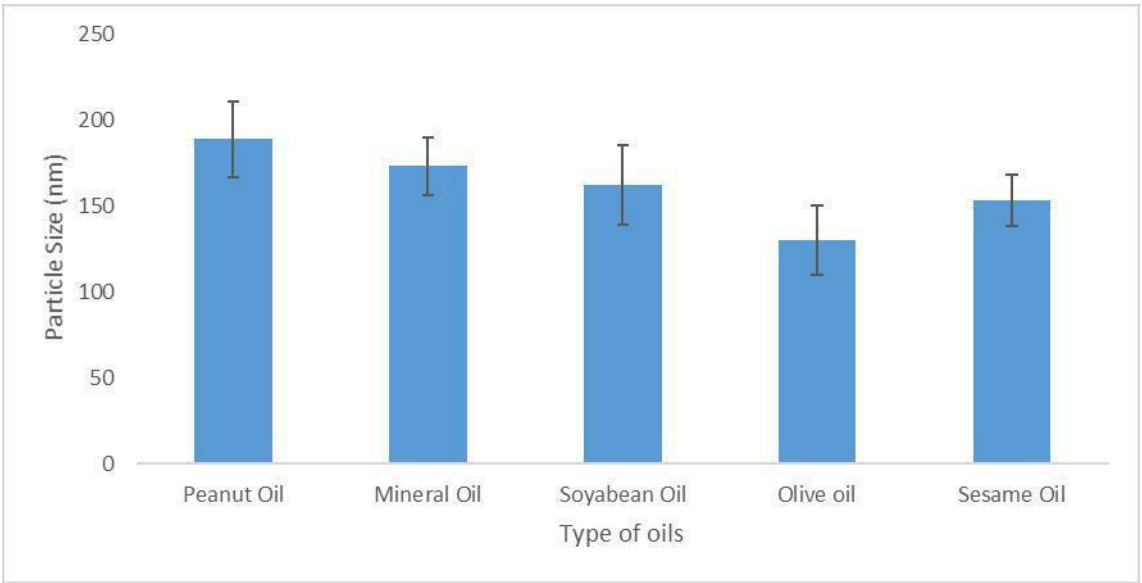

Figure 9: Impact of type of oil on particle size

4. Conclusion

The results show that our system is capable of producing W/O nano-emulsions with a range of surfactants, oils and aqueous phase composition. Both methods can be exploited to form nano-emulsions with range of particle size. In all the variables tested, surfactant to oil ratio was the main factor in determining the final particle size of nano-emulsion droplets. Moreover, surfactant type also plays an important role among other contributing processes. The real originality of the system lies in the utilization of peristaltic pump to add aqueous phase at a constant rate in the method A that helps to control the process and makes it more reproducible. Whereas other originality lies the first time use of this spontaneous emulsification pathway to produce W/O nano-emulsions. The system offers possibility of hydrophilic molecules for drug delivery and opens avenues for researchers doing research in developing different drug delivery systems for the encapsulating the hydrophilic molecules.

References

1. Liu, H. and T.J. Webster, *Nanomedicine for implants: A review of studies and necessary experimental tools.* Biomaterials, 2007. **28**(2): p. 354-369.
2. Mirza, A.Z. and F.A. Siddiqui, *Nanomedicine and drug delivery: a mini review.* International Nano Letters, 2014. **4**(1): p. 94.
3. Wu, H., et al., *Topical transport of hydrophilic compounds using water-in-oil nanoemulsions.* International Journal of Pharmaceutics, 2001. **220**(1): p. 63-75.
4. Mou, D., et al., *Hydrogel-thickened nanoemulsion system for topical delivery of lipophilic drugs.* International Journal of Pharmaceutics, 2008. **353**(1): p. 270-276.
5. Ding, S., et al., *A new method for the formulation of double nanoemulsions.* Soft Matter, 2017. **13**(8): p. 1660-1669.
6. Akram, S., et al., *Toward the Formulation of Stable Micro and Nano Double Emulsions through a Silica Coating on Internal Water Droplets.* Langmuir, 2019. **35**(6): p. 2313-2325.
7. Jaiswal, M., R. Dudhe, and P.K. Sharma, *Nanoemulsion: an advanced mode of drug delivery system.* 3 Biotech, 2015. **5**(2): p. 123-127.
8. Bouchemal, K., et al., *Nano-emulsion formulation using spontaneous emulsification: solvent, oil and surfactant optimisation.* International Journal of Pharmaceutics, 2004. **280**(1): p. 241-251.
9. McClements, D.J., *Nanoemulsions versus microemulsions: terminology, differences, and similarities.* Soft Matter, 2012. **8**(6): p. 1719-1729.
10. Anton, N., J.-P. Benoit, and P. Saulnier, *Design and production of nanoparticles formulated from nano-emulsion templates—A review.* Journal of Controlled Release, 2008. **128**(3): p. 185-199.
11. Wooster, T.J., M. Golding, and P. Sanguansri, *Impact of Oil Type on Nanoemulsion Formation and Ostwald Ripening Stability.* Langmuir, 2008. **24**(22): p. 12758-12765.
12. Taylor, P., *Ostwald ripening in emulsions.* Advances in Colloid and Interface Science, 1998. **75**(2): p. 107-163.
13. Welin-Berger, K. and B. Bergenståhl, *Inhibition of Ostwald ripening in local anesthetic emulsions by using hydrophobic excipients in the disperse phase.* International Journal of Pharmaceutics, 2000. **200**(2): p. 249-260.
14. Tadros, T., et al., *Formation and stability of nano-emulsions.* Advances in Colloid and Interface Science, 2004. **108-109**: p. 303-318.
15. Solans, C. and I. Solé, *Nano-emulsions: Formation by low-energy methods.* Current Opinion in Colloid and Interface Science, 2012. **17**(5): p. 246-254.
16. Gulotta, A., et al., *Nanoemulsion-Based Delivery Systems for Polyunsaturated (ω-3) Oils: Formation Using a Spontaneous Emulsification Method.* Journal of Agricultural and Food Chemistry, 2014. **62**(7): p. 1720-1725.
17. Anton, N. and T.F. Vandamme, *The universality of low-energy nano-emulsification.* International Journal of Pharmaceutics, 2009. **377**(1): p. 142-147.
18. Guttoff, M., A.H. Saberi, and D.J. McClements, *Formation of vitamin D nanoemulsion-based delivery systems by spontaneous emulsification: Factors affecting particle size and stability.* Food Chemistry, 2015. **171**: p. 117-122.
19. Mehrnia, M.-A., et al., *Crocin loaded nano-emulsions: Factors affecting emulsion properties in spontaneous emulsification.* International Journal of Biological Macromolecules, 2016. **84**: p. 261-267.
20. Saberi, A.H., Y. Fang, and D.J. McClements, *Fabrication of vitamin E-enriched nanoemulsions: Factors affecting particle size using spontaneous emulsification.* Journal of Colloid and Interface Science, 2013. **391**: p. 95-102.

21. Peng, L.-C., et al., *Optimization of water-in-oil nanoemulsions by mixed surfactants.* Colloids and Surfaces A: Physicochemical and Engineering Aspects, 2010. **370**(1): p. 136-142.
22. Housaindokht, M.R. and A. Nakhaei Pour, *Study the effect of HLB of surfactant on particle size distribution of hematite nanoparticles prepared via the reverse microemulsion.* Solid State Sciences, 2012. **14**(5): p. 622-625.
23. *Intermolecular and Surface Forces*, in *Intermolecular and Surface Forces (Third Edition)*, J.N. Israelachvili, Editor. 2011, Academic Press: Boston. p. iii.
24. Wang, L., et al., *Design and optimization of a new self-nanoemulsifying drug delivery system.* Journal of Colloid and Interface Science, 2009. **330**(2): p. 443-448.
25. Porras, M., et al., *Properties of water-in-oil (W/O) nano-emulsions prepared by a low-energy emulsification method.* Colloids and Surfaces A: Physicochemical and Engineering Aspects, 2008. **324**(1): p. 181-188.
26. Usón, N., M.J. Garcia, and C. Solans, *Formation of water-in-oil (W/O) nano-emulsions in a water/mixed non-ionic surfactant/oil systems prepared by a low-energy emulsification method.* Colloids and Surfaces A: Physicochemical and Engineering Aspects, 2004. **250**(1): p. 415-421.
27. Koroleva, M.Y. and E.V. Yurtov, *Nanoemulsions: the properties, methods of preparation and promising applications.* Russian Chemical Reviews, 2012. **81**(1): p. 21-43.

SECTION 3

Additional Research Work & List of Publications

Executive Summary

This section consists of two parts, the first part is chapter 6 which consists of overall conclusion & perspective of our studies. The second part consists a bird eye view of some of additional research work, in which I worked in collaboration during my PhD. At the end this part contains list of the publications achieved during the PhD.

CHAPTER 6

Conclusion & Perspective

Conclusion & Perspectives

The objective of PhD work was the development of the novel methods of formation of simple, inverse & double emulsion systems by using several strategies. We were seeking to draw a comparative analysis of different technologies used to produce nano particle generated in the form of the emulsion system. The technologies we investigated during the PhD process were Microfluidization, Ultrasonication & Spontaneous emulsification.

During the first study, it was observed that combination of Microfluidization & spontaneous emulsification can be transposed to produce double emulsions at nano scale successfully. The study provided a firm theoretical background & foundational research work to produce double emulsions at nano scale by combination of classical methods of production of double emulsions at micro scale.

The second study was the continuation of our first study in a way but using combination of different technologies & addressing more solutions faced by the formulation scientist for production of double emulsions at industrial scale. One of the most important challenge regarding double emulsions at nano scale is their low encapsulation efficiency. Our study responded to this challenge by formation of silica shell at the interface of the primary W/O nano-emulsion. This was never reported in literature before that the encapsulation efficiency of double emulsions at nano scale without any modification of the internal phase. The method was

simple, reproducible & can be exploited for encapsulation of hydrophilic & lipophilic molecules at industrial scale.

The third study provided an alternative way of encapsulation of hydrophilic molecules by creation of W/O nano-emulsion by spontaneous emulsification. The study filled gaps in research on W/O nano-emulsions as there are very limited research available on this interesting drug delivery system. The study concluded that W/O nano-emulsions can be effectively produced by spontaneous emulsification. The system also offered an alternative opportunity for encapsulation of hydrophilic drugs in addition to double emulsions & liposomes & can be exploited at the industrial scale.

APPENDICES

Additional Research Work & List of Publications

Additional Research Work: Appendix A

Development of doxorubicin hydrochloride loaded pH-sensitive liposomes: Investigation on the impact of chemical nature of lipids and liposome composition on pH-sensitivity.

Rehman AU[1], Omran Z[2], Anton H[3], Mély Y[3], Akram S[4], Vandamme TF[5], Anton N[6]

1 Université de Strasbourg, CNRS, CAMB UMR 7199, F-67000 Strasbourg, France ; Bahauddin Zakariya University (BZU) Multan, Pakistan.

2 Department of Pharmaceutical Chemistry, Faculty of Pharmacy, Umm AlQura University, Kingdom of Saudi Arabia. Electronic address: zhomran@uqu.edu.sa.

3 Université de Strasbourg, CNRS, LBP UMR 7213, F-67000 Strasbourg, France.

4 Université de Strasbourg, CNRS, CAMB UMR 7199, F-67000 Strasbourg, France.

5 Université de Strasbourg, CNRS, CAMB UMR 7199, F-67000 Strasbourg, France. Electronic address: vandamme@unistra.fr.

6 Université de Strasbourg, CNRS, CAMB UMR 7199, F-67000 Strasbourg, France. Electronic address: nanton@unistra.fr.

Abstract

This study investigates the impact of the chemical nature of lipids and additive on the formulation and properties of pH sensitive liposomes. The objective is to understand the respective role of the formulation parameters on the liposome properties in order to optimize the conditions for efficient encapsulation of doxorubicin (DOX). These liposomes should be stable at physiological pH, and disrupt in slightly acidic media such as the tumor microenvironment to release their DOX load. The major challenge for encapsulating DOX in pH sensitive liposomes lies in the fact that this drug is soluble at low pH (when the pH-sensitive liposomes are not stable), but the DOX aqueous solubility decreases in the pH conditions corresponding to the stability of the pH-sensitive liposomes. The study of pH-sensitivity of liposomes was conducted using carboxyfluorescein (CF) encapsulated in high concentration, i.e. quenched, and following the dye dequenching as sensor of the liposome integrity. We studied the impact of (i) the chemical nature of lipids (dioleoyl phosphatidyl ethanolamine (DOPE), palmitoyl-oleoyl phosphatidyl ethanolamine (POPE) and dimyristoyl phosphatidyl ethanolamine (DMPE)) and (ii) the lipid/stabilizing agent ratio (alpha-tocopheryl succinate), on the pH sensitivity of the liposomes. Optimized liposome formulations were then selected for the encapsulation of DOX by an active loading procedure, i.e. driven by a difference in pH inside and outside the liposomes. Numerous experimental conditions were explored, in function of the pH gradient and liposome composition, which allowed identifying critical parameters for the efficient DOX encapsulation in pH-sensitive liposomes.

Additional Research Work: Appendix B

Spontaneous nano-emulsification with tailor-made amphiphilic polymers and related monomers

Asad Ur Rehman [a,b], Mayeul Collot [c], Andrey S. Klymchenko [c], Salman Akram [a], Bilal Mustafa [a], Thierry Vandamme [a], Nicolas Anton [a*]

a University of Strasbourg, CNRS, CAMB UMR 7199, F-67000 Strasbourg,

France b Bahauddin Zakariya University (BZU) Multan, Pakistan

c University of Strasbourg, CNRS, LBP UMR 7021, F-67000 Strasbourg, France

Abstract

In general, nano-emulsions are submicron droplets composed of liquid oil phase dispersed in liquid aqueous bulk phase. They are stable and very powerful systems when it regards the encapsulation of lipophilic compounds and their dispersion in aqueous medium. On the other hand, when the properties of the nano-emulsions aim to be modified, e.g. for changing their surface properties, decorating the droplets with targeting ligands, or modifying the surface charge, the dynamic liquid / liquid interfaces make it relatively challenging. In this study, we have explored the development of nano-emulsions which were not anymore stabilized with a classical low-molecular weight surfactant, but instead, with an amphiphilic polymer based on poly(maleic anhydride-alt-1-octadecene) (PMAO) and Jeffamine®, a hydrophilic amino-terminated PPG/PEG copolymer. Using a polymer as stabilizer is a potential solution for the nano-emulsion functionalization, ensuring the droplet stabilization as well as being a platform for the droplet decoration with ligands (for instance after addition of function groups in the terminations of the chains). The main idea of the present work was to understand if the spontaneous emulsification –commonly performed with nonionic surfactants– can be transposed with amphiphilic polymers, and a secondary objective was to identify the main parameters impacting on the process. PMAO was modified with two different Jeffamine®, additionally different oils and different formulation conditions were evaluated. As a control, the parent monomer, octadecyl succinic anhydride (OSA) was also modified and studied in the similar way as that of polymer. The generated nano-emulsions were mainly studied by dynamic light scattering and electron microscopy, that allows discriminating the crucial parameters in the spontaneous process, originally conducted with polymers as only stabilizer. Keywords: Spontaneous emulsification; PMAO; nano-emulsion; surfactant; Jeffamine.

Additional Research Work: Appendix C

List of Publications

-Research Articles

1. Toward the Formulation of Stable Micro and Nano Double Emulsions through a Silica Coating on Internal Water Droplets.
Akram S, Wang X, Vandamme TF, Collot M, Rehman AU, Messaddeq N, Mély Y, Anton N.
Langmuir. 2019 Feb 12;35(6):2313-2325.

2. Development of doxorubicin hydrochloride loaded pH-sensitive liposomes: Investigation on the impact of chemical nature of lipids
and liposome composition on pH-sensitivity.
Rehman AU, Omran Z, Anton H, Mély Y, Akram S, Vandamme TF, Anton N.
European Journal of Pharmaceutics and Biopharmaceutics, 2018 Dec;133:331-338.

3. A new method for the formulation of double nanoemulsions.
Ding S, Anton N2, Akram S, Er-Ra k M, Anton H, Klymchenko A, Yu W, Vandamme TF, Serra CA
Soft Matter. 2017 Feb 22;13(8):1660-1669

4. Spontaneous nano-emulsi cation with tailor-made amphiphilic polymers and related monomers
Rehman, A.U.; Collot, M.; Klymchenko, A.S.; Akram, S.; Mustafa, B.; Vandamme, T.F.; Anton, N
European Journal of Pharmaceutical Research, 2019, 1(1) 27-36

-Review Articles

1. Biomedical Imaging: Principles, Technologies, Clinical Aspects, Contrast Agents, Limitations and Future Trends in Nanomedicines
Justine Wallyn, Nicolas Anton, Salman Akram, Thierry F.
Vandamme Pharmaceutical Research, June 2019, 36:78

-Book Chapters

1. Transitional Nanoemulsi cation Methods
Elsevier: Nanoemulsions Formulation, Applications, and Characterization
2018, Pages 77-100

2. Lipid Nano-Carriers: Formulation, Properties, And Applications
Elsevier (Accepted Manuscript

Salman AKRAM

Synthèse, optimisation, caractérisation physico-chimique, fonctionnalisation et application biomédicale de nanoparticules

Résumé

Techniques d'émulsification et systèmes d'émulsion, nanoparticules

L'objectif principal de cette thèse de recherche est d'analyser les systèmes d'administration de médicaments sous forme de particules, en particulier les émulsions sous différents angles. À cet égard, la présente thèse couvre de manière exhaustive trois aspects principaux de ces systèmes d'administration de médicaments. Premièrement, il donne un aperçu détaillé des différentes techniques d'émulsification, telles que la microfluidisation, les ultrasons et les méthodes de transition, et fournit une comparaison et les avantages relatifs de ces techniques par rapport à d'autres. Deuxièmement, la thèse donne également une vue détaillée de différents systèmes d'émulsion tels que les émulsions inverses et doubles à l'échelle micro et nanométrique et aborde des solutions à certains des problèmes clés associés à ces systèmes. Troisièmement, la thèse couvre également différentes techniques de caractérisation physico-chimiques pour analyser ces différents systèmes, leur fonctionnalisation et leur application en tant que systèmes de libération de médicaments. Enfin, il ouvre de nouvelles perspectives pour d'autres chercheurs travaillant dans le domaine de la nanomédecine, afin d'exploiter ces systèmes pour améliorer l'administration de médicaments.

Résumé en anglais

Emulsfication Techniques & Emulsion Systems, Nano Particles

The main point of focus of this research thesis is to analyse the particulate drug delivery systems specially emulsions from different angles. In this regard, the present thesis comprehensively covers three main aspects of these drug delivery systems. First, it gives a detailed overview of different emulsification techniques such as microfluidization, ultrasonication & transitional methods & provides a comparison and relative advantages of these techniques over another. Secondly, thesis also gives a detailed view of different emulsion systems such as inverse & double emulsions at both micro and nano scale and addresses solutions to some of the key problems associated with these systems. Thirdly, the thesis also covers different physicochemical characterization techniques for analysing these different systems, their functionalization & application as drug delivery systems. In last, it opens future avenues for other researchers working in field of nanomedicine, to exploit these systems in improving drug delivery.